

9-2009

# Minimizing Energy Use in Large Groundwater Supply Systems

Mikaela Martin

Follow this and additional works at: [https://scholarworks.umass.edu/cee\\_ewre](https://scholarworks.umass.edu/cee_ewre)



Part of the [Environmental Engineering Commons](#)

---

Martin, Mikaela, "Minimizing Energy Use in Large Groundwater Supply Systems" (2009). *Environmental & Water Resources Engineering Masters Projects*. 71.

<https://doi.org/10.7275/669D-WW96>

This Article is brought to you for free and open access by the Civil and Environmental Engineering at ScholarWorks@UMass Amherst. It has been accepted for inclusion in Environmental & Water Resources Engineering Masters Projects by an authorized administrator of ScholarWorks@UMass Amherst. For more information, please contact [scholarworks@library.umass.edu](mailto:scholarworks@library.umass.edu).

# **MINIMIZING ENERGY USE IN LARGE GROUNDWATER SUPPLY SYSTEMS**

A Master's Project Presented by

Mikaela A. Martin

Submitted to the Department of Civil and Environmental Engineering  
of the University of Massachusetts  
in partial fulfillment of the requirements for the degree of

**MASTER OF SCIENCE**

September 2009

Environmental Engineering

# MINIMIZING ENERGY USE IN LARGE GROUNDWATER SUPPLY SYSTEMS

A Master's Project Presented

by

MIKAELA A. MARTIN

Approved as to style and content by:

---

Dr. David P. Ahlfeld, Chair

---

Dr. Casey Brown, Member

---

Dr. Paul Barlow, Member

---

Dr. John E. Tobiason  
Graduate Program Director  
Environmental Engineering

## **Acknowledgements**

This research would not be possible without the support of many people.

I thank my advisor, Dr. Ahlfeld, whose knowledge, help, support, and encouragement allowed me to work on and complete this project. I look to my continuing work with him.

I thank my family: my fiancé Nick who kept me sane throughout the process and my parents and sister for their constant encouragement.

## **Abstract**

Two optimization formulations have been developed. The first formulation minimizes the energy required to pump water from an aquifer. This formulation is non-linear, requiring the use of quadratic terms in the objective function. The second formulation minimizes the maximum lift in an aquifer and is called the MINIMAX formulation. This formulation is linear and may be an acceptable substitution for the minimize energy formulation under conditions where there are small differences in initial lifts at the wells and where the demand is sufficient to require pumping at all wells such that the lifts at all wells are equal.

The minimize energy and MINIMAX formulations were applied to four test models: a confined, homogeneous aquifer with two wells; a confined, homogeneous aquifer with 20 wells; a confined, heterogeneous aquifer with 20 wells; and an unconfined, homogeneous aquifer. The MINIMAX formulation produced the same results as the minimize energy formulation when the non-pumping lifts were the same. As the non-pumping lifts varied, the MINIMAX formulation deviated from the minimize energy formulation.

A case study of the Lancaster subbasin of Antelope Valley, California, was used to further test the minimize energy and MINIMAX formulations. Two minimize energy formulations were examined, the first lifting water to the ground surface elevation at each well and the second lifting the water to a single reference elevation that took the value of the maximum ground surface elevation that was used in the first formulation. The MINIMAX formulation was applied to the case where the water was lifted to the reference elevation. The difference in total energy between the MINIMAX and minimize energy formulations was less than 10%, but the distribution of pumping among the wells varied greatly.

## Table of Contents

Acknowledgements .....	iii
Abstract .....	iv
Table of Contents .....	v
List of Tables .....	vi
List of Figures .....	vii
1 Introduction .....	1
2 Optimization Formulations .....	3
2.1 Minimize energy formulation .....	3
2.2 Minimize maximum lift formulation .....	4
2.3 Analytical examination of minimize energy formulation .....	4
3 Test Models .....	10
3.1 MODFLOW and GWM .....	10
3.2 Description of the model domain .....	11
3.3 Results and discussion .....	13
3.3.1 Confined aquifer model .....	14
3.3.1.1 Two-well model .....	14
3.3.1.2 Twenty-well model .....	19
3.3.1.3 Limitations of the MINIMAX formulation .....	24
3.3.2 Heterogeneity .....	27
3.3.3 Unconfined aquifer .....	29
3.4 Conclusions from the test models .....	35
4 Antelope Valley Case Study .....	36
4.1 Site description .....	36
4.2 Literature review of previous Antelope Valley models .....	39
4.2.1 Antelope Valley groundwater basin model .....	40
4.2.2 Lancaster flow simulation model .....	42
4.2.3 Lancaster simulation/optimization model .....	44
4.2.4 Lancaster simulation/optimization model using GWM .....	47
4.3 Model description .....	48
4.4 Application of minimize energy formulation to the Lancaster subbasin .....	51
4.5 Results and discussion .....	53
4.5.1 Minimize energy formulations compared to LANOPT results .....	55
4.5.2 Uniform reference elevation .....	64
4.5.2.1 Minimize energy formulation using a uniform reference elevation ....	64
4.5.2.2 MINIMAX formulation using a uniform reference elevation .....	70
4.5.3 Comparison of minimize energy and MINIMAX formulations .....	78
4.6 Conclusions from the Antelope Valley case study .....	82
5 Conclusions .....	84
6 References .....	85

## List of Tables

Table 4-1. Sources of recharge to the LAN model .....	44
Table 4-2. Comparison of total and managed water demand for each year .....	50
Table 4-3. Total injection for each year proposed by Scenario 2 of the LANOPT model .....	52
Table 4-4. Summary of scenarios used in the Antelope Valley case study .....	54
Table 4-5. Initial lifts at each well .....	59
Table 4-6. Lifts at the end of the last withdrawal period of the LANOPT-GS scenario ..	62
Table 4-7. Lifts at the end of the last withdrawal period of the MINENG-GS-GS1 scenario .....	63
Table 4-8. Lifts at the end of the last withdrawal period of the MINENG-GS-GS2 scenario .....	63
Table 4-9. Comparison of energy requirements for each formulation.....	79

## List of Figures

Figure 2-1. Two-well confined aquifer system.....	5
Figure 3-1. Two-well model domain showing the well locations .....	12
Figure 3-2. 20-well model domain showing the well locations.....	12
Figure 3-3. Percent error in total energy in MINIMAX formulation as compared to minimize energy formulation for the two-well model.....	16
Figure 3-4. Pumping distribution for the two-well model resulting from the minimize energy and MINIMAX formulations when the initial lifts are equal .....	16
Figure 3-5. Pumping distribution for the two-well model resulting from the minimize energy and MINIMAX formulations when the normalized maximum non-pumping lift is 1.11.....	17
Figure 3-6. Pumping distribution for the two-well model resulting from the minimize energy and MINIMAX formulations when the normalized maximum non-pumping lift is 1.24.....	17
Figure 3-7. Maximum relative difference between pumping rates for the two-well model .....	18
Figure 3-8. Average relative difference between pumping rates for the two-well model .....	18
Figure 3-9. Relative difference between drawdowns for the two-well model.....	19
Figure 3-10. Percent error in total energy in MINIMAX formulation as compared to minimize energy formulation for the 20-well model.....	20
Figure 3-11. Maximum relative difference between pumping rates for the 20-well model .....	20
Figure 3-12. Average relative difference between pumping rates for the 20-well model .....	21
Figure 3-13. Comparison of minimize energy and MINIMAX pumping distributions from the 20-well model where the non-pumping lifts at each well are equal .....	22
Figure 3-14. Comparison of minimize energy and MINIMAX pumping distributions from the 20-well model where the relative difference between non-pumping lifts is 1.97.....	22
Figure 3-15. Examples of the change in drawdown across the domain as the ground surface slope changes; the drawdown decreases when the initial lift is increased and the drawdown increases when the initial lift is decreased .....	23
Figure 3-16. Relative difference between drawdowns for the 20-well model.....	23
Figure 3-17. Pumping rate and lift resulting from the 20-well MINIMAX formulation with a normalized maximum non-pumping lift of 1.46 and a demand of $4 \times 10^5 \text{ m}^3/\text{d}$ .....	24
Figure 3-18. Pumping rate and lift resulting from the 20-well MINIMAX formulation with a normalized maximum non-pumping lift of 1.46 and a demand of $3 \times 10^5 \text{ m}^3/\text{d}$ .....	25
Figure 3-19. Pumping rate and lift resulting from the 20-well MINIMAX formulation with a normalized maximum non-pumping lift of 1.46 and a demand of $2 \times 10^5 \text{ m}^3/\text{d}$ .....	25
Figure 3-20. Pumping rate and lift resulting from the 20-well MINIMAX formulation with a normalized maximum non-pumping lift of 1.46 and a demand of $1 \times 10^5 \text{ m}^3/\text{d}$ .....	26
Figure 3-21. Pumping rate and lift resulting from the 20-well MINIMAX formulation with a normalized maximum non-pumping lift of 1.11 and a demand of $3 \times 10^5 \text{ m}^3/\text{d}$ .....	26
Figure 3-22. Test well model domain showing the western region with $T=400 \text{ m}^2/\text{d}$ and the eastern region with $T=200 \text{ m}^2/\text{d}$ .....	27
Figure 3-23. Comparison of minimize energy and MINIMAX pumping distribution under heterogeneous conditions where the non-pumping lifts at each well are equal.....	28



Figure 3-24. Comparison of minimize energy and MINIMAX pumping distribution under heterogeneous conditions where the relative difference between non-pumping lifts is 1.35	28
Figure 3-25. Comparison of minimize energy and MINIMAX pumping distribution under heterogeneous conditions where the relative difference between non-pumping lifts is 1.97	29
Figure 3-26. Pumping distribution of the unconfined and confined equal non-pumping lifts cases resulting from the minimize energy formulation	31
Figure 3-27. Drawdown distribution of the unconfined and confined equal non-pumping lifts cases resulting from the minimize energy formulation	31
Figure 3-28. Percent error in total energy in MINIMAX formulation as compared to minimize energy formulation for the 20-well, unconfined model	32
Figure 3-29. Maximum relative difference between pumping rates for the 20-well, unconfined model	32
Figure 3-30. Average relative difference between pumping rates for the 20-well, unconfined model	33
Figure 3-31. Comparison of minimize energy and MINIMAX pumping distribution from the unconfined aquifer where the non-pumping lifts at each well are equal	34
Figure 3-32. Comparison of minimize energy and MINIMAX pumping distribution from the unconfined aquifer where the relative difference between non-pumping lifts is 1.2.	34
Figure 4-1. Map showing the location of Antelope Valley and the model domain. Figure from Phillips et al. (2003)	37
Figure 4-2. AV model grid and boundaries, from Leighton and Phillips (2003)	41
Figure 4-3. Active region of the LAN model grid, in the Lancaster subbasin of Antelope Valley; figure from Phillips et al. (2003)	43
Figure 4-4. Uniformly spaced grid used for the LANOPT model, from Phillips et al. (2003)	45
Figure 4-5. Map showing well locations as black dots; the managed wells are circled. Figure adapted from Phillips et al. (2003).	50
Figure 4-6. Grouping of the managed wells into northern, middle, and southern regions. Figure adapted from Phillips et al. (Phillips et al. 2003).	55
Figure 4-7. Total energy required for pumping for each year the LANOPT-GS, MINENG-GS-GS1, and MINENG-GS-GS2 scenarios	56
Figure 4-8. Total amount of water injected yearly in the LANOPT-GS, MINENG-GS-GS1, and MINENG-GS-GS2 scenarios	57
Figure 4-9. Distribution of pumping for the LANOPT-GS scenario	58
Figure 4-10. Distribution of injection for the LANOPT-GS scenario	58
Figure 4-11. Distribution of pumping for the MINENG-GS-GS1 scenario	60
Figure 4-12. Distribution of injection for the MINENG-GS-GS1 scenario	60
Figure 4-13. Distribution of pumping for the MINENG-GS-GS2 scenario	61
Figure 4-14. Distribution of injection for the MINENG-GS-GS2 scenario	61
Figure 4-15. Energy required for pumping for the MINENG-UE scenario	64
Figure 4-16. Regional pumping distribution for the MINENG-UE scenario	65
Figure 4-17. Pumping distribution within the northern region for the MINENG-UE scenario	65

Figure 4-18. Pumping distribution within the middle region for the MINENG-UE scenario .....	66
Figure 4-19. Pumping distribution within the southern region for the MINENG-UE scenario .....	66
Figure 4-20. Regional injection distribution for the MINENG-UE scenario .....	67
Figure 4-21. Injection distribution within the northern region for the MINENG-UE scenario .....	67
Figure 4-22. Injection distribution within the middle region for the MINENG-UE scenario .....	68
Figure 4-23. Injection distribution within the southern region for the MINENG-UE scenario .....	68
Figure 4-24. Heads at wells within the northern region for the MINENG-UE scenario ..	69
Figure 4-25. Heads at wells within the middle region for the MINENG-UE scenario ....	69
Figure 4-26. Heads at wells within the southern region for the MINENG-UE scenario ..	70
Figure 4-27. Energy required for pumping for the MINIMAX-UE scenario .....	71
Figure 4-28. Regional pumping distribution for the MINIMAX-UE scenario .....	72
Figure 4-29. Pumping distribution within the northern region for the MINIMAX-UE scenario .....	72
Figure 4-30. Pumping distribution within the middle region for the MINIMAX-UE scenario .....	73
Figure 4-31. Pumping distribution within the southern region for the MINIMAX-UE scenario .....	73
Figure 4-32. Regional injection distribution for the MINIMAX-UE scenario .....	74
Figure 4-33. Injection distribution within the northern region for the MINIMAX-UE scenario .....	74
Figure 4-34. Injection distribution within the middle region for the MINIMAX-UE scenario .....	75
Figure 4-35. Injection distribution within the southern region for the MINIMAX-UE scenario .....	75
Figure 4-36. Heads at wells within the northern region for the MINIMAX-UE scenario	76
Figure 4-37. Heads at wells within the middle region for the MINIMAX-UE scenario ..	76
Figure 4-38. Heads at wells within the southern region for the MINIMAX-UE scenario	77
Figure 4-39. Lifts at wells within the northern region for the MINIMAX-UE scenario ..	77
Figure 4-40. Lifts at wells within the middle region for the MINIMAX-UE scenario ....	78
Figure 4-41. Lifts at wells within the southern region for the MINIMAX-UE scenario ..	78
Figure 4-42. Comparison of pumping rates for the LANOPT-UE, MINENG-GS-UE, MINENG-UE, and MINIMAX-UE scenarios for the northern region .....	80
Figure 4-43. Comparison of pumping rates for the LANOPT-UE, MINENG-GS-UE, MINENG-UE, and MINIMAX-UE scenarios for the middle region .....	80
Figure 4-44. Comparison of pumping rates for the LANOPT-UE, MINENG-GS-UE, MINENG-UE, and MINIMAX-UE scenarios for the southern region .....	81
Figure 4-45. Comparison of injection rates for the LANOPT-UE, MINENG-GS-UE, MINENG-UE, and MINIMAX-UE scenarios for the northern region .....	81
Figure 4-46. Comparison of injection rates for the LANOPT-UE, MINENG-GS-UE, MINENG-UE, and MINIMAX-UE scenarios for the middle region .....	82

Figure 4-47. Comparison of injection rates for the LANOPT-UE, MINENG-GS-UE, MINENG-UE, and MINIMAX-UE scenarios for the southern region.....	82
----------------------------------------------------------------------------------------------------------------------------------------------	----

## **1 Introduction**

Energy consumption for groundwater pumping is substantial. Moving and treating water in California consumes 15,000 GWh/year, comprising 6.5% of the total energy consumption in the state. In the three regions of California that are responsible for two-thirds of the groundwater use in the state, groundwater pumping consumes 2,250 GWh/year, comprising 1% of the total energy consumption (California Energy Commission 2004). Most of the energy cost is due to moving the water. The energy required to lift the groundwater increases with decreasing groundwater levels.

Groundwater depletion is caused primarily by sustained pumping. Water level declines have occurred in many places in the United States as a result of groundwater extraction, though the problem of groundwater depletion is most well known in the High Plains and Southwest regions of the country. The High Plains aquifer underlies parts of eight states. Water level declines of more than 100 feet as compared to predevelopment levels have been observed in some areas; in other areas the saturated thickness has been reduced by half. In the Southwest, there have been water level declines of 300 to 500 feet in Arizona, resulting in up to 12.5 feet of measured subsidence, and Las Vegas has had up to 300 feet of groundwater level decline. Along the Gulf Coast, water level declines of 200 feet in Louisiana have resulted in saltwater encroachment from the Gulf of Mexico, while pumping in Houston, Texas, has caused up to 400 feet of groundwater level decline, resulting in 10 feet of subsidence. The Chicago-Milwaukee area has had up to 900 feet of groundwater level decline (Bartolino and Cunningham 2003). Antelope Valley, California, located on the western edge of the Mojave Desert, has had more than 200 feet of groundwater level decline, resulting in six feet of land subsidence (Leighton and Phillips 2003). Groundwater depletion results in greater pumping costs because, as the depth to the water increases, the water must be lifted higher to reach the land surface, requiring more energy to power the pump to lift the water.

Optimization is used to help decision makers choose among multiple solutions to a problem. Optimization has been used in groundwater to minimize pumping costs in multi-well systems. The pumping cost can be expressed linearly, as a function of the pumping rate of the well only, or it can be expressed as a non-linear function that includes the pumping rate of the well and the head at the well. Theodossiou (2004) uses a

non-linear objective function representing the relative cost of pumping that includes the pumping rate at the well, the initial depth to the water table, and the drawdown resulting from pumping to create an objective function that minimizes the product of pumping rate and lift. The response matrix approach is used to link the MINOS solver to a two-dimensional finite difference groundwater flow simulation model of an unconfined aquifer underlying the Kokkinohoria area in southern Cyprus. Tsai et al. (2009) uses a parallel genetic algorithm to solve a multi-objective management model that includes a non-linear objective function minimizing the product of the pumping rate and the lift and that also considers the efficiency of the pump. It is applied to a three-dimensional model that uses MODFLOW to model an aquifer underlying Chandler, Arizona. Increasing the weight of the minimize energy objective function as compared to the other objectives resulted in a reduction of the amount of energy required to pump water from the system by more than 60% and the amount of drawdown by more than 24%.

An optimization algorithm has several criteria that it should meet. It should be able to handle large-scale transient problems and to accommodate mild non-linear responses, such as unconfined aquifers, so as to be applicable to a variety of problems. The formulation needs to be numerically robust. As such, a linear formulation is desirable. Non-linear optimization formulations often have local minima which may result in the optimization program finding a non-optimal solution (Ahlfeld and Mulligan 2000).

The purpose of this research is to determine if optimization can be effectively applied to adjust groundwater pumping schedules for multi-well fields to reduce energy use. This is achieved by developing an optimization formulation that minimizes the energy required to pump groundwater. The formulation needs to minimize energy costs by choosing a pumping schedule to meet water demands.

## 2 Optimization Formulations

Two optimization formulations have been developed. The first formulation is a non-linear formulation that minimizes the energy required to pump water from an aquifer. The second formulation minimizes the maximum lift in an aquifer and is linear.

### 2.1 Minimize energy formulation

The energy required to pump water from a well is a function of the product of lift and flow rate at the well. The power,  $\dot{E}_{work}$ , required to lift the water is

$$\dot{E}_{work} = \rho g Q L \quad (\text{Eq. 2.1})$$

where  $\rho$  is the density of the water,  $g$  is the gravitational rate constant,  $Q$  is pumping rate, and  $L$  is the required lift, which is the difference between the ground surface elevation,  $H$ , and the hydraulic head,  $h$ , at the well. The energy required to pump the water can then be calculated as

$$E = \dot{E}_{work} \Delta t = \rho g Q (H - h) \Delta t \quad (\text{Eq. 2.2})$$

where  $\Delta t$  is the time over which the water is pumped. This equation can be simplified to

$$E = \alpha Q (H - h) \quad (\text{Eq. 2.3})$$

where  $\alpha$  is a conversion factor that incorporates  $\rho$ ,  $g$ , and  $\Delta t$ . The conversion factor can also incorporate electricity costs.

The objective of the minimize energy formulation is to minimize the total energy use as a function of hydraulic head and flow rate from the wells. The formulation can be described in the following way:

$$\text{Minimize } Z = \sum_{i=1}^n \alpha Q_i (H_i - h_i) \quad (\text{Eq. 2.4})$$

$$\text{such that } \sum_{i=1}^n Q_i \geq D$$

where  $Z$  is the objective function,  $Q_i$  is the withdrawal rate at a given well,  $n$  is the number of wells,  $H_i$  is the ground surface elevation at a well,  $h_i$  is the head at a well, and  $D$  is the demand that must be met with pumping. The formulation will not pump any more water than is needed to meet the demand, since extracting more water would require more energy. In effect the demand will be met as an equality in all cases. Since

the hydraulic head depends on the pumping rate, the objective function is nonlinear and may be quadratic.

## 2.2 Minimize maximum lift formulation

The minimize maximum lift (MINIMAX) formulation is a proposed substitute for the minimize energy formulation. Since energy is a product of lift and flow rate, minimizing the lift will, under some conditions shown herein, yield the same solution as the minimize energy formulation and often yield an acceptable approximation. It may be preferable to use the MINIMAX formulation because it is a linear formulation, eliminating the possibility of finding non-optimal solutions due to local minima of a non-linear function. The formulation can be described in the following way:

$$\begin{aligned} &\text{Minimize } Z = R && \text{(Eq. 2.5)} \\ &\text{such that } \sum_{i=1}^n Q_i \geq D \\ &\text{and } H_i - h_i \leq R, \quad i = 1, 2, \dots, n \end{aligned}$$

The MINIMAX formulation will select rates so that all of the lifts are identical and equal to the value of R, provided that the demand is large enough to equalize the lifts. If the demand is small, R will take the value of the maximum lift. The formulation will not pump any more water than is needed to meet the demand, since extracting more water than required would lower heads in the aquifer, thereby increasing the lifts. As with the minimize energy formulation, in effect, the demand will be met as an equality in all cases.

## 2.3 Analytical examination of minimize energy formulation

The minimize energy formulation can be examined analytically for a simple case to illustrate the expected results with both unequal non-pumping lifts and with equal non-pumping lifts. Consider a system with a confined aquifer and two wells (Figure 2-1).

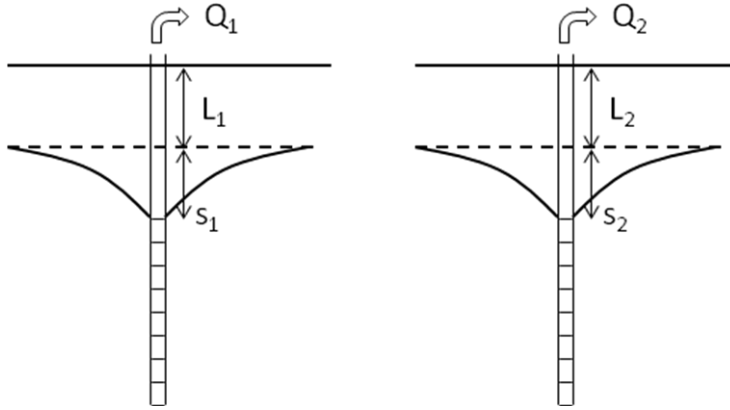


Figure 2-1. Two-well confined aquifer system

Assume that pumping at each well may affect the head at the other well and that the response of the head at each well is non-symmetric. The minimize energy formulation for the system can be described as follows:

$$\begin{aligned} \text{Minimize } Z &= Q_1(L_1 + s_1) + Q_2(L_2 + s_2) \\ \text{such that } Q_1 + Q_2 &= D \end{aligned} \quad (\text{Eq. 2.6})$$

where  $L_1$  and  $L_2$  are the non-pumping lifts at each well,  $s_1$  and  $s_2$  are the drawdowns at each well,  $Q_1$  and  $Q_2$  are the withdrawal rates at each well, and  $D$  is the demand that must be met through pumping.

The drawdown at each well can be expressed using response coefficients. The response matrix approach is often used in solving groundwater optimization problems (Gorelick 1983). It is based on the principle of superposition, which applies to all linear systems. The principle of superposition states that the net response of the system at a given place and time caused by multiple stresses is the sum of responses that would be caused by each stress individually. The principle of superposition applies to groundwater systems with linear governing equations and boundary conditions and allows the impact of multiple stresses on head to be predicted. For example, the drawdown at a location due to multiple pumping wells can be calculated by adding the drawdown at that location from each individual well. Doubling or halving the pumping at a well would double or halve the drawdown at a location due to that well. The principle of superposition is not valid when the governing equation is nonlinear, such as for unconfined flow, or when the boundary conditions are nonlinear (Ahlfeld and Mulligan 2000; Das and Datta 2001).



The response matrix approach to groundwater optimization develops a relationship between hydraulic head and stress. The response of the head at a location to a change in stress can be described using the Taylor series:

$$h_i(\mathbf{q}) = h_i^0(\mathbf{q}_0) + \sum_{j=1}^n \frac{\partial h_i}{\partial q_j}(\mathbf{q}_0)(q_j - q_j^0) + \sum_{j=1}^n \sum_{k=1}^n \left[ \frac{\partial^2 h_i}{\partial q_j \partial q_k}(\mathbf{q}_0) \frac{(q_j - q_j^0)(q_k - q_k^0)}{2!} \right] + \dots \quad (\text{Eq. 2.7})$$

where  $h_i$  is the head at location  $i$ ,  $h_i^0$  is the initial head at location  $i$ ,  $\mathbf{q}$  is the vector of new stresses with elements  $q_j$ ,  $\mathbf{q}_0$  is the vector of original stresses with elements  $q_j^0$ , and  $n$  is the number of locations considered for applications of stress. For a linear system, where head is a linear function of stress, the second order and higher derivatives of  $h$  with respect to  $q$  are zero and the first order derivative of  $h$  with respect to  $q$  is constant. Under such conditions,  $\partial h / \partial q$  is independent of  $\mathbf{q}_0$ . Setting  $\mathbf{q}_0$  equal to zero allows the Taylor series to be simplified to

$$h_i(\mathbf{q}) = h_i^0 + \sum_{j=1}^n \frac{\partial h_i}{\partial q_j} q_j. \quad (\text{Eq. 2.8})$$

In terms of drawdown, the response of the system at a location to stress can be expressed as

$$s_i(\mathbf{q}) = \sum_{j=1}^n \frac{\partial s_i}{\partial q_j} q_j \quad (\text{Eq. 2.9})$$

where  $s_i$  is the drawdown at location  $i$ .

The partial derivatives  $\partial h_i / \partial q_j$  describe the response of the head at each location to the applied stresses and are called response coefficients. The perturbation method is often used to calculate the response coefficients (Ahlfeld and Mulligan 2000). A groundwater flow simulation model is used to determine the response of groundwater flow to changes in stress by running the model multiple times, first with the stresses as described by  $\mathbf{q}_0$  as a base condition, then subsequent times by changing one stress at a time. The response coefficients are calculated by using a forward difference approximation:

$$\frac{\partial h_i}{\partial q_j} \approx \frac{\Delta h_i}{\Delta q_j} = \frac{h_i(\mathbf{q}_{\Delta j}) - h_i(\mathbf{q}_0)}{q_{\Delta j} - q_j^0} \quad (\text{Eq. 2.10})$$

where  $q_{Aj}$  is the perturbed flow rate at well  $j$  and  $\mathbf{q}_{Aj}$  varies from  $\mathbf{q}_0$  only in element  $j$  by the amount  $(q_{Aj} - q_j^0)$ . The collection of response coefficients is called the response matrix. The response matrix connects the optimization formulation to the groundwater flow simulation model.

Assuming that pumping at each well may affect the head at the other well and that the response of the head at each well is non-symmetric, the drawdown at each well can be expressed as

$$s_1 = \frac{\partial s_1}{\partial Q_1} Q_1 + \frac{\partial s_1}{\partial Q_2} Q_2 = \beta_{11} Q_1 + \beta_{12} Q_2 \quad (\text{Eq. 2.11})$$

and

$$s_2 = \frac{\partial s_2}{\partial Q_1} Q_1 + \frac{\partial s_2}{\partial Q_2} Q_2 = \beta_{21} Q_1 + \beta_{22} Q_2 \quad (\text{Eq. 2.12})$$

where  $\beta_{ij} = \frac{\partial s_i}{\partial Q_j}$  is the response coefficient. The minimize energy formulation then becomes

$$\text{Minimize} \quad (\text{Eq. 2.13})$$

$$Z = Q_1 (L_1 + \beta_{11} Q_1 + \beta_{12} Q_2) + Q_2 (L_2 + \beta_{21} Q_1 + \beta_{22} Q_2)$$

$$\text{such that } Q_1 + Q_2 = D,$$

giving two equations with two unknowns ( $Q_1$  and  $Q_2$ ). Eliminating  $Q_2$  by substitution and rearranging the remaining equation gives

$$Z = Q_1 L_1 + \beta_{11} Q_1^2 + (\beta_{12} + \beta_{21}) Q_1 D - (\beta_{12} + \beta_{21}) Q_1^2 + D L_2 - Q_1 L_2 + \beta_{22} (D - Q_1)^2. \quad (\text{Eq. 2.14})$$

At the minimum  $Z$ ,  $\partial Z / \partial Q_1$  is equal to zero. The equation can be solved for  $Q_1$  by taking the derivative and setting it equal to zero, at which point  $Q_2$ ,  $s_1$ , and  $s_2$  can be calculated:

$$Q_1 = \frac{D}{2} + \frac{D}{2} \frac{(\beta_{22} - \beta_{11})}{((\beta_{11} + \beta_{22}) - (\beta_{12} + \beta_{21}))} - \frac{(L_1 - L_2)}{2((\beta_{11} + \beta_{22}) - (\beta_{12} + \beta_{21}))} \quad (\text{Eq. 2.15})$$

$$Q_2 = \frac{D}{2} - \frac{D}{2} \frac{(\beta_{22} - \beta_{11})}{((\beta_{11} + \beta_{22}) - (\beta_{12} + \beta_{21}))} + \frac{(L_1 - L_2)}{2((\beta_{11} + \beta_{22}) - (\beta_{12} + \beta_{21}))} \quad (\text{Eq. 2.16})$$

$$s_1 = (\beta_{11} + \beta_{12})\frac{D}{2} + \frac{D}{2} \frac{(\beta_{22} - \beta_{11})(\beta_{11} - \beta_{12})}{((\beta_{11} + \beta_{22}) - (\beta_{12} + \beta_{21}))} \quad (\text{Eq. 2.17})$$

$$s_1 = (\beta_{11} + \beta_{12})\frac{D}{2} + \frac{D}{2} \frac{(\beta_{22} - \beta_{11})(\beta_{11} - \beta_{12})}{((\beta_{11} + \beta_{22}) - (\beta_{12} + \beta_{21}))} - \frac{(L_1 - L_2)(\beta_{11} - \beta_{12})}{2((\beta_{11} + \beta_{22}) - (\beta_{12} + \beta_{21}))}$$

$$s_2 = (\beta_{21} + \beta_{22})\frac{D}{2} + \frac{D}{2} \frac{(\beta_{22} - \beta_{11})(\beta_{21} - \beta_{22})}{((\beta_{11} + \beta_{22}) - (\beta_{12} + \beta_{21}))} \quad (\text{Eq. 2.18})$$

$$- \frac{(L_1 - L_2)(\beta_{21} - \beta_{22})}{2((\beta_{11} + \beta_{22}) - (\beta_{12} + \beta_{21}))}$$

Under certain conditions, the minimize energy formulation gives the same results as the MINIMAX formulation. If the initial non-pumping lifts are the same and the response of the head at each well is symmetric, then it can be assumed that

$$\beta_{11} = \beta_{22} = \beta_1 \quad (\text{Eq. 2.19})$$

and

$$\beta_{12} = \beta_{21} = \beta_2 \quad (\text{Eq. 2.20})$$

resulting in equal pumping and drawdown (and therefore equal lifts) at both wells:

$$Q_1 = Q_2 = \frac{D}{2} \quad (\text{Eq. 2.21})$$

$$s_1 = s_2 = \frac{D}{2}(\beta_1 + \beta_2). \quad (\text{Eq. 2.22})$$

If the initial non-pumping lifts are the same, the response of the head at each well is symmetric, and the pumping at one well does not affect the head at the other (i.e., the wells are far apart and the transmissivity is large), then the objective function simplifies further with

$$\beta_{11} = \beta_{22} = \beta \quad (\text{Eq. 2.23})$$

$$\beta_{12} = \beta_{21} = 0 \quad (\text{Eq. 2.24})$$

$$s_1 = \beta Q_1 \quad (\text{Eq. 2.25})$$

$$s_2 = \beta Q_2 \quad (\text{Eq. 2.26})$$

and resulting once again in equal pumping and drawdown at both wells:

$$Q_1 = Q_2 = \frac{D}{2} \quad (\text{Eq. 2.27})$$

$$s_1 = s_2 = \frac{D}{2} \beta. \quad (\text{Eq. 2.28})$$

The minimize energy and MINIMAX formulations provide the same solution of equal pumping and equal drawdown in cases where the initial lifts at each well are equal. For a confined aquifer, both the ground surface and the piezometric surface can slope; the solution is the same as long as the initial lifts are uniform. As the initial, non-pumping lift varies between wells, it is expected that the solution provided by the MINIMAX formulation will deviate from that provided by the minimize energy formulation. In cases where the differences among initial lifts are small, the MINIMAX formulation provide an acceptable approximation of the solution from the minimize energy formulation.

Katsifarakis (2008) presented a similar analytical examination of the minimize energy formulation for the case of a horizontal aquifer under steady state conditions for any number and configuration of wells. It was assumed that the initial non-pumping lift was equal at all wells. It was proved that, in infinite and semi-infinite aquifers, the hydraulic head is the same at all wells when the pumping cost is minimized.

### **3 Test Models**

A simple model has been created to examine the minimize energy and MINIMAX formulations. The test problem is run with MODFLOW and Ground-Water Management (GWM).

#### **3.1 MODFLOW and GWM**

MODFLOW (McDonald and Harbaugh 1988) is a modular, three-dimensional, finite-difference groundwater flow model. It is an open source program that was developed and is maintained by the U.S. Geological Survey. The model can simulate both steady and transient flow in heterogeneous, confined or unconfined systems. Its modular nature allows the use of packages to modify the code for particular applications in which additional stresses to the model are added to the basic groundwater flow process. The packages include recharge, evapotranspiration, well flow, and river seepage, among others.

Ground-Water Management (GWM) is an optimization process that is coupled with MODFLOW (Ahlfeld, Barlow, and Mulligan 2005). The current version of GWM, MF2005-GWM, couples GWM with MODFLOW 2005 (Harbaugh 2005). GWM uses the response matrix approach to solve linear, non-linear, and mixed-binary linear groundwater management formulations. The management formulations consist of decision variables, constraints, and an objective function.

The decision variables are flow rate, external, or binary variables. Flow rate decision variables represent well withdrawal or injection rates and are defined by their MODFLOW grid locations and active stress periods. External variables are used to represent sources or sinks of water that do not directly affect the state of the groundwater flow system. Binary variables are associated with flow rate and external variables and indicate the status of the associated variables. A binary variable with a value of one indicates that the associated variables are active. A binary variable with a value of zero indicates that the associated variables are inactive. The constraints place limits on the flow rate and external decision variables. Constraints can be placed on the values of the decision variables, on the linear summation of the decision variables, on the hydraulic head or state of the system, and on streamflow. The hydraulic head can be constrained

through placing upper and lower head bounds at a location, limiting drawdown at a location, limiting the difference between hydraulic heads at two locations, and limiting the gradient in head between two locations. The objective function maximizes or minimizes the weighted sum of the decision variables.

Two enhanced versions of GWM have recently been developed (Baker 2008). The GWM STA version adds the ability to use state variables in the groundwater management formulation, through the addition of the STA package to GWM. The state variables consist of hydraulic head and streamflow type variables. The state variables can be added to the objective function and can be included in the summation constraints. They are dependent on the flow rate variables and are calculated using the response matrix approach. The GWM QUAD version allows quadratic objective functions by incorporating quadratic programming. The objective function is no longer limited to maximizing or minimizing the weighted sum of the decision variables, but can also incorporate quadratic terms. The quadratic terms can consist of two flow rate variables, a flow rate variable and a state variable, or two state variables. The inclusion of quadratic terms in the objective function allows energy costs, which are a product of flow rate variables and hydraulic head, to be represented.

### **3.2 Description of the model domain**

The model domain is  $100 \text{ km}^2$  with 100 rows and 100 columns, each with 100 m spacing. The eastern and western edges are constant head boundaries with heads of 100 m and the northern and southern edges are no flow boundaries. There is one horizontal, confined aquifer with a transmissivity of  $300 \text{ m}^2/\text{d}$ . There is no recharge. The simulation is steady state. The optimization simulations are run using two different well fields. The first well field contains two wells, located at row 50, columns 25 and 75 (Figure 3-1). The well placement is not exactly symmetrical. As a result, the pumping from both wells is not identical when the model domain has otherwise symmetrical conditions, as would be expected for symmetrical well placement, though the pumping rates are close due to the near symmetry of the well placement. The second well field contains 20 wells, scattered throughout the model domain (Figure 3-2). Flow rate decision variables and hydraulic head state variables are located at each well.

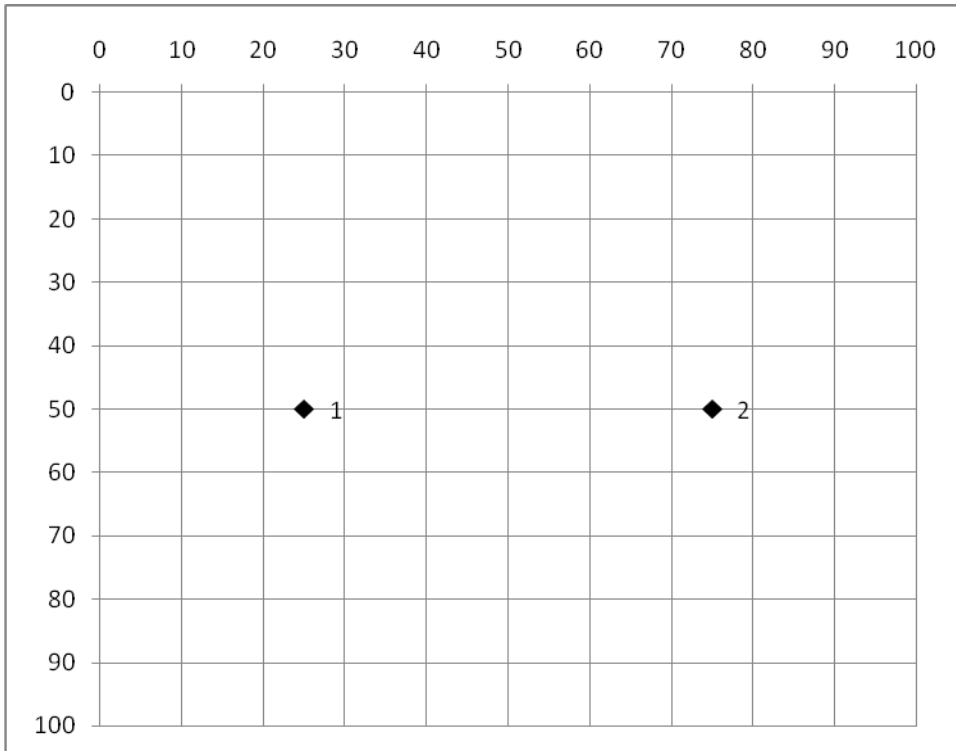


Figure 3-1. Two-well model domain showing the well locations

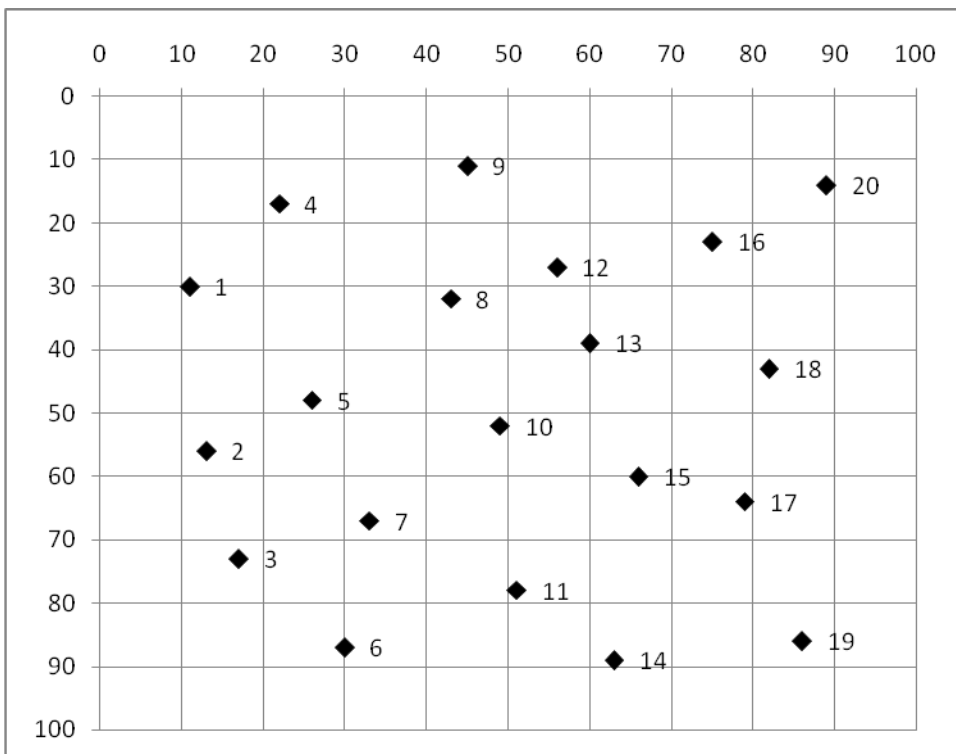


Figure 3-2. 20-well model domain showing the well locations

Initially, the ground surface is horizontal and parallel to the aquifer top so that the non-pumping lifts at all wells are uniform. The effect of differing non-pumping lifts on the minimize energy and MINIMAX formulations is examined by tilting the ground surface such that the elevation of the ground surface decreases from the west edge to the east edge of the domain, resulting in differing non-pumping lifts. The amount by which the non-pumping lifts differ across the domain is normalized by dividing the maximum non-pumping lift among all of the wells by the average non-pumping lift of all of the wells for each simulation. The variation in lifts can be described by the normalized maximum non-pumping lift:

$$\text{Normalized Maximum Non – Pumping Lift} = \frac{L_{\max}}{L_{\text{average}}} \quad (\text{Eq. 3.1})$$

where  $L_{\max}$  is the maximum non-pumping lift among all wells for a given simulation and  $L_{\text{average}}$  is the average non-pumping lift among all wells for a given simulation. The deviation between the minimize energy and MINIMAX formulations is examined by varying the normalized maximum non-pumping lift between 1.0 (where all lifts are equal) and 2.0.

### 3.3 Results and discussion

The results of the optimization runs are analyzed by examining how the minimize energy and MINIMAX formulation results differ as the variation in lifts across the domain increases.

The difference in the total energy required to pump groundwater for each formulation can be described by the percent error of the MINIMAX formulation as compared to the minimize energy formulation:

$$\% \text{ Error} = \frac{|E_{\text{total},\text{MINIMAX}} - E_{\text{total},\text{energy}}|}{E_{\text{total},\text{energy}}} \cdot 100\% \quad (\text{Eq. 3.2})$$

where  $E_{\text{total},\text{MINIMAX}}$  is the total energy for MINIMAX formulation (kWh/d) and  $E_{\text{total},\text{energy}}$  is the total energy for minimize energy formulation (kWh/d). It is also useful to examine the relative difference between pumping rates at a given well for each formulation:



$$\text{Relative Difference in Pumping} = \frac{\left| Q_{i,MINIMAX} - Q_{i,energy} \right|}{\frac{Q_{i,MINIMAX} + Q_{i,energy}}{2}} \quad (\text{Eq. 3.3})$$

where  $Q_{i,MINIMAX}$  is an optimal pumping rate of a well as determined by the MINIMAX formulation and  $Q_{i,energy}$  is the optimal pumping rate of the same well as determined by the minimize energy formulation. The maximum relative difference for each simulation describes the extent of variation between the pumping rates; the average relative difference describes the overall fit of the MINIMAX results to the minimize energy results. The difference in drawdown between the minimize energy and MINIMAX formulations is calculated in the same way, where  $s_{i,MINIMAX}$  is the resulting drawdown at a well as determined by the MINIMAX formulation and  $s_{i,energy}$  is the resulting drawdown at the same well as determined by the minimize energy formulation:

$$\text{Relative Difference in Drawdown} = \frac{s_{i,MINIMAX} - s_{i,energy}}{\frac{s_{i,MINIMAX} + s_{i,energy}}{2}} \quad (\text{Eq. 3.4})$$

The absolute value operator is omitted for the drawdown calculation in order to be able to determine which formulation causes greater drawdown at a well.

### 3.3.1 Confined aquifer model

The simplest model used to examine the minimize energy and MINIMAX formulations is a homogeneous, confined aquifer, as described in the model description. The two-well model is used to gain a basic understanding of the differences between the two formulations and the 20-well model is used to examine how the formulations differ when a large number of wells are pumping.

#### 3.3.1.1 Two-well model

For the two-well model, both the minimize energy and MINIMAX formulations are required to meet a demand of  $5 \times 10^4 \text{ m}^3/\text{d}$ . The minimize energy formulation takes the form

$$\text{Minimize } Z = Q_1(H_1 - h_1) + Q_2(H_2 - h_2) \quad (\text{Eq. 3.5})$$

$$\text{such that } Q_1 + Q_2 \geq 5 \times 10^4 \frac{m^3}{d}.$$

The MINIMAX formulation takes the form

$$\text{Minimize } Z = R \quad (\text{Eq. 3.6})$$

$$\text{such that } Q_1 + Q_2 \geq 5 \times 10^4 \frac{m^3}{d}$$

$$\text{and } H_1 - h_1 \leq R$$

$$H_2 - h_2 \leq R.$$

For both formulations,  $Q_1$  and  $Q_2$  represent the flow rate decision variables at each well,  $h_1$  and  $h_2$  represent the hydraulic head state variables at each well, and  $H_1$  and  $H_2$  represent the ground surface elevations at each well. The normalized maximum lift varies between 1.0 and 1.3. Above the normalized maximum lift of 1.3, the MINIMAX formulation is unable to equalize the lifts and pumps only from the eastern well, which has the smaller initial lift, in order to minimize the maximum lift.

When the non-pumping lifts are equal at both wells, the MINIMAX formulation gives the same results as the minimize energy formulation. As the slope of the ground surface deviates from that of the aquifer, causing greater variation in the non-pumping lifts, the results of the MINIMAX formulation deviate from the results of the minimize energy formulation. The percent error of the total energy required for the MINIMAX formulation as compared to the energy required for the minimize energy formulation increases to 4.8% as the normalized maximum lift increases from 1.0 to 1.3 (Figure 3-3). The pumping distribution between wells is the same when the lifts are equal (Figure 3-4). As the normalized maximum lift increases, representing greater differences between non-pumping lifts, the pumping decreases at the western well, where the lift is greater, and increases at the eastern well, where the lift is smaller, for both formulations (Figure 3-5 and Figure 3-6). The maximum relative difference in pumping at a single well increases to 1.73 (Figure 3-7) and the average relative difference increases to 1.01 (Figure 3-8). The MINIMAX formulation changes the pumping distribution more than the minimize energy formulation in order to equalize the lifts at both wells, whereas the minimize energy formulation is able to balance the increase in pumping with the decrease in lift.

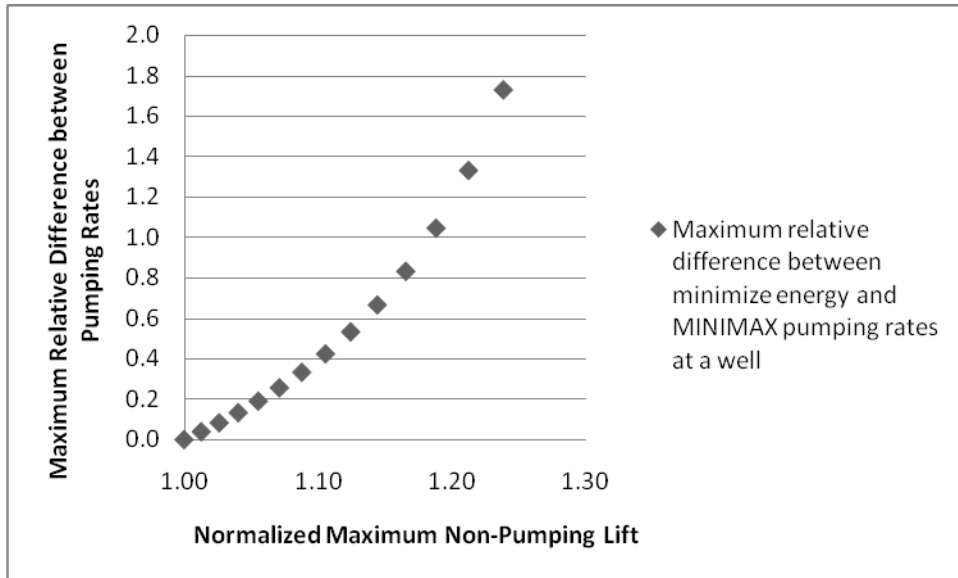


Figure 3-3. Percent error in total energy in MINIMAX formulation as compared to minimize energy formulation for the two-well model

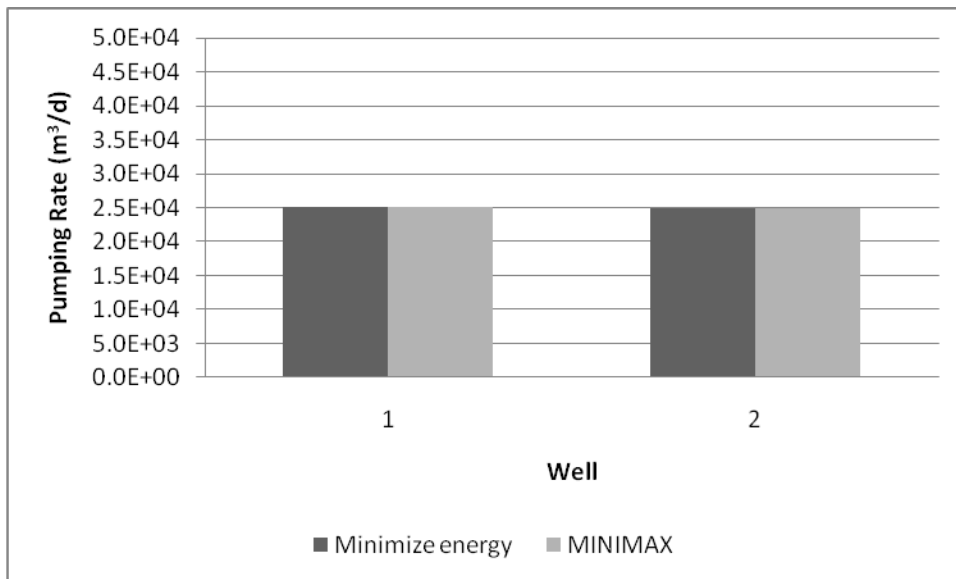


Figure 3-4. Pumping distribution for the two-well model resulting from the minimize energy and MINIMAX formulations when the initial lifts are equal

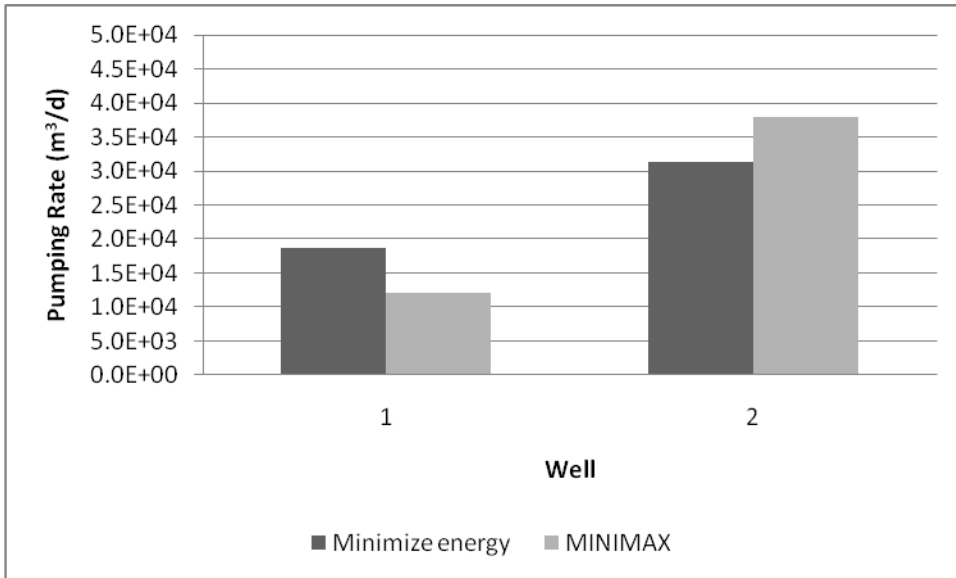


Figure 3-5. Pumping distribution for the two-well model resulting from the minimize energy and MINIMAX formulations when the normalized maximum non-pumping lift is 1.11

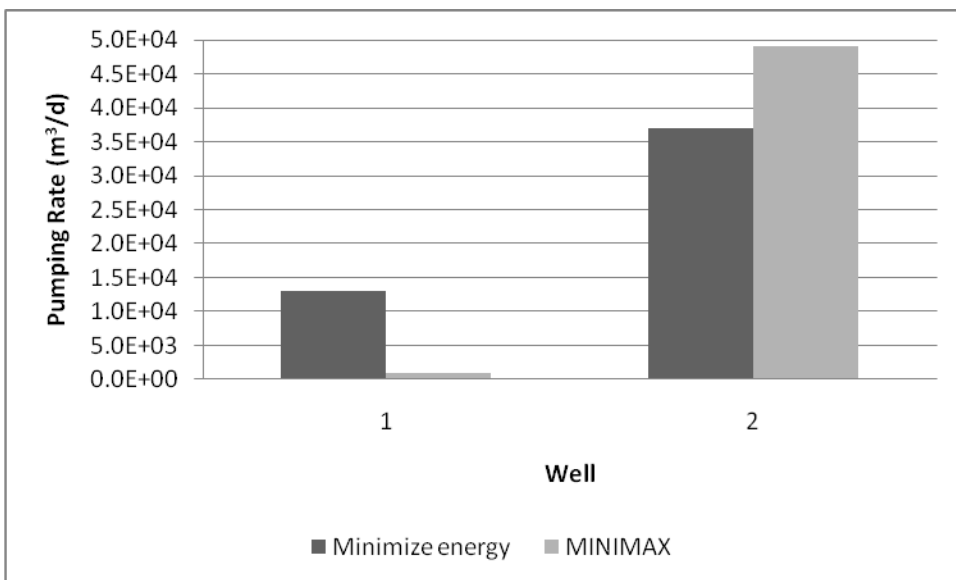


Figure 3-6. Pumping distribution for the two-well model resulting from the minimize energy and MINIMAX formulations when the normalized maximum non-pumping lift is 1.24

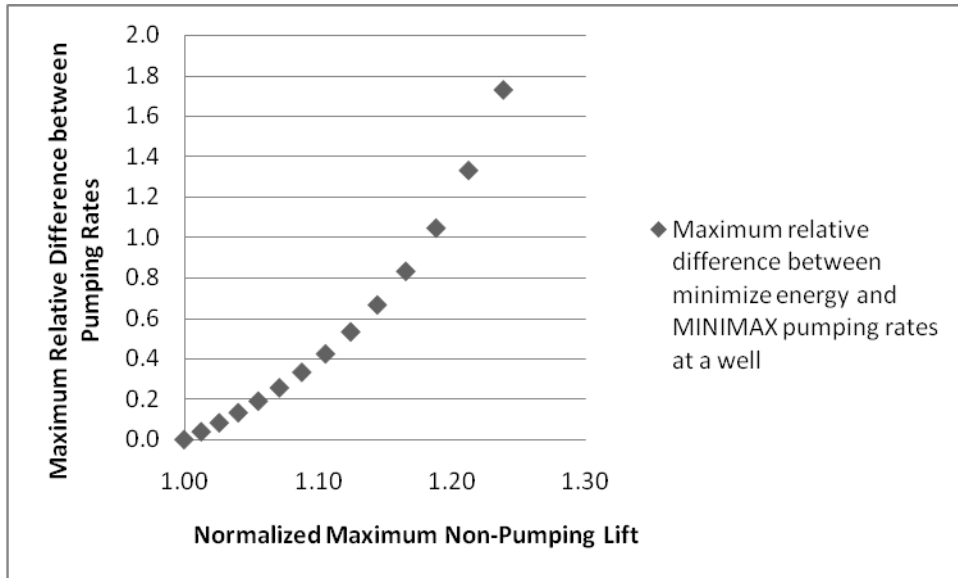


Figure 3-7. Maximum relative difference between pumping rates for the two-well model

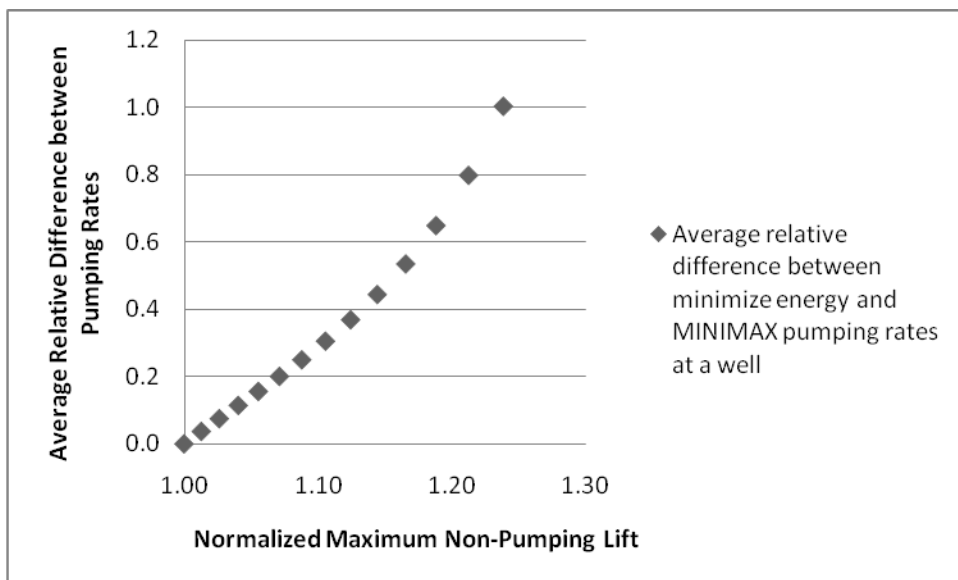


Figure 3-8. Average relative difference between pumping rates for the two-well model

When the land surface is parallel with the aquifer, the drawdown at both wells for both the minimize energy and MINIMAX formulations is 78.5 m. As the slope of the ground surface deviates from that of the aquifer, the drawdown at Well 1 decreases and the drawdown at Well 2 increases for both formulations. At the normalized maximum lift of 1.24, the drawdown at Well 1 is 46.1 m and the drawdown at Well 2 is 111.1 m for the minimize energy formulation; the drawdown at Well 1 is 13.7 m and the drawdown at

Well 2 is 143.7 m for the MINIMAX formulation. The relative difference in drawdown is -1.08 at Well 1 and 0.26 at Well 2 (Figure 3-9).

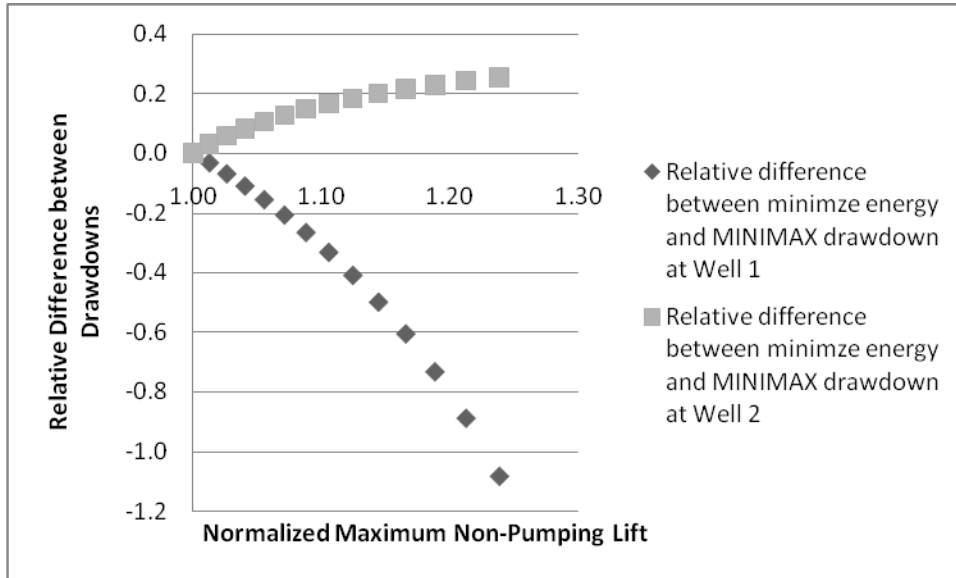


Figure 3-9. Relative difference between drawdowns for the two-well model

### 3.3.1.2 Twenty-well model

The 20-well model uses a water demand of  $1 \times 10^6 \text{ m}^3/\text{d}$ . The MINIMAX formulation is unable to equalize the lifts at small normalized maximum lifts in the 20-well model when using the lower demand that was used for the two-well model. The higher demand is used to examine the effect of greater variations in initial lifts among the wells. Limitations of the MINIMAX formulation are discussed more in a subsequent section.

When the ground surface and aquifer are parallel to each other, such that the non-pumping lifts are equal at all wells, MINIMAX gives the same results as the minimize energy formulation. As the slope of the ground surface deviates from that of the aquifer, causing greater variation in the non-pumping lifts, the MINIMAX formulation deviates from the minimize energy formulation. The percent error increases to 3.3% as the normalized maximum difference in non-pumping lift increases from 1.0 to 2.0 (Figure 3-10). The maximum relative difference in pumping at a single well increases to 0.49 (Figure 3-11) and the average relative difference increases to 0.25 (Figure 3-12).

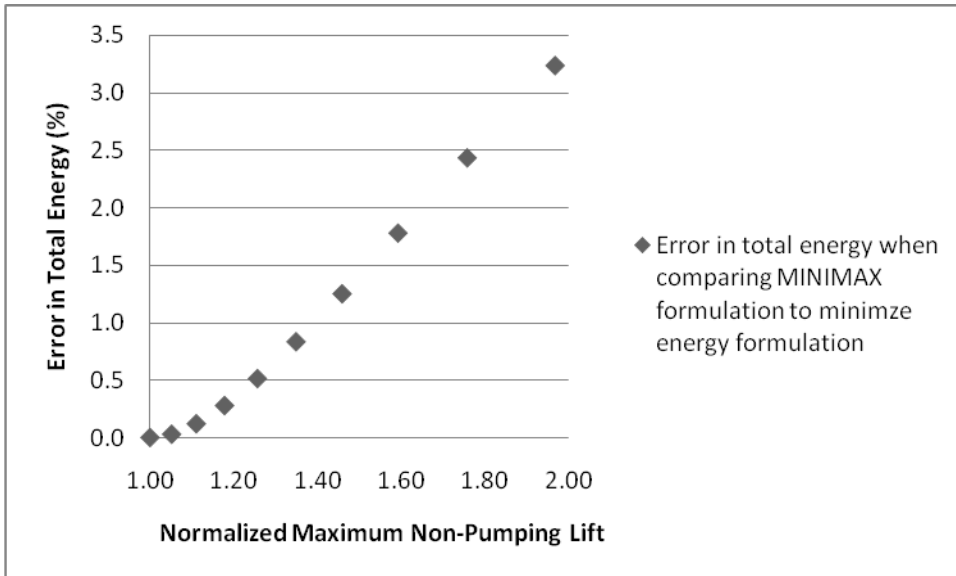


Figure 3-10. Percent error in total energy in MINIMAX formulation as compared to minimize energy formulation for the 20-well model

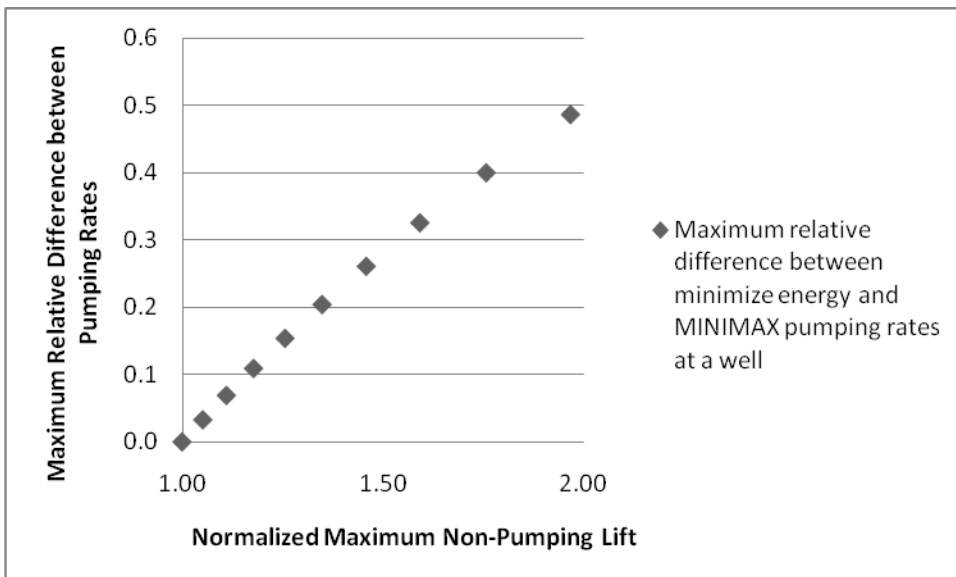


Figure 3-11. Maximum relative difference between pumping rates for the 20-well model

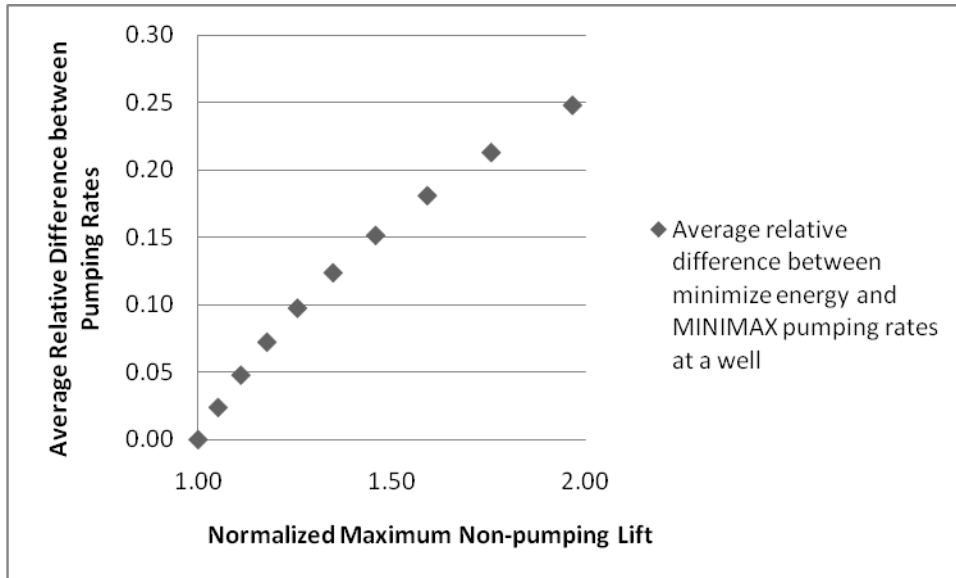


Figure 3-12. Average relative difference between pumping rates for the 20-well model

Under the equal non-pumping lifts condition, the pumping rates are distributed across the wells such that more water is pumped from the wells nearest the sources of water at the constant head boundaries on the western and eastern borders and less water is pumped from the wells located closer to the center of the aquifer (Figure 3-13). As the non-pumping lifts near the eastern border decrease, more water is withdrawn from the wells located in the eastern half of the aquifer and less water is withdrawn from the wells in the western half of the aquifer (Figure 3-14). As with the two-well case, the pumping distribution changes more with the MINIMAX formulation than with the minimize energy formulation, since the MINIMAX formulation must pump less where the initial lift is large and more where the initial lift is small in order to equalize the lift at each well.



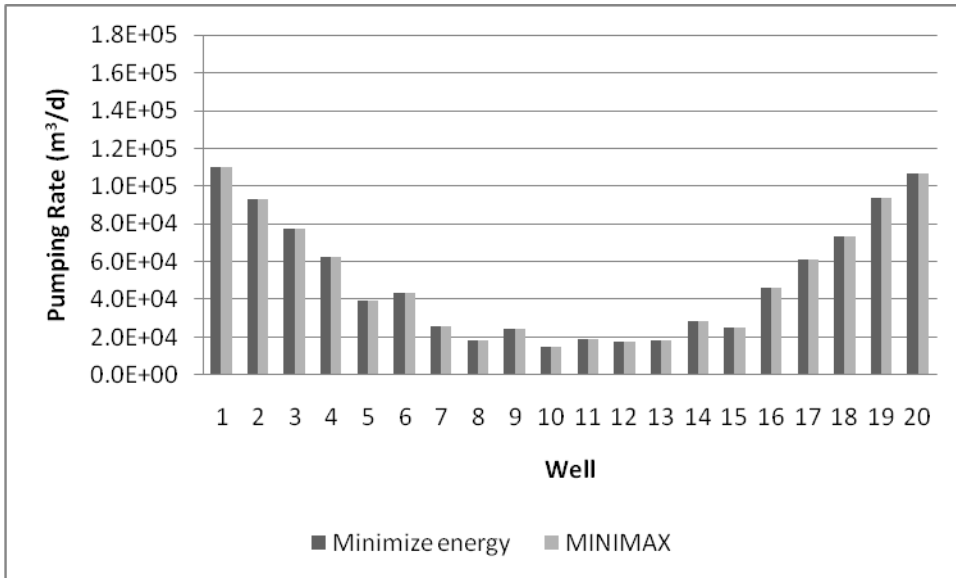


Figure 3-13. Comparison of minimize energy and MINIMAX pumping distributions from the 20-well model where the non-pumping lifts at each well are equal

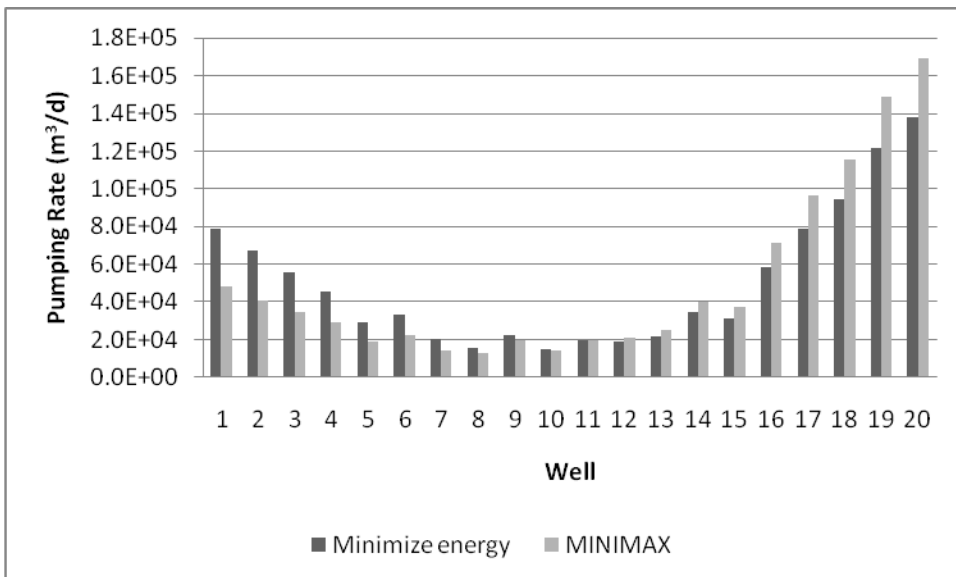


Figure 3-14. Comparison of minimize energy and MINIMAX pumping distributions from the 20-well model where the relative difference between non-pumping lifts is 1.97

When the land surface is horizontal, the drawdown at all wells for both the minimize energy and MINIMAX formulations is 383.0 m. As the slope of the ground surface deviates from that of the aquifer, the drawdowns in the wells located in the western portion of the domain decrease and the drawdowns in the wells located in the eastern portion of the domain increase for both formulations, as demonstrated in Figure 3-15 for the minimize energy formulation. At the normalized maximum lift of 2.0, the

drawdown at Well 1 is 296.0 m and the drawdown at Well 20 is 473.1 m for the minimize energy formulation; the drawdown at Well 1 is 209.1 m and the drawdown at Well 20 is 563.2 m for the MINIMAX formulation. The relative difference in drawdown is -0.34 at Well 1 and 0.17 at Well 20 (Figure 3-16).

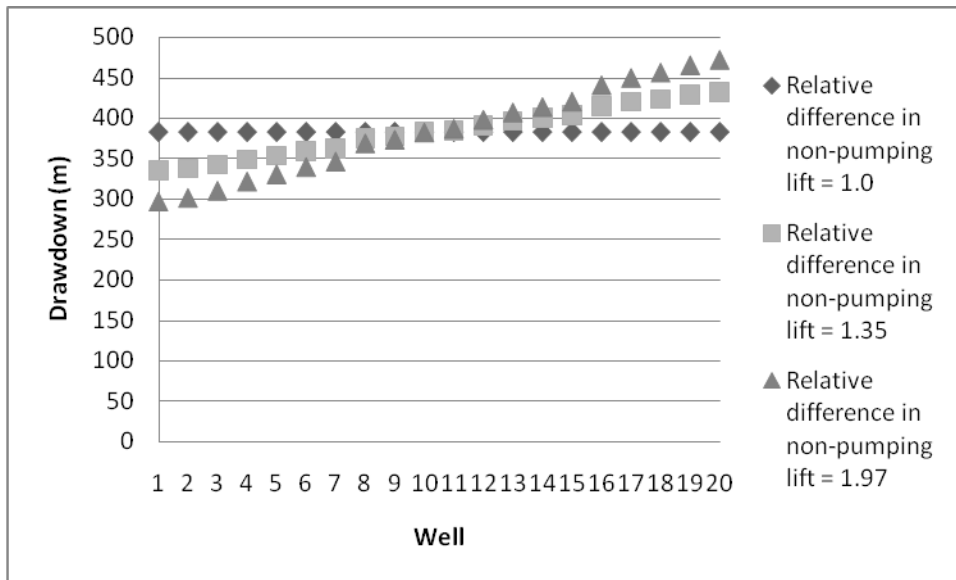


Figure 3-15. Examples of the change in drawdown across the domain as the ground surface slope changes; the drawdown decreases when the initial lift is increased and the drawdown increases when the initial lift is decreased

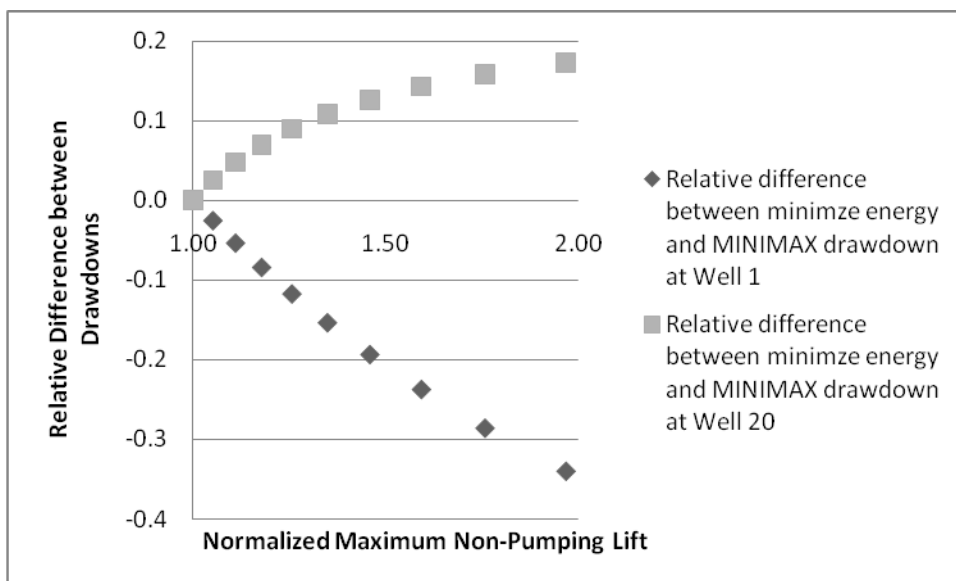


Figure 3-16. Relative difference between drawdowns for the 20-well model

### 3.3.1.3 Limitations of the MINIMAX formulation

When there is a large difference between the initial, non-pumping lifts, or when the demand is low, the demand may be insufficient to allow the optimization program to withdraw enough water to equalize the lifts at the wells. When this occurs, the MINIMAX formulation only pumps at some of the wells in order to minimize the maximum lift. Figure 3-17 through Figure 3-21 demonstrate how the pumping distribution and resulting lifts change with demand and normalized maximum non-pumping lift for the 20-well model. When the demand is  $4 \times 10^5 \text{ m}^3/\text{d}$ , pumping occurs at all wells and the lifts are all equal (Figure 3-17). As the demand decreases (Figure 3-18, Figure 3-19, and Figure 3-20), the pumping is distributed among fewer wells. The lift at the wells becomes more varied such that fewer locations have a lift equal to the value of the maximum lift. Figure 3-18, Figure 3-19, and Figure 3-20 demonstrate low demand cases where there is large variation in non-pumping lift. Comparing Figure 3-18 and Figure 3-21 shows that decreasing the normalized maximum lift can result in pumping from all of the wells and equal lifts at all wells when there had been pumping at only a few of the wells with the greater normalized maximum lift.

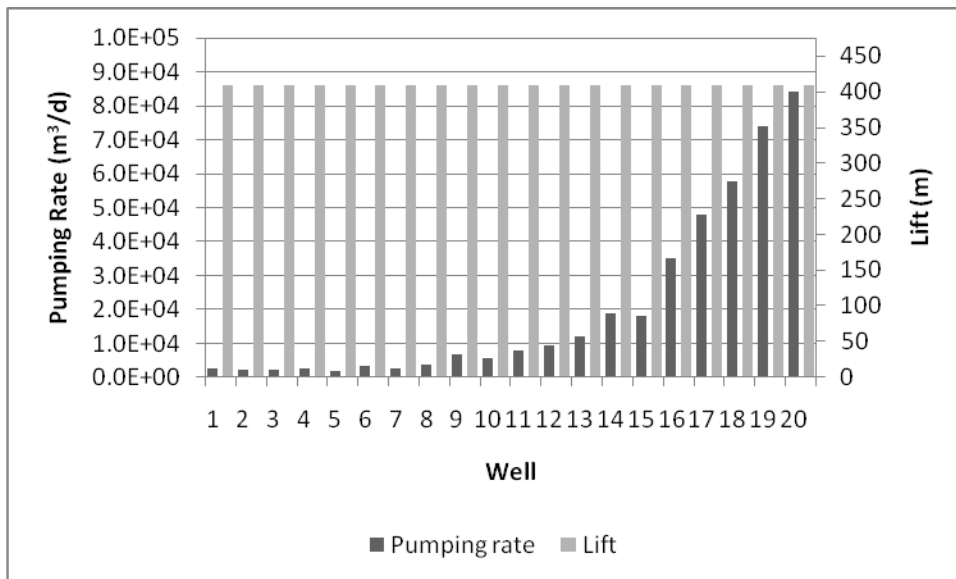


Figure 3-17. Pumping rate and lift resulting from the 20-well MINIMAX formulation with a normalized maximum non-pumping lift of 1.46 and a demand of  $4 \times 10^5 \text{ m}^3/\text{d}$

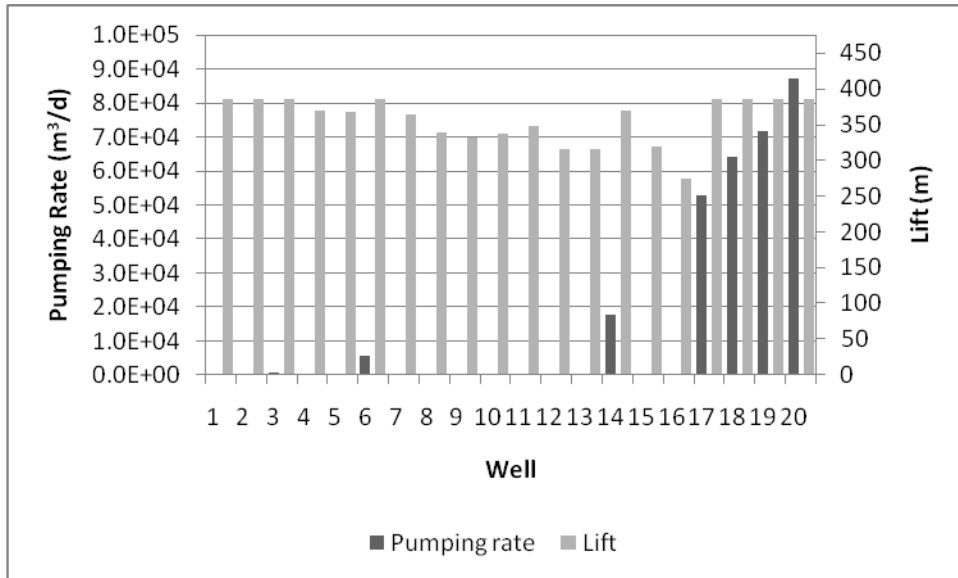


Figure 3-18. Pumping rate and lift resulting from the 20-well MINIMAX formulation with a normalized maximum non-pumping lift of 1.46 and a demand of  $3 \times 10^5 \text{ m}^3/\text{d}$

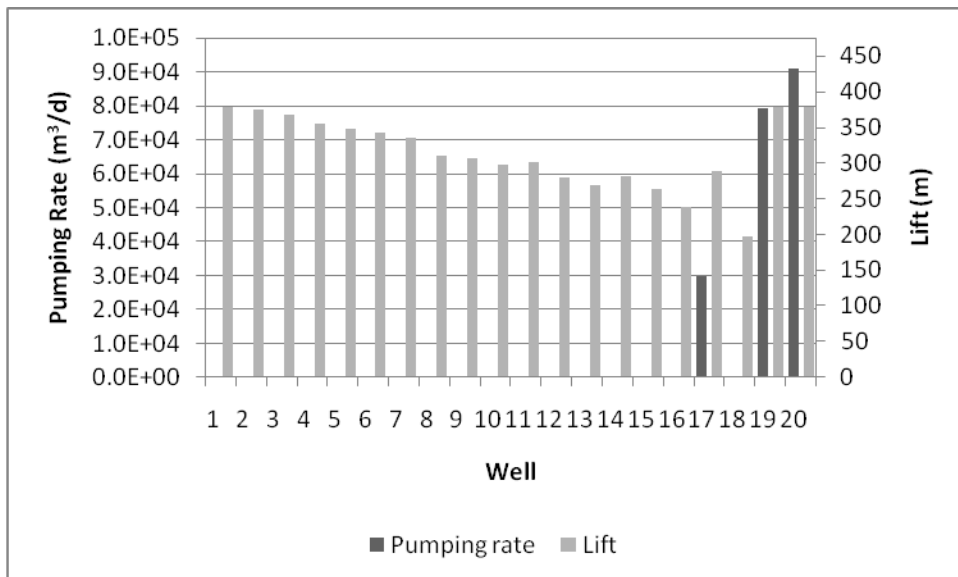


Figure 3-19. Pumping rate and lift resulting from the 20-well MINIMAX formulation with a normalized maximum non-pumping lift of 1.46 and a demand of  $2 \times 10^5 \text{ m}^3/\text{d}$

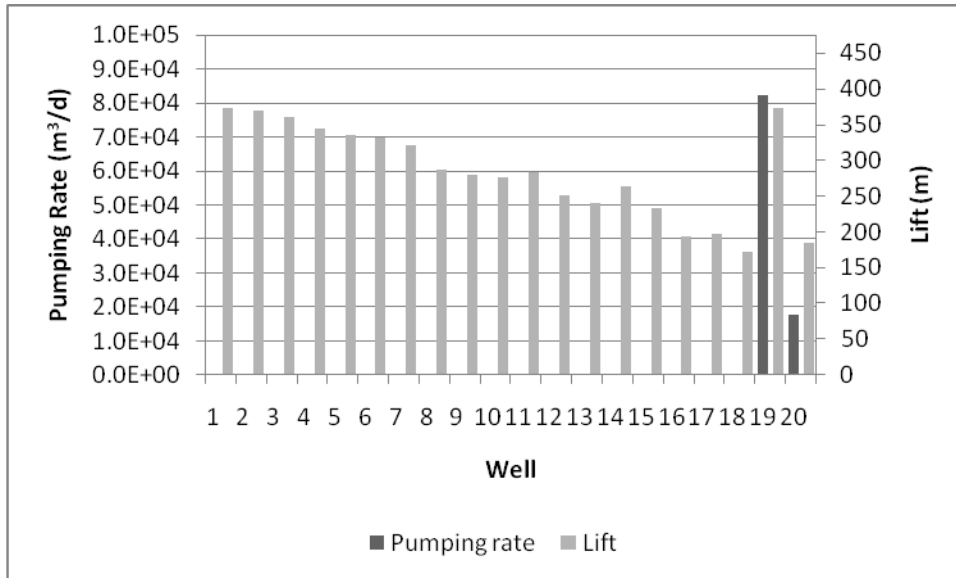


Figure 3-20. Pumping rate and lift resulting from the 20-well MINIMAX formulation with a normalized maximum non-pumping lift of 1.46 and a demand of  $1 \times 10^5 \text{ m}^3/\text{d}$

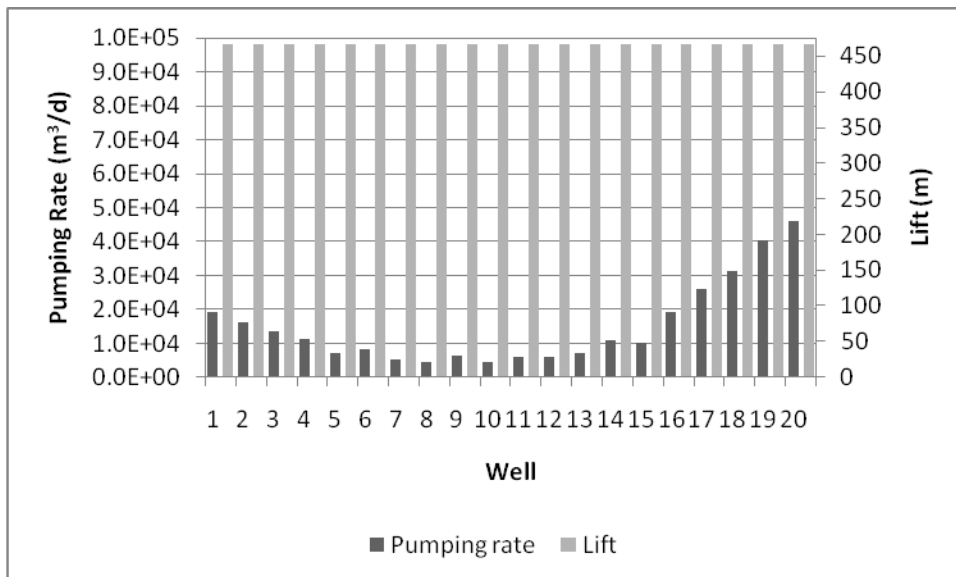


Figure 3-21. Pumping rate and lift resulting from the 20-well MINIMAX formulation with a normalized maximum non-pumping lift of 1.11 and a demand of  $3 \times 10^5 \text{ m}^3/\text{d}$

Although the MINIMAX formulation may provide results in cases of low demand or high variations in initial lift, the correlation of the MINIMAX results with the results of the minimize energy formulation are not predictable. The error in energy costs between the MINIMAX and minimize energy formulations in cases where the MINIMAX formulation does not result in equal lifts may be larger or smaller than cases where the MINIMAX formulation results in equal lifts.

### 3.3.2 Heterogeneity

The effect of heterogeneity across the aquifer was examined by varying the transmissivity in different regions of the aquifer. The transmissivity in the western half of the aquifer was changed from  $300 \text{ m}^2/\text{d}$  to  $400 \text{ m}^2/\text{d}$  and the transmissivity in the eastern half of the aquifer was changed from  $300 \text{ m}^2/\text{d}$  to  $200 \text{ m}^2/\text{d}$  (Figure 3-22). The model was otherwise unchanged from the 20-well scenario.

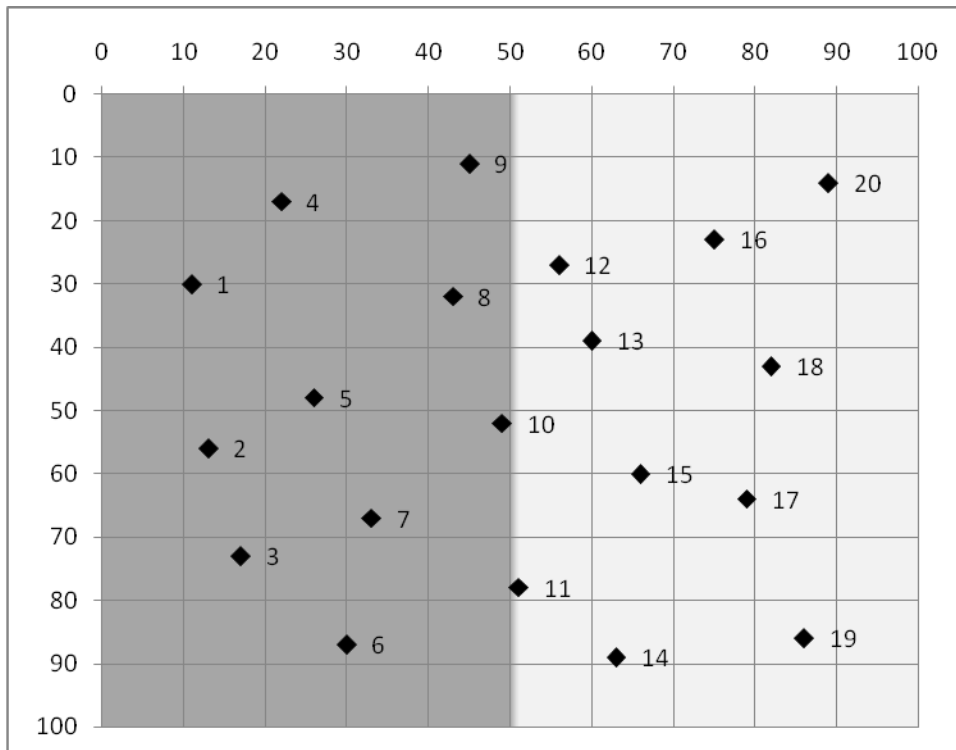


Figure 3-22. Test well model domain showing the western region with  $T=400 \text{ m}^2/\text{d}$  and the eastern region with  $T=200 \text{ m}^2/\text{d}$

As before, when the ground surface and the aquifer are parallel to each other, the minimize energy and MINIMAX formulations give the same results. For the case of varying transmissivities, more water is withdrawn from the region of the aquifer with the higher transmissivity (Figure 3-23). As the non-pumping lift in the lower transmissivity region decreases as compared to the lift in the higher transmissivity region, more water is withdrawn from the lower transmissivity region of the aquifer for both the minimize energy and the MINIMAX formulations. As with the homogeneous case, as the non-pumping lifts near the eastern border decrease, more water is withdrawn from the wells

located in the eastern half of the aquifer and less water is withdrawn from the wells in the western half of the aquifer (Figure 3-24 and Figure 3-25). However, less water is withdrawn from the wells in the eastern region for the heterogeneous case as compared to the homogeneous case due to the lower transmissivity in the eastern region for the heterogeneous case.

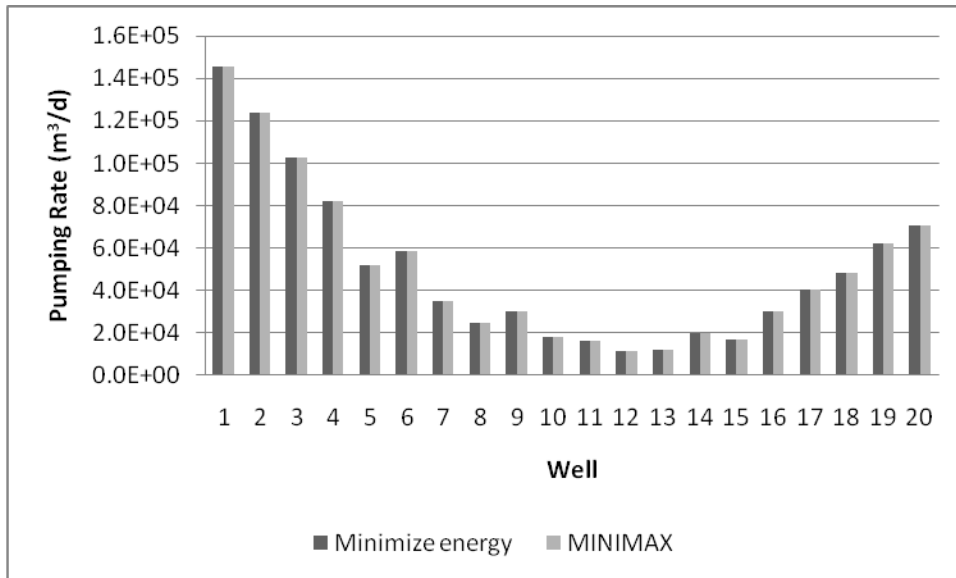


Figure 3-23. Comparison of minimize energy and MINIMAX pumping distribution under heterogeneous conditions where the non-pumping lifts at each well are equal

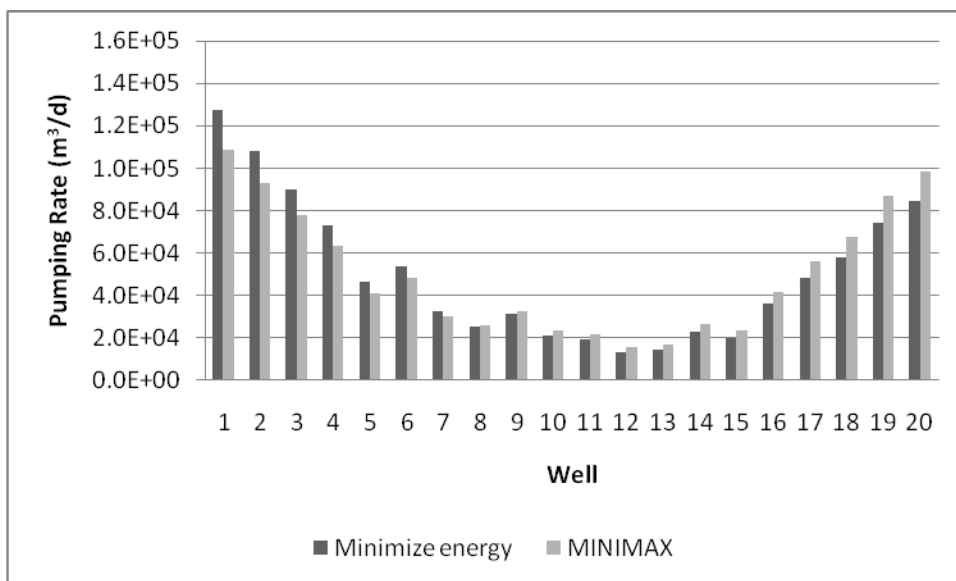


Figure 3-24. Comparison of minimize energy and MINIMAX pumping distribution under heterogeneous conditions where the relative difference between non-pumping lifts is 1.35

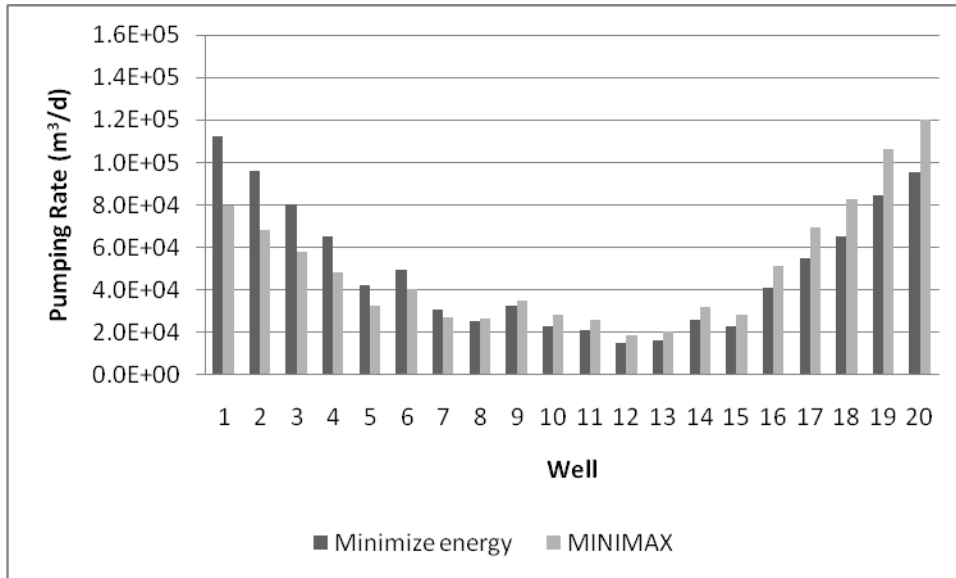


Figure 3-25. Comparison of minimize energy and MINIMAX pumping distribution under heterogeneous conditions where the relative difference between non-pumping lifts is 1.97

### 3.3.3 Unconfined aquifer

The single layer in the test model was converted from a confined aquifer to an unconfined aquifer in order to examine the application of the minimize energy and MINIMAX formulations to an unconfined aquifer. The optimization problem was solved using sequential linear programming. The aquifer thickness was increased to 400 m to prevent the groundwater flow process failing to converge. The same hydraulic conductivity of 3.0 m/d as used in the confined case with an aquifer thickness of 100 m was used for the unconfined aquifer. A demand of  $7.0 \times 10^5 \text{ m}^3/\text{d}$  for the 20-well scenario was used.

Although the minimize energy and MINIMAX formulations produce the same results for the confined case where the non-pumping lifts are equal, the unconfined case results in small differences between the results produced by the two formulations. By examining the results of the two optimization simulations, it has been determined that the differences in pumping rates and heads between the two formulations is due to the convergence criteria specified in the solution file. The heads resulting from the MINIMAX formulation were all equal, but the heads of the minimize energy formulation varied from well to well. The average percent difference of flow rates at given well between the two formulations is 0.04% and the average percent difference of the head at



a given well between the two formulations is 0.001%. Each iteration of the minimize energy formulation produced heads closer to those resulting from the MINIMAX formulation. Changing the convergence criteria from  $10^{-4}$  to  $10^{-6}$  for the minimize energy formulation requires 39 iterations instead of 10 iterations and produces heads that are closer to those produced by the MINIMAX formulation; the average percent difference of the head at a given well between the two formulations is 0.0004% with the smaller convergence criteria. Since the differences between the results of the minimize energy and MINIMAX formulations are very small and are due to the convergence criteria of the SLP solver, it can be said that the minimize energy and the MINIMAX formulations produce the same results for the case with equal non-pumping lifts.

A confined model using the same parameters as the unconfined model was constructed in order to compare the unconfined results with the confined results for the case with equal non-pumping lifts. The pumping distribution was very similar between the unconfined and the confined models (Figure 3-26). There was an average difference of 0.06% between the confined and unconfined results produced by the minimize energy formulation and an average difference of 0.02% between the confined and unconfined results produced by the MINIMAX formulation. The drawdown in the unconfined aquifer was greater than that in the confined aquifer (Figure 3-27). The drawdown in the unconfined aquifer was 74 m and the drawdown in the confined aquifer was 67 m. More energy is required to pump from the unconfined aquifer than from the confined aquifer as a result of the greater drawdown. For this example, pumping from the unconfined aquifer requires 1.5% more energy than pumping from the unconfined aquifer.

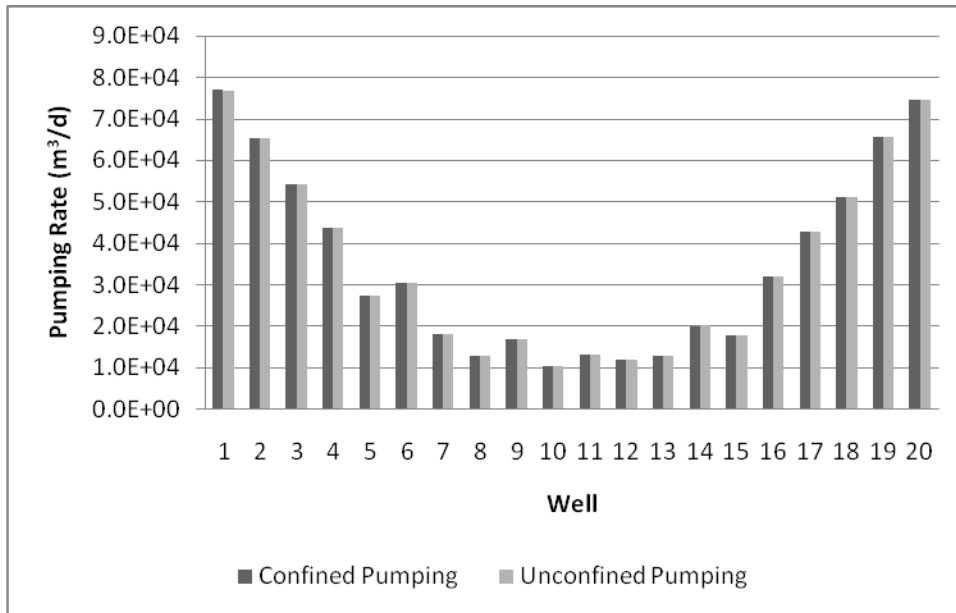


Figure 3-26. Pumping distribution of the unconfined and confined equal non-pumping lifts cases resulting from the minimize energy formulation

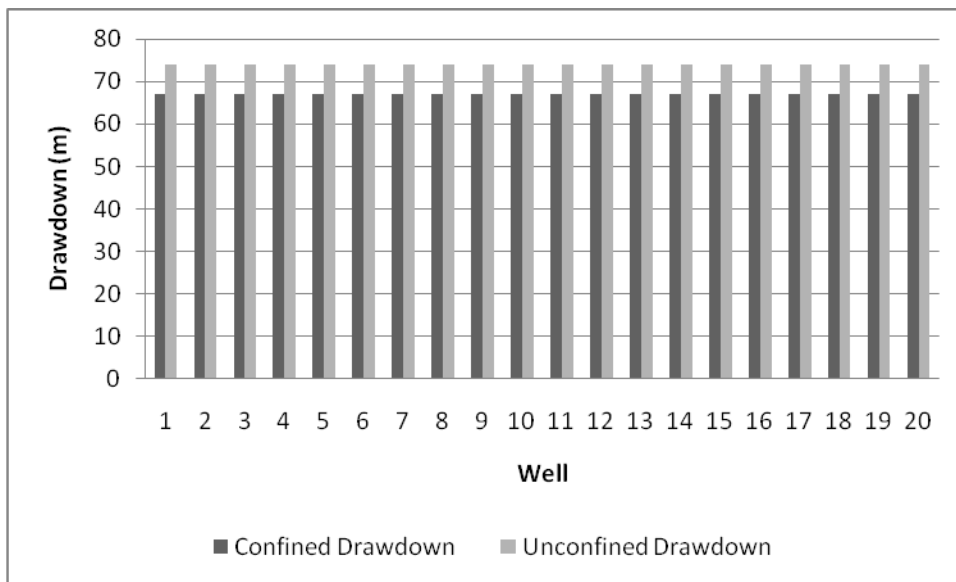


Figure 3-27. Drawdown distribution of the unconfined and confined equal non-pumping lifts cases resulting from the minimize energy formulation

As the slope of the ground surface deviates from that of the aquifer, causing greater variation in the non-pumping lifts, the MINIMAX formulation deviates from the minimize energy formulation. The percent error increases to 3.0% as the normalized maximum difference in non-pumping lift increases from 1.0 to 1.2 (Figure 3-28). The maximum relative difference in pumping at a single well increases to 1.4 (Figure 3-29)

and the average relative difference increases to 0.53 (Figure 3-30). The demand is insufficient for the MINIMAX formulation to be able to withdraw enough water to equalize the lifts at all wells when the normalized maximum lift is greater than 1.2 for this case.

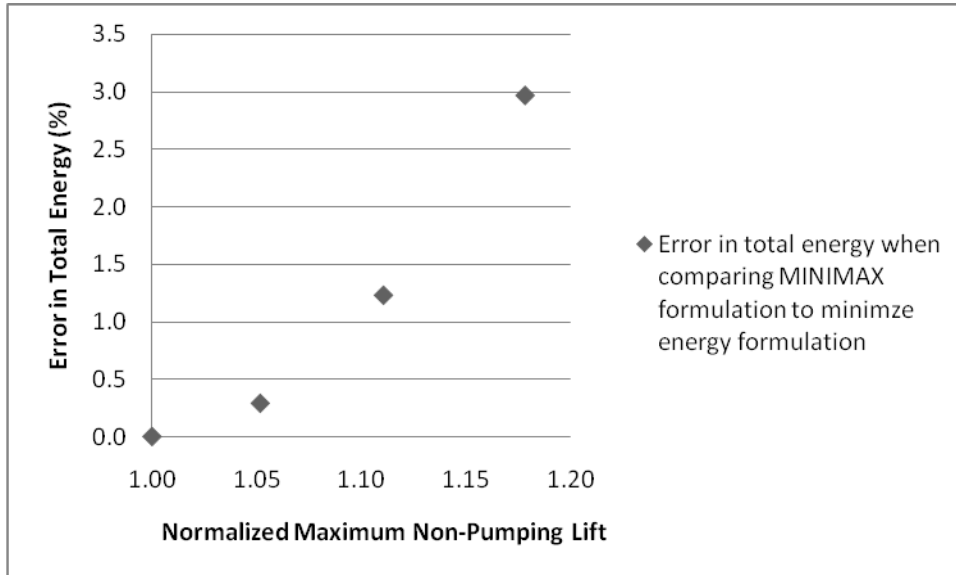


Figure 3-28. Percent error in total energy in MINIMAX formulation as compared to minimize energy formulation for the 20-well, unconfined model

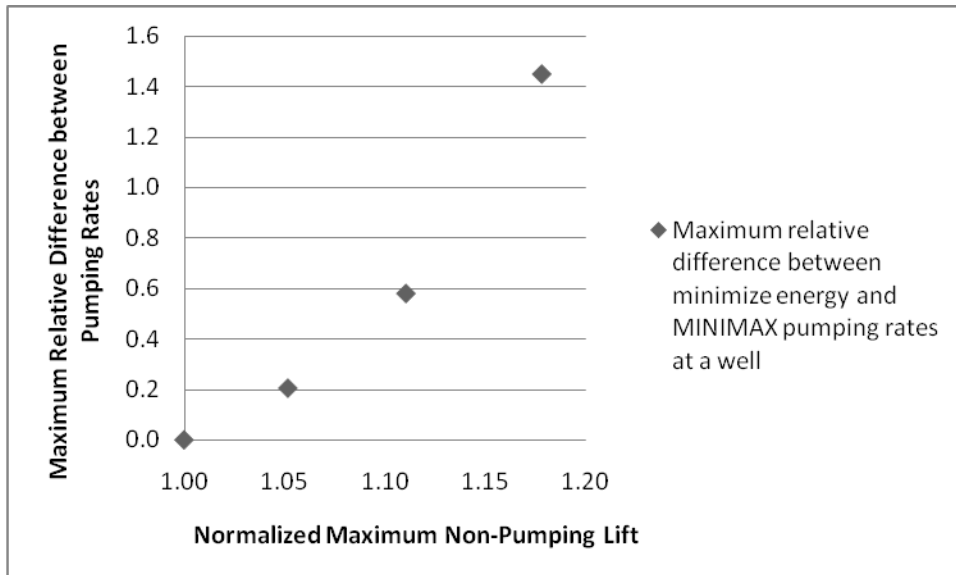


Figure 3-29. Maximum relative difference between pumping rates for the 20-well, unconfined model

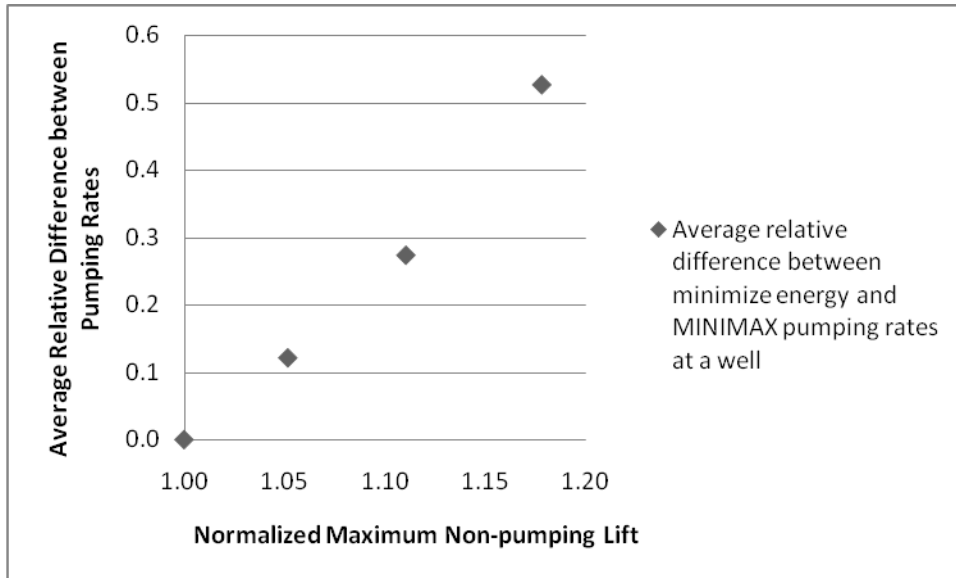


Figure 3-30. Average relative difference between pumping rates for the 20-well, unconfined model

Under the equal non-pumping lifts condition, the pumping rates are distributed across the wells such that more water is pumped from the wells nearest the constant head boundaries on the western and eastern borders and less water is pumped from the wells located closer to the center of the aquifer (Figure 3-31). As the non-pumping lifts near the eastern border decrease, more water is withdrawn from the wells located in the eastern half of the aquifer and less water is withdrawn from the wells in the western half of the aquifer (Figure 3-32). The pumping distribution changes more with the MINIMAX formulation than with the minimize energy formulation.

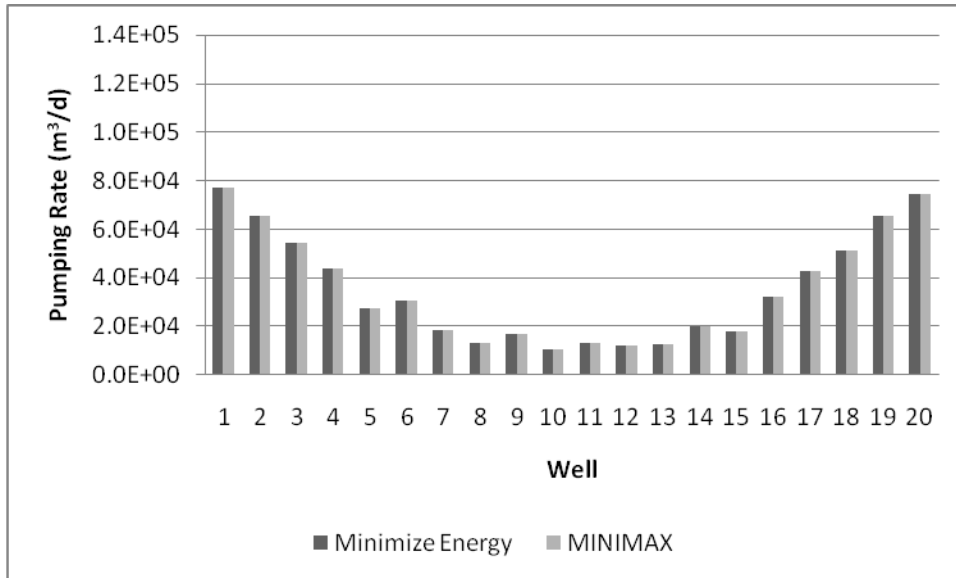


Figure 3-31. Comparison of minimize energy and MINIMAX pumping distribution from the unconfined aquifer where the non-pumping lifts at each well are equal

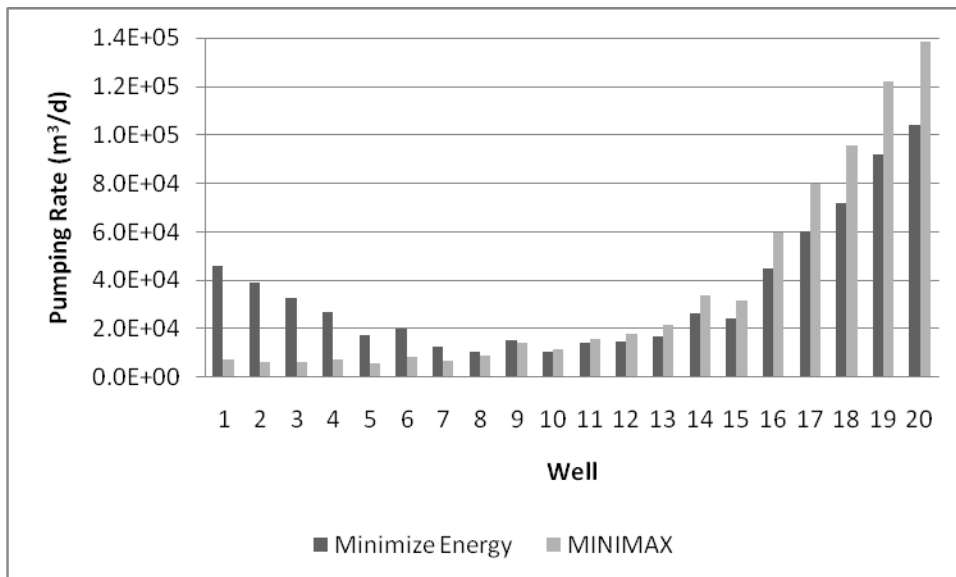


Figure 3-32. Comparison of minimize energy and MINIMAX pumping distribution from the unconfined aquifer where the relative difference between non-pumping lifts is 1.2

The differences between the results from the MINIMAX and minimize energy formulations increase faster with variation in non-pumping lift for the unconfined case than for the confined case. For the unconfined case, the MINIMAX formulation must distribute more pumping to areas with lower lifts than for the confined case due to the greater drawdown that occurs in the unconfined aquifer as compared to the confined aquifer.

### **3.4 Conclusions from the test models**

From these test cases, it has been determined that the MINIMAX formulation can be an acceptable substitute for the minimize energy formulation when there are only small variations among initial lifts and when the demand is sufficiently large that all wells are pumping for the MINIMAX formulation. The MINIMAX formulation provides the same results as the minimize energy formulation when the non-pumping initial lifts at each well are the same regardless of whether the aquifer is confined or unconfined, homogeneous or heterogeneous. If the aquifer is confined, the ground surface and the piezometric surface can both slope; only the difference in slope matters. Due to the larger drawdown that occurs in unconfined aquifers as compared to confined aquifers, the error between the MINIMAX and the minimize energy formulations increases faster with increasing variation in non-pumping lift than occurs for confined aquifers.

## **4 Antelope Valley Case Study**

The capabilities of the minimize energy formulation were further tested by applying it to the Antelope Valley region of California. This region was used to test the formulation with a large, multi-well field, transient problem. Section 4.1 contains a site description of Antelope Valley and section 4.2 contains a literature review of previous groundwater modeling work involving Antelope Valley. Sections 4.3 through 4.6 describe the application and results of using the minimize energy and MINIMAX formulations with the Antelope Valley case study.

### **4.1 Site description**

Antelope Valley is located in California in the western corner of the Mojave Desert, 50 miles northeast of Los Angeles (Figure 4-1). It is bounded by the Tehachapi Mountains to the northwest, the San Gabriel Mountains to the southwest, and low-lying hills to the north and east, creating a topographically-closed valley. Altitudes in the valley range from 3500 feet near the foothills to 2270 feet at the playas. The surrounding mountains have elevations as great as 10,064 feet. (Leighton and Phillips 2003)

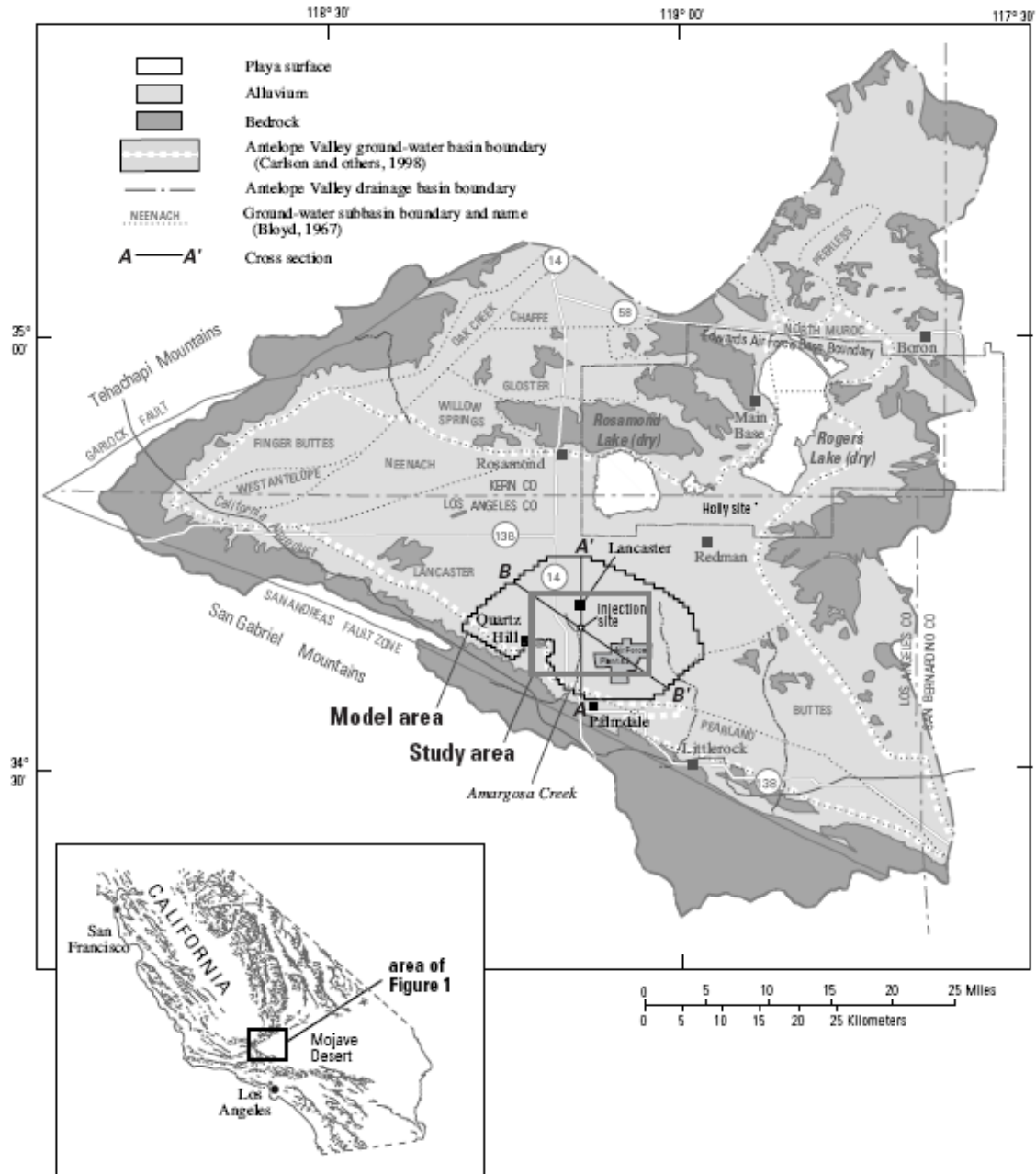


Figure 4-1. Map showing the location of Antelope Valley and the model domain. Figure from Phillips et al. (2003)

The Antelope Valley groundwater basin was defined by Carlson et al. (1998). It covers an area of 940 square miles. The hydrology of the area was first mapped by Johnson (1911) and then by Thompson (1929). The basin contains seven subbasins based on geologic features, water levels, faults, and other groundwater divides (Thayer 1946; Bloyd 1967; Durbin 1978; Carlson and Phillips 1998; Carlson et al. 1998; Nishikawa,



Rewis, and Martin 2001; Metzger, Ikehara, and Howle 2002; Leighton and Phillips 2003; Phillips et al. 2003). Historically, the groundwater system has been portrayed as two aquifers: an upper, unconfined aquifer separated from a lower, deep aquifer by lacustrine deposits (Durbin 1978). More recently, the groundwater system has been divided into three aquifers based on the age of the deposits as well as hydrologic properties and depths of unconsolidated deposits (Leighton and Phillips 2003). The upper aquifer is partially confined and partially unconfined and includes all portions of the system above approximately 1950 ft above sea level; the middle aquifer is confined and ranges from approximately 1550 ft to 1950 ft; the lower aquifer is confined and consists of the elevations between the bedrock and 1550 ft.

Antelope Valley has an arid to semiarid climate. The average annual precipitation at the Lancaster Flight Service Station was 7.6 in/year between 1974 and 2008 with a low of 1.85 inches in 1990 (Western Regional Climate Center). Pan evaporation rates have been measured at 114 in/year (Leighton and Phillips 2003). The low amounts of precipitation along with high evapotranspiration rates results in negligible recharge to the groundwater from direct precipitation. As such, the only significant source of natural recharge is infiltration of precipitation runoff from the surrounding mountains. Other sources of recharge include irrigation return flow and infiltration of reclaimed treated wastewater. Discharge is primarily from groundwater extraction. Groundwater pumping peaked in 1951 at 395,000 ac-ft and had a post-development low of 70,600 ac-ft in 1990. The decrease in groundwater pumping prior to 1990 was due to decreases in agricultural demand and importation of water from the California State Water Project. The increase in demand after 1990 was due to increased urban growth and the associated demand. Prior to development, which began around 1915, discharge was primarily from evapotranspiration. After development, the groundwater levels dropped due to groundwater extraction, leading to minimal discharge via evapotranspiration (Leighton and Phillips 2003).

The water table was less than 50 ft below the land surface in most of the Lancaster subbasin and less than 200 feet below the ground surface in the western and southern portions of the subbasin prior to development. Groundwater extraction has exceeded natural recharge since the 1920s, resulting in a decline in groundwater levels to

more than 100 ft below the ground surface. In the eastern and western portions of the Lancaster subbasin where agricultural pumping is concentrated, the water table has declined to 200 to 300 feet below the surface; near Palmdale, where most of the public supply pumping occurs, the water table has declined to 500 ft below the ground surface. (Leighton and Phillips 2003)

Substantial land subsidence has resulted from the groundwater level decline. Land subsidence is caused by compaction of compressible sediments due to declines in groundwater levels. Land subsidence of 6 ft has been observed in Lancaster between 1930 and 1992 and at least 1 ft of land subsidence has been observed in 290 square miles of Antelope Valley (Ikehara and Phillips 1994). More recent research has shown that the land subsidence is continuing to occur (Galloway et al. 1998).

More than half of the water used in Antelope Valley is currently imported from northern California via the California State Water Project (SWP). Part of the groundwater management plan involves injecting treated water from the SWP into the aquifer during low demand winter months for extraction and use during the higher demand summer months. The purpose of the injection program is to stop the decline of groundwater levels and to avoid land subsidence while meeting groundwater demands. Pilot-scale tests of injection have been conducted using existing wells in Lancaster that show that injection is hydraulically feasible (Phillips et al. 2003).

#### **4.2 Literature review of previous Antelope Valley models**

Extensive testing and monitoring have been conducted in Antelope Valley. The collected data have been used to create numerical models of the Antelope Valley groundwater basin. Models created previous to this study are described below. A simulation and subsidence model of the entire groundwater basin was created by Leighton and Phillips (2003). A simulation and an optimization model of a smaller portion of the groundwater basin surrounding Lancaster was created by Phillips et al. (2003) and modified by Baro-Montes (2007). The optimization models were used to examine the effects of injecting water from the SWP into the aquifer.

#### **4.2.1 Antelope Valley groundwater basin model**

The Antelope Valley groundwater basin model (AV model) is a simulation and land subsidence model of the Antelope Valley groundwater basin (Leighton and Phillips 2003). It uses the US Geological Survey's modular three-dimensional finite difference groundwater flow model, MODFLOW (McDonald and Harbaugh 1988). The Interbed Storage 1 (IBS1) Package (Leake and Prudic 1991) is used along with basic MODFLOW code to simulate aquifer-system compaction and land subsidence. The Horizontal Flow Barrier (HBF) Package (Hsieh and Freckleton 1993) is used to simulate the effect of horizontal barriers to groundwater flow.

The AV model is discretized using 43 rows and 60 columns, with each cell having one-mile long sides (Figure 4-2). The model has three layers, representing the upper, middle, and lower aquifers. There are 2083 active cells: 921 in layer 1, 626 in layer 2, and 536 in layer 3. The temporal discretization uses 81 stress periods of one year. The model is calibrated using 1915 water levels for steady-state conditions and 1915-1995 water levels and subsidence data for transient-state conditions. (Leighton and Phillips 2003)

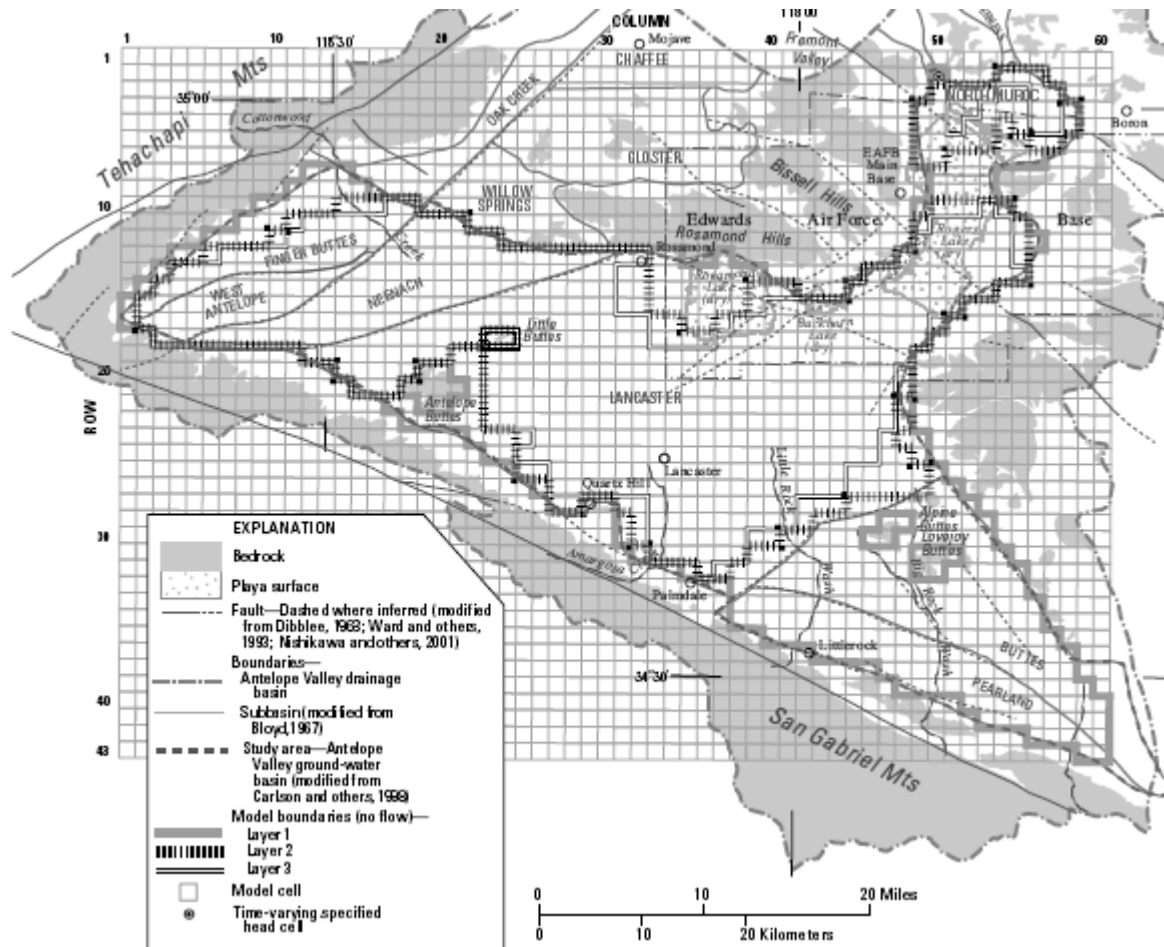


Figure 4-2. AV model grid and boundaries, from Leighton and Phillips (2003)

The results of the calibrated model showed that groundwater storage declined by more than 8.5 million ac-ft from 1915 to 1995 due to compaction and groundwater extraction from storage. During the period of peak pumping (1949-1953), 79% of the extracted groundwater came from storage; during the last five years of the simulation (1991-1995), 17% of the extracted groundwater came from storage. (Leighton and Phillips 2003)

The AV model was used to examine the effects of two pumping scenarios on the groundwater basin between the years of 1995 and 2025. In Scenario 1, the annual pumping remained the same as it was for 1995. This scenario resulted in water levels rising in areas where there had been much greater historical agricultural pumping and water levels declining and subsidence continuing where pumping for public supply was concentrated. In Scenario 2, the public supply increased 3.3% annually compared to 1995

and agricultural pumping and irrigation return flows were 75% greater than 1995 levels. This scenario resulted in significant water level declines of 150 ft in the south-central portion of the basin and an additional 5 ft of subsidence in the central portion of the basin. (Leighton and Phillips 2003)

#### **4.2.2 Lancaster flow simulation model**

The Lancaster groundwater subbasin flow simulation (LAN) model (Phillips et al. 2003) has a smaller domain than the AV model, encompassing an 11 mile by 19 mile area surrounding the injection pilot study site. Subsidence is not simulated in this model because further subsidence is not considered an acceptable outcome. Water level constraints are used to avoid additional subsidence. MODFLOW is used with the PCG2 numerical solver (Hill 1990).

The model is discretized using a variable cell size grid with 77 rows and 101 columns (Figure 4-3). Rows 1, 2, and 75-77 and columns 1-3 and 99-101 are inactive. Small cells (approximately 100 ft on each side) are used near the injection site, with cell size increasing by a factor of 1.1 with distance from the injection site to a maximum dimension of approximately 1980 ft. The variable grid is used due to the availability of densely spaced data near the injection site during the pilot testing; the data are more sparsely spaced as the distance from the injection wells increases. The model has two layers, representing the upper and middle aquifers. The lacustrine unit acts as a no-flow barrier between the lower aquifer and the upper and middle aquifers. Layer 1 contains no-flow boundaries on the northwest, southwest, and eastern borders; specified flux boundaries on the southeaster border; and specified head boundaries on the northern border of the domain. All of the lateral boundaries in layer 2 are no-flow boundaries. (Phillips et al. 2003)

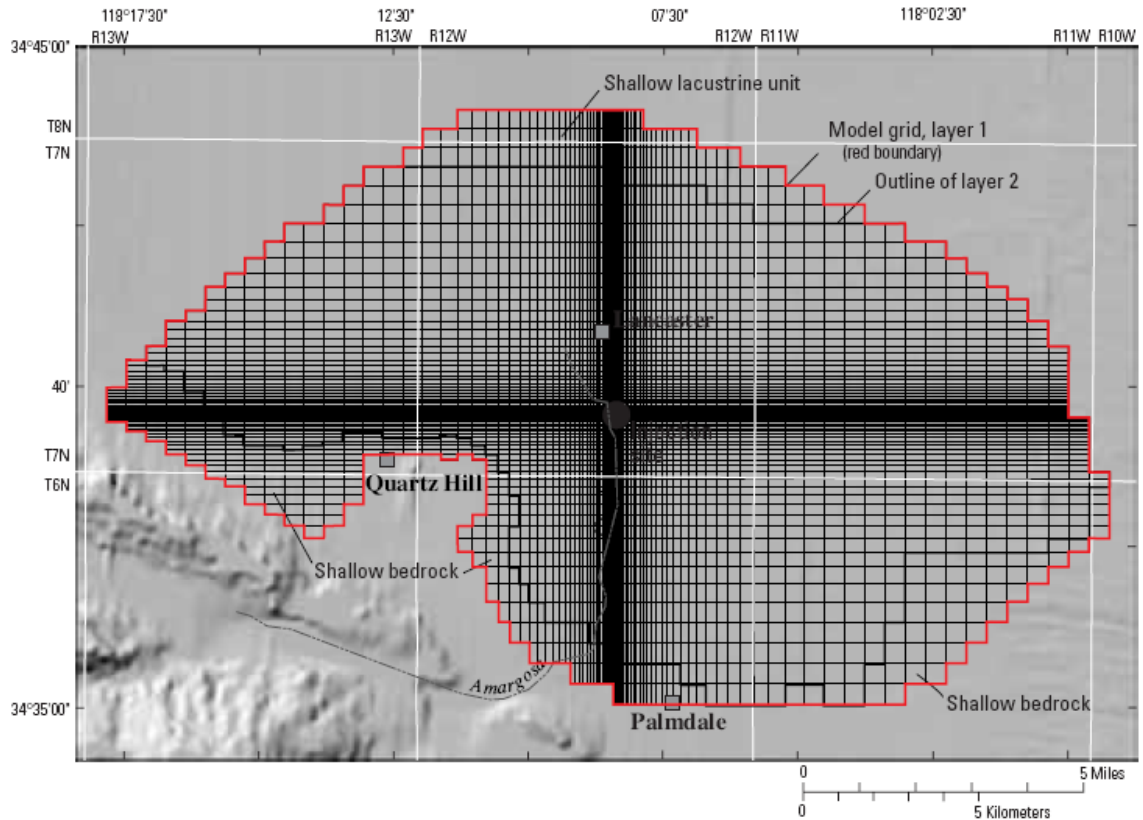


Figure 4-3. Active region of the LAN model grid, in the Lancaster subbasin of Antelope Valley; figure from Phillips et al. (2003)

Sources of recharge (Table 4-1) include contributions from runoff from the surrounding mountains, interbasin flow, agricultural return flow, and infiltration of treated wastewater. Approximately 4100 ac-ft/year of recharge is contributed from Amargosa Creek and other streams. Agricultural recharge is assumed to be 30% of the total amount of water used for irrigation. Reclaimed wastewater ponds contribute approximately 8000 ac-ft/year of recharge. Interbasin flow from the southeastern boundary contributes approximately 7650 ac-ft/year. The northern boundary straddles a groundwater mound, which contributes 5130 ac-ft/year of recharge. Insignificant sources of recharge include upward flow from the lower aquifer, direct infiltration of precipitation, and urban sources. Discharge from the aquifer is only considered to occur through groundwater extraction. (Phillips et al. 2003)

Table 4-1. Sources of recharge to the LAN model

Source of Recharge		Amount (ac-ft/year)	Amount (cfd)	Amount (m <sup>3</sup> /d)
Infiltration	Amargosa Creek	2835	3.38E+05	9.58E+03
	Other streams	1300	1.55E+05	4.39E+03
Agricultural return flow **		--	--	--
Treated wastewater ponds		8000	9.55E+05	2.70E+04
Southeastern specified-flux boundary		7650	9.13E+05	2.59E+04
Northern specified-head boundary		5130	6.12E+05	1.73E+04
Total (without agricultural recharge)		24915	2.97E+06	8.42E+04

\*\* Agricultural recharge is assumed to be 30% of the total amount of water used for irrigation.

Calibrated parameters from the AV model were used as a starting point in the LAN model and adjusted during calibration. The Spring 1983 water levels were used to assign initial heads to every well both because of data availability and because 1983 occurs during the time between the agricultural decline and rapid urban expansion, thus representing quasi-steady-state conditions. The LAN model simulated the period of time between May 1993 and August 1998 with 185 stress periods of one month (30.4375 days). There were 15 time steps for each stress period with the length of each time step increasing by a factor of 1.2. Extraction and injection rates were defined for each stress period. The model was calibrated to simulate long-term and seasonal water levels. The calibrated model closely simulated conditions near the injection wells and reasonably simulated conditions farther away from the injection wells. (Phillips et al. 2003)

#### 4.2.3 Lancaster simulation/optimization model

The purpose of the Lancaster groundwater subbasin simulation/optimization (LANOPT) model (Phillips et al. 2003) is to aid in planning and managing a large-scale injection program in Antelope Valley for the purpose of maximizing heads throughout the aquifer to limit subsidence and stop declining water levels. The LAN model was modified and incorporated into a linear programming problem to optimize the injection program. MODMAN version 3.0 (Greenwald 1993) was used to formulate the optimization problem. MODMAN runs the MODFLOW-based groundwater flow problem multiple times to generate a response matrix. LINDO (Schrage 1991) was used





wells pump at predetermined rates and are not a part of the optimization problem. Determining the location of the wells is not part of the optimization problem. Multiple wells located in one cell are represented as one well. Each well or well group is simulated as four wells: separate wells are used for extraction and injection and separate wells are used for the upper and middle aquifers. Injection is only allowed during the injection period of each year; extraction is allowed from all wells throughout the entire year. (Phillips et al. 2003)

The objective of the model is to maximize the minimum head in the aquifer, in effect seeking to equalize the heads at all locations. Minimum head constraints are used to limit drawdown and to prevent subsidence in subsidence-prone areas. Maximum head constraints limiting the head to 100 ft below the ground surface are used to avoid high water table conditions. The amount of water extracted and injected at each well is constrained by the extraction and injection capacity of each well. The amount of water extracted must meet the groundwater demand for each year. The initial groundwater demand in 2000 is assumed to be the same as the demand during 1995. The initial demand increases linearly with time according to the assumed population growth rates. The increase in the urban demand is applied to all non-agricultural wells and the agricultural demand is assumed to remain steady at 1995 levels. The availability of water from the SWP is not considered; it is assumed that sufficient water will be available for injection. (Phillips et al. 2003)

Four hypothetical management scenarios were tested using the LANOPT model. Scenario 1 is not an optimization problem. It uses the present (1995) management without injection and without any increase in groundwater demand to test the sustainability of the current management. Scenario 2 uses only the existing wells for extraction and injection and allows injection during 6 months of the year. Scenario 3 uses the existing and proposed wells and allows injection during 6 months of the year. Scenario 4 uses the existing and proposed wells but only allows injection during 4 months of the year. Scenario 1 resulted in large drawdowns and the minimum heads specified for the other scenarios were violated at all locations. The LANOPT model was used to attempt to optimize the pumping distribution for the first scenario to meet those

head constraints, but no feasible solution was found. Feasible solutions were found for the three optimization scenarios. (Phillips et al. 2003)

#### **4.2.4 Lancaster simulation/optimization model using GWM**

The LANOPT model was modified for use with another computer program for optimization, Ground-Water Management (Baro-Montes 2007). The LANOPT files originally used MODFLOW-96 (Harbaugh and McDonald 1996) and were modified to run with MODFLOW 2000 (Harbaugh et al. 2000). The simulation period began in April 2000 and ended in March 2010 with 60 2-month stress periods so that there were 10 full withdrawal and injection cycles, beginning with a withdrawal period. The GWM model uses MF2K-GWM (Ahlfeld, Barlow, and Mulligan 2005) for the groundwater management process. There were no other changes or calibrations to the LANOPT model. Two optimization formulations were used to test the GWM program: maximizing pumping and maximizing the minimum head (MAXIMIN).

There are 10 managed wells (or well groups), designated as 9A, 9B, 9E, 15R, 22B, 27F, 27H, 27P, 30B, and 34N. The wells are represented as single, screened entities with specified fractions of water from each layer. Separate decision variables are used for the extraction and injection periods. Injection is only allowed during the injection periods and extraction is only allowed during the extraction periods. Only one flow rate per well per injection or withdrawal period is used, though the flow rate may change from year to year. As such, there are 20 decision variables per well and 200 decision variables total. (Baro-Montes 2007)

The objective of the maximize pumping formulation is to maximize the amount of water withdrawn from the aquifer. Maximizing pumping is achieved by maximizing the weighted sum of the decision variables, where pumping is maximized by applying positive cost coefficients to withdrawal flow variables and injection is minimized by applying negative cost coefficients to injection flow variables. As with the LANOPT model, upper and lower head bounds are used to prevent subsidence and high water table issues. Summation constraints are used for annual demands, creating linear relations between decision variables. The summation constraints only include flow variables active during withdrawal periods. (Baro-Montes 2007)

The objective of the MAXIMIN formulation is achieved by using head state variables that are linked to the objective function via external variables. The state variables are applied at the same locations as the wells at the end of each extraction and injection period, resulting in 200 state variables. To ensure that the effect of pumping is felt throughout the domain, 9 state variables were applied near the eastern border. A lower head bound was not used for this formulation since the objective was to maximize heads. (Baro-Montes 2007)

The upper layer was modeled both as unconfined and confined for the maximize pumping formulation. The sequential linear programming (SLP) algorithm available in GWM was used to minimize errors associated with the non-linearity resulting from the response of the unconfined aquifer to stresses (Ahlfeld and Mulligan 2000). The confined version of the upper aquifer was modeled using the linear programming algorithm available in GWM. The confined results were similar to the unconfined results; the confined model gives the largest amount of withdrawal, requires the least amount of injection and has a larger storage capacity than the unconfined version of the model. Since the upper layer is unconfined, the SLP unconfined version of the model was determined to be the most accurate (Baro-Montes 2007). Ahlfeld and Baro-Montes (2008) used this model with MF2K-GWM to further test the SLP algorithm to solve non-linear problems.

The results from the maximize pumping and MAXIMIN formulations both meet their objectives, showing that GWM can be used with large-scale, transient problems. Due to the nature of the formulations, the maximize pumping formulation withdraws more water than necessary and the MAXIMIN formulation limits the amount of water extracted from the aquifer to that required to meet the annual demands. (Baro-Montes 2007)

#### **4.3 Model description**

This project uses the model modified by Baro-Montes (2007). The input files were slightly modified so as to work with MF2005-GWM with the state variables and quadratic programming capabilities. As stated previously, this model has 37 rows and 60 columns, covering an area of approximately 200 square miles. The model uses two

layers, representing the upper and middle aquifers. Layer 1 contains no-flow boundaries on the northwest, southwest, and eastern borders; specified flux boundaries on the southeaster border; and specified head boundaries on the northern border of the domain. All of the lateral boundaries in layer 2 are no-flow boundaries. The model simulates 10 years using 60 2-month stress periods. Each year contains a six-month withdrawal period followed by a six-month injection period.

Groundwater is extracted during the summer months and is injected during the winter months using the 10 managed wells. The wells are designated as 9A, 9B, 9E, 15R, 22B, 27F, 27H, 27P, 30B, and 34N and are represented as single, screened entities with specified fractions of water from each layer. Some of the “managed wells” represent multiple wells that are located in the same cell. Figure 4-5 shows the locations of the managed wells. The 75 unmanaged wells provide year-round background pumping. The withdrawal from the managed wells required to meet the yearly demand comprises an average of 26% of the total withdrawal (Table 4-2). The amount of water required from the managed wells increases from 24% to 28% of the total demand over the ten years of the simulation. Water is injected using the ten managed wells as well; no water is injected using the unmanaged wells. A different demand is used than was used in Baro-Montes (2007) due to a calculation error that was discovered at the start of this project.

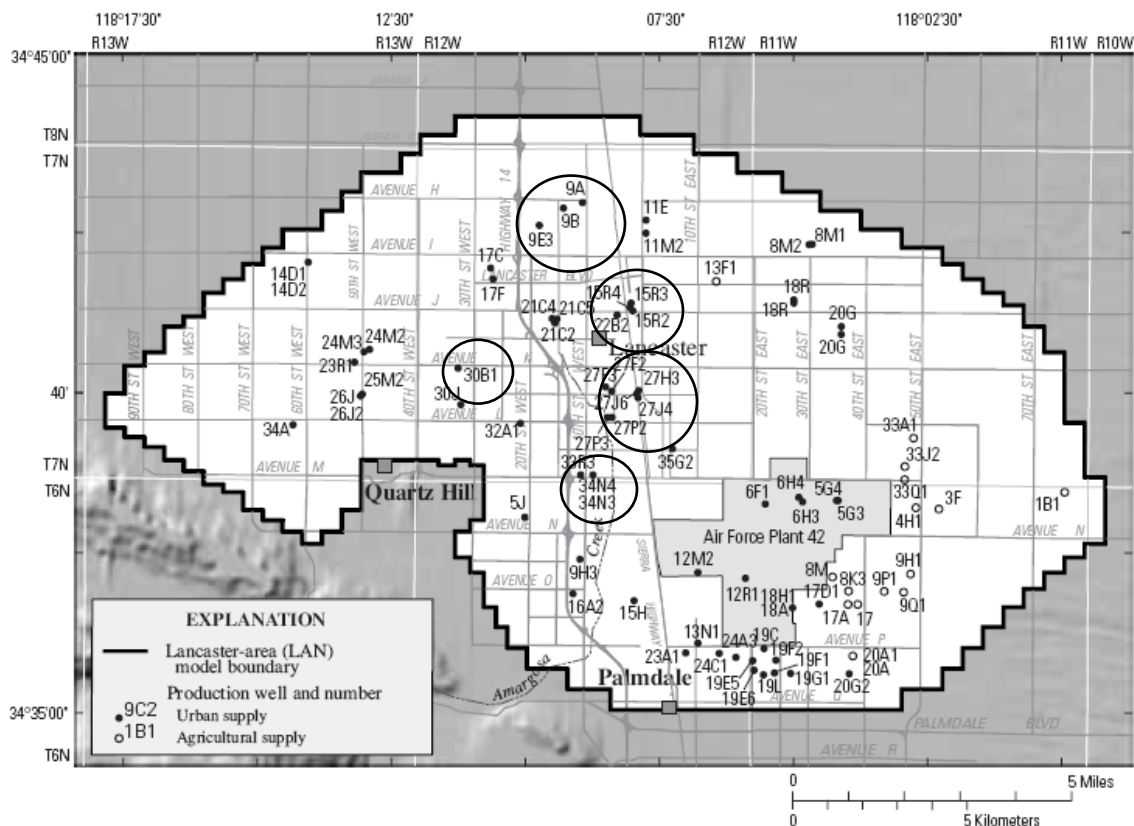


Figure 4-5. Map showing well locations as black dots; the managed wells are circled. Figure adapted from Phillips et al. (2003).

Table 4-2. Comparison of total and managed water demand for each year

Year	Total withdrawal, including managed demand		Demand that must be met by managed wells		Fraction of total
	cfd	m <sup>3</sup> /d	cfd	m <sup>3</sup> /d	
1	4.46E+06	1.26E+05	1.09E+06	3.07E+04	0.24
2	4.53E+06	1.28E+05	1.12E+06	3.19E+04	0.25
3	4.60E+06	1.30E+05	1.16E+06	3.30E+04	0.25
4	4.67E+06	1.32E+05	1.20E+06	3.41E+04	0.26
5	4.75E+06	1.34E+05	1.24E+06	3.52E+04	0.26
6	4.83E+06	1.37E+05	1.28E+06	3.63E+04	0.27
7	4.90E+06	1.39E+05	1.32E+06	3.74E+04	0.27
8	4.95E+06	1.40E+05	1.36E+06	3.86E+04	0.27
9	5.05E+06	1.43E+05	1.40E+06	3.97E+04	0.28
10	5.16E+06	1.46E+05	1.44E+06	4.08E+04	0.28

Separate decision variables are used for the extraction and injection periods. Injection is only allowed during the injection periods and extraction is only allowed during the extraction periods. Only one flow rate per well per injection or withdrawal

period is used, though the flow rate may change from year to year. There are 20 decision variables per well resulting in 200 decision variables for the entire model. There are 10 head state variables located at each managed well, one for the end of each injection period per year.

#### 4.4 Application of minimize energy formulation to the Lancaster subbasin

The minimize energy formulation minimizes the total energy required to extract water from the aquifer over the ten-year simulation period while meeting the water demand for each year. The amount of water injected into the aquifer in a given year is limited to the amount of water withdrawn by the managed wells in that year (Eq. 4.1).

$$\text{Minimize} \quad Z = \sum_t \sum_i Q_{i,t} (H_i - h_{i,t}(Q_{i,t})) \quad (\text{Eq. 4.1})$$

$$\text{such that} \quad \sum_i Q_{i,t} \geq D_t \text{ for each year}$$

$$\sum_i Q_{i,t} \geq \sum_i I_{i,t} \text{ for each year}$$

$$\text{and} \quad h_{i,t} \leq 2300 \text{ ft.}$$

An upper head bound of 2300 feet is used to avoid high water table conditions such as evapotranspiration and liquefaction.

Table 4-3 shows the total amount of water injected each year as determined in Scenario 2 of the LANOPT model, in which injection is allowed for six months of the year and only existing wells are used. The original proposal is used as the base condition to which the results of the minimize energy formulation are compared.

Table 4-3. Total injection for each year proposed by Scenario 2 of the LANOPT model

Year	Injection	
	cfd	m <sup>3</sup> /d
1	9.41E+05	2.66E+04
2	9.32E+05	2.64E+04
3	9.22E+05	2.61E+04
4	9.13E+05	2.59E+04
5	9.04E+05	2.56E+04
6	8.94E+05	2.53E+04
7	8.85E+05	2.51E+04
8	8.75E+05	2.48E+04
9	8.65E+05	2.45E+04
10	4.21E+05	1.19E+04

An alternative constraint on the amount of water injected into the aquifer is used to limit the amount of water injected into the aquifer each year to the amount that was injected in the original scenario. Under that constraint, the minimize energy formulation becomes

$$\text{Minimize} \quad Z = \sum_{i,t} Q_{i,t} (H_i - h_{i,t}(Q)) \text{ for each year} \quad (\text{Eq. 4.2})$$

$$\text{such that} \quad \sum_i Q_{i,t} \geq D_t \text{ for each year}$$

$$\sum_i I_{i,t} \leq \sum_i I_{i,t,LANOPT} \text{ for each year}$$

$$\text{and} \quad h_{i,t} \leq 2300 \text{ ft}.$$

This constraint is used to examine the results of the minimize energy formulation more closely.

By using the ground surface elevation at each well,  $H_i$ , in the minimize energy formulation, it is assumed that the water will be used locally and will not need to be pumped to higher elevations in order to be used. This assumption can be removed by using a uniform reference elevation,  $H$ , for all wells, representing the maximum elevation to which the water withdrawn from any of the wells would be pumped. Using a uniform reference elevation provides an upper bound on the energy required to pump the groundwater as determined by the minimize energy formulation; using the ground surface elevation provides a lower bound on the energy to pump the groundwater as determined by the minimize energy formulation. Using a uniform reference elevation, the minimize energy formulation becomes

$$\begin{aligned}
&\text{Minimize} && Z = \sum_t \sum_i Q_{i,t} (H - h_{i,t}(Q_{i,t})) && (\text{Eq. 4.3}) \\
&\text{such that} && \sum_i Q_{i,t} \geq D_t \text{ for each year} \\
&&& \sum_i Q_{i,t} \geq \sum_i I_{i,t} \text{ for each year} \\
&\text{and} && h_{i,t} \leq 2300 \text{ ft} .
\end{aligned}$$

#### 4.5 Results and discussion

The minimize energy formulation was tested by applying it to the Lancaster subbasin region of Antelope Valley, California. Seven scenarios are examined in the following sections. The pumping and injection distribution resulting from the LANOPT Scenario 2 (Phillips et al. 2003) is used as a surrogate for current operation practices to which the other scenarios are compared. The energy required for each scenario is determined by lifting the water to either the ground surface elevation or to the uniform reference elevation, as described in section 4.4. The LANOPT-GS scenario uses the pumping and injection rates from the LANOPT Scenario 2 results and the required energy is calculated by lifting the water to the ground surface. The MINENG-GS-GS1 scenario uses the minimize energy formulation in which the water is lifted to the ground surface and the energy is calculated by lifting the water to the ground surface at each well. The MINENG-GS-GS2 is the same as MINENG-GS-GS1 except that the injection is limited to that of the LANOPT scenario. The LANOPT-UE scenario uses the pumping and injection rates from the LANOPT Scenario 2 results and the required energy is calculated by lifting the water to a uniform elevation at each well. MINENG-GS-UE uses the pumping and injection distribution from MINENG-GS-GS1, but the energy is calculated by lifting the water to the uniform elevation. MINENG-UE uses the minimize energy formulation in which the water is lifted to a uniform elevation and the energy is also calculated using the uniform elevation. MINIMAX-UE uses the MINIMAX formulation, lifting the water to the uniform elevation. The scenarios are summarized in Table 4-4.



Table 4-4. Summary of scenarios used in the Antelope Valley case study

Scenario name	Source of pumping rates	Elevations used to calculate energy
LANOPT-GS	LANOPT Scenario 2 results	Ground surface elevations
MINENG-GS-GS1	Minimize energy formulation using ground surface elevations	Ground surface elevations
MINENG-GS-GS2	Minimize energy formulation using ground surface elevations, constraining the injection to the amount of water injected in the LANOPT scenario	Ground surface elevations
LANOPT-UE	LANOPT Scenario 2 results	Uniform elevation
MINENG-GS-UE	Minimize energy formulation using ground surface elevations	Uniform elevation
MINENG-UE	Minimize energy formulation using uniform elevation	Uniform elevation
MINIMAX-UE	MINIMAX formulation using uniform elevation	Uniform elevation

The spatial distribution of pumping and injection across the aquifer is examined by dividing the wells into three regions. Since the groundwater flow is primarily from north to south, the wells are assigned regions based on their locations. The northern region contains the wells designated as 9A, 9B, and 9E, the middle region contains the wells designated as 15R, 22B, and 30B, and the southern region contains the wells designated as 27F, 27H, 27P, and 34N (Figure 4-6). The total pumping and injection from each region is then averaged across the total number of wells in that region in order to compare the three regions.



distributions of the MINENG-GS-GS1 and MINENG-GS-GS2 scenarios use 25-30% of the energy required by the LANOPT-GS scenario. The LANOPT-GS scenario requires  $33.4 \times 10^6$  kWh of energy over the 10-year simulation to pump the groundwater. The MINENG-GS-GS1 optimization scenario requires  $8.89 \times 10^6$  kWh of energy over the 10-year simulation. The MINENG-GS-GS2 optimization scenario requires  $9.30 \times 10^6$  kWh of energy over the 10-year simulation. The energy requirements of both optimization scenarios increase by small amounts each year.

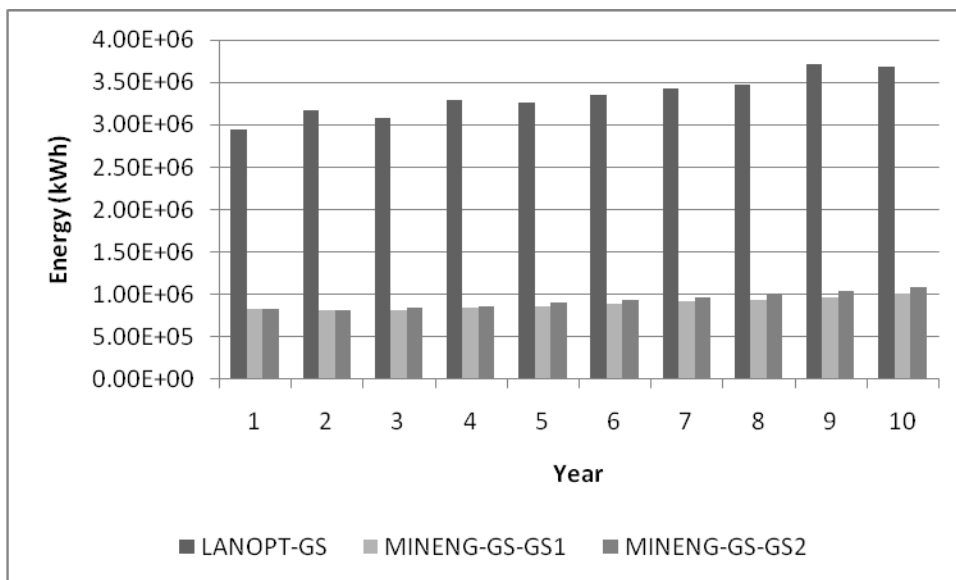


Figure 4-7. Total energy required for pumping for each year the LANOPT-GS, MINENG-GS-GS1, and MINENG-GS-GS2 scenarios

The MINENG-GS-GS1 scenario injects more water than the LANOPT-GS scenario (Figure 4-8). Excluding the final year of the simulation, the amount of water injected in the MINENG-GS-GS1 scenario as compared to the LANOPT-GS scenario increases by 16 to 61% over the first nine years (the last year shows a 211% increase, due to end effects of the simulation). However, the MINENG-GS-GS2 scenario demonstrates that limiting the injection in the minimize energy formulation to the injection of the LANOPT-GS scenario results in only a small increase in the total energy from the MINENG-GS-GS1 scenario to the MINENG-GS-GS2 scenario, as compared to the difference in energy requirements between the LANOPT-GS scenario and MINENG-GS-GS1 scenario. This indicates that, for the Lancaster subbasin, redistributing the pumping

and injection to better balance pumping and lift has more effect on minimizing the energy requirements to withdraw water from the aquifer than increasing the injection.

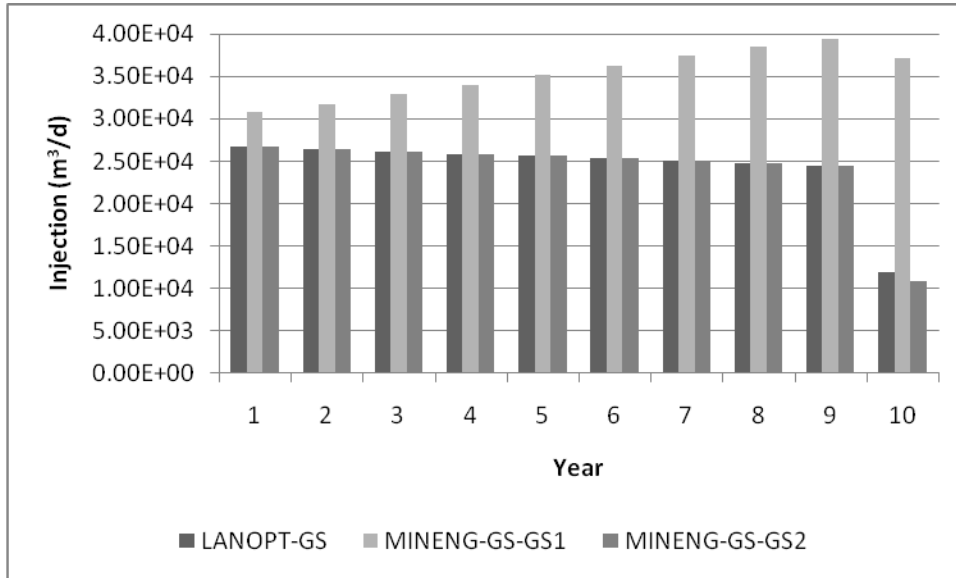


Figure 4-8. Total amount of water injected yearly in the LANOPT-GS, MINENG-GS-GS1, and MINENG-GS-GS2 scenarios

The pumping in the LANOPT-GS scenario is concentrated in the southern region (Figure 4-9). Over the 10-year simulation period, 20% of the total water demand is met by the three wells located in the northern region, 14% is met by the three wells in the middle region, and 66% is met by the four wells in the southern region.

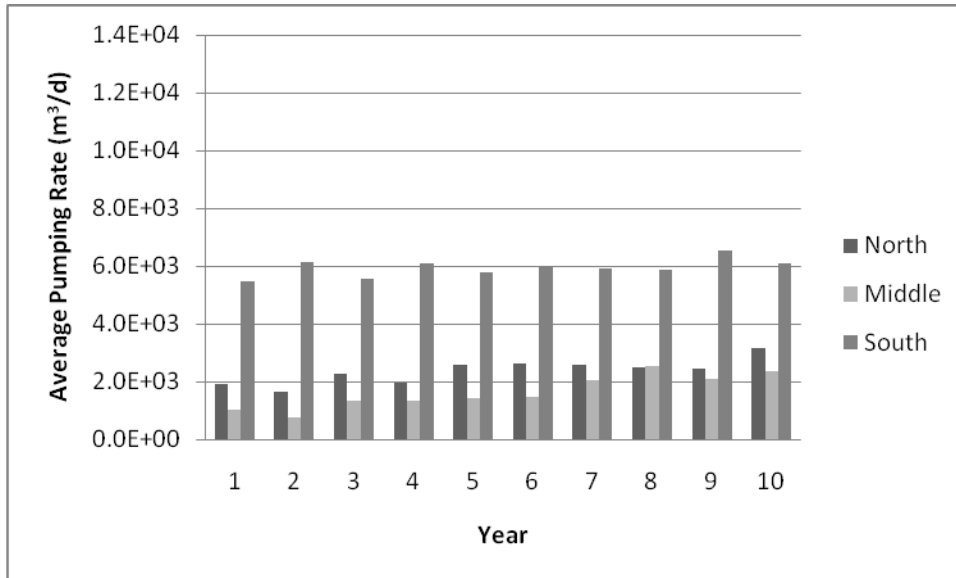


Figure 4-9. Distribution of pumping for the LANOPT-GS scenario

The injection in the LANOPT-GS scenario is more evenly distributed than the pumping. (Figure 4-10). Over the 10-year simulation period, 35% of the injected water is injected using the wells in the southern region, 35% is injected using the wells in the middle region, and 30% is injected using the wells in the northern region.

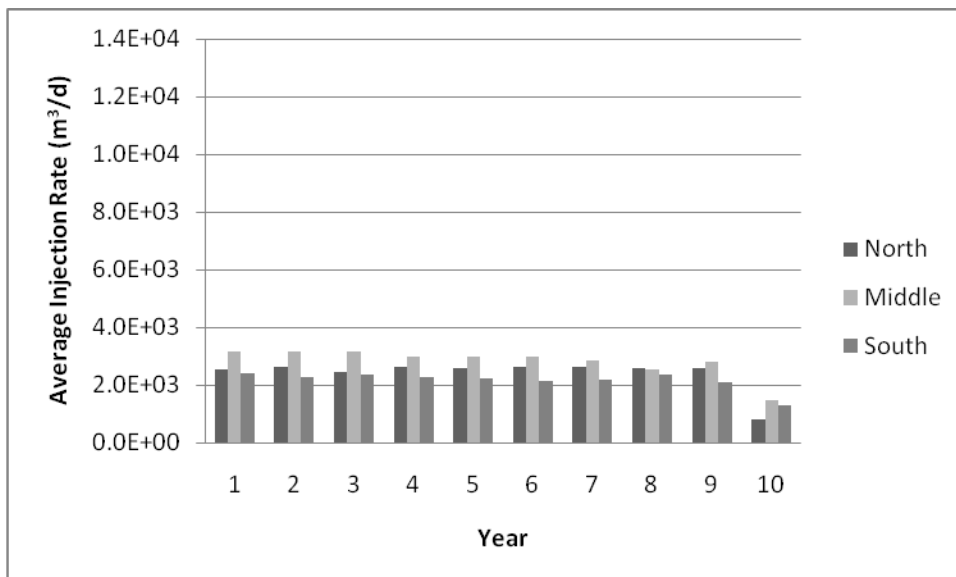


Figure 4-10. Distribution of injection for the LANOPT-GS scenario

The land surface and initial head are sloped in such a way that the initial lift in the northern section of the aquifer is much smaller than the initial lift in the

southern section of the aquifer. The initial lift varies from 40 m at well 9B to 118 m at well 34N (Table 4-5). As such, it is expected that the minimize energy formulation would pump more water from wells in the northern region and less water from the wells in the southern region in order to take advantage of the low lifts in the northern region.

Table 4-5. Initial lifts at each well

Well	Ground Surface Elevation	Initial Head	Initial Lift
	m	m	m
9A	707	666	41
9B	706	666	40
9E	707	663	44
15R	727	654	73
22B	724	654	70
27F	744	649	96
27H	745	650	95
27P	751	649	102
30B	728	658	69
34N	768	650	118

The pumping for the MINENG-GS-GS1 scenario primarily occurs in the northern region, where the initial lift was the lowest (Figure 4-11). Over the 10-year simulation period, 91% of the water demand is met by pumping from the wells in the northern region and 9% is met by pumping from wells in the middle region. There is no pumping from any of the four wells in the southern region.

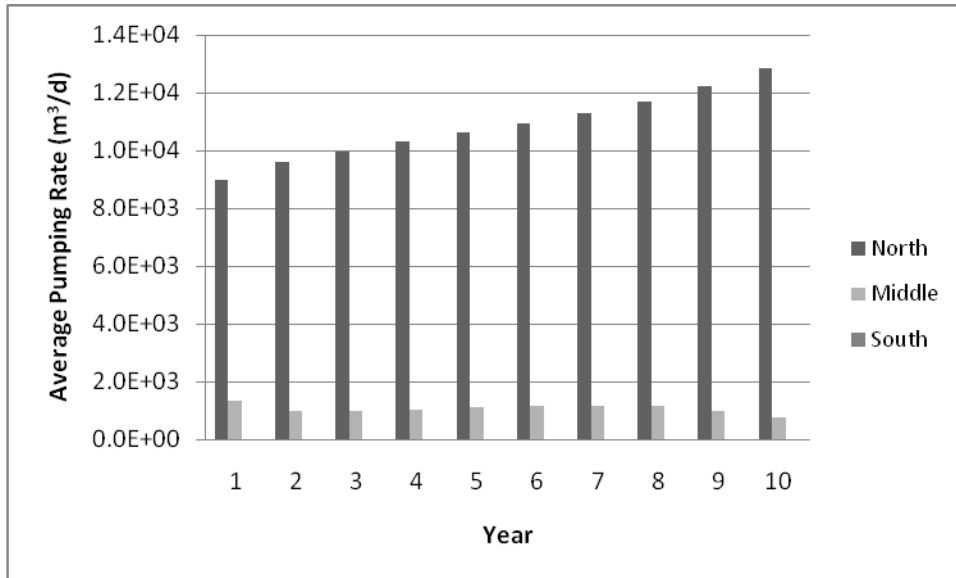


Figure 4-11. Distribution of pumping for the MINENG-GS-GS1 scenario

During the first eight years of the simulation, water is only injected using wells in the northern region. In the ninth year, a small fraction of the injected water is injected using wells in the middle and southern regions, and equal amounts of water are injected in all of the wells during the last year. Overall, 92% of the total water injected is injected using the wells in the northern region, and 4% is injected using wells in both the middle and southern regions (Figure 4-12).

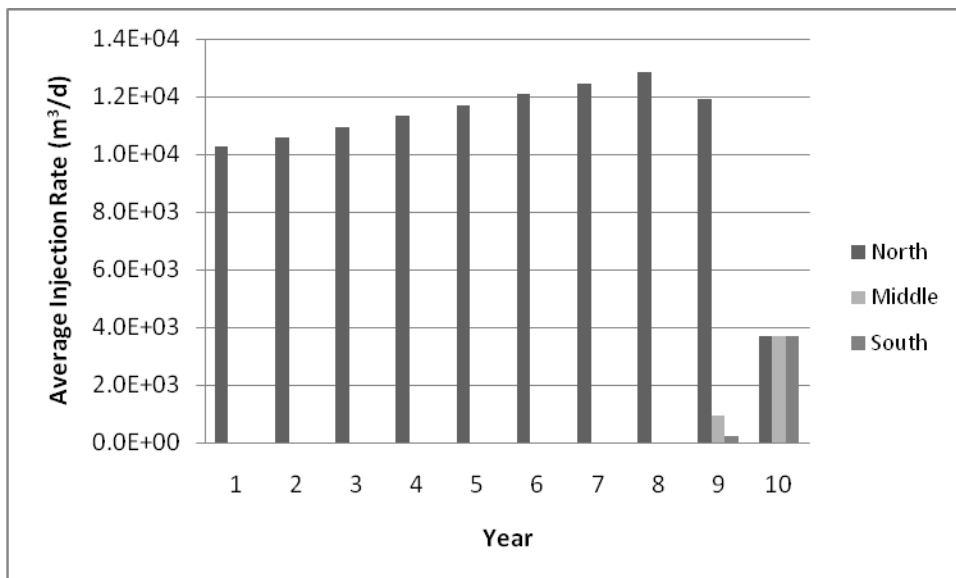


Figure 4-12. Distribution of injection for the MINENG-GS-GS1 scenario

The pumping and injection distribution for the MINENG-GS-GS2 scenario were similar to those of the first optimization scenario. Most of the pumping occurred in the northern region and no pumping occurred in the southern region (Figure 4-13). Injection occurred only in the northern region during the first nine years of the simulation, then was evenly distributed among all wells during the final year of the simulation (Figure 4-14).

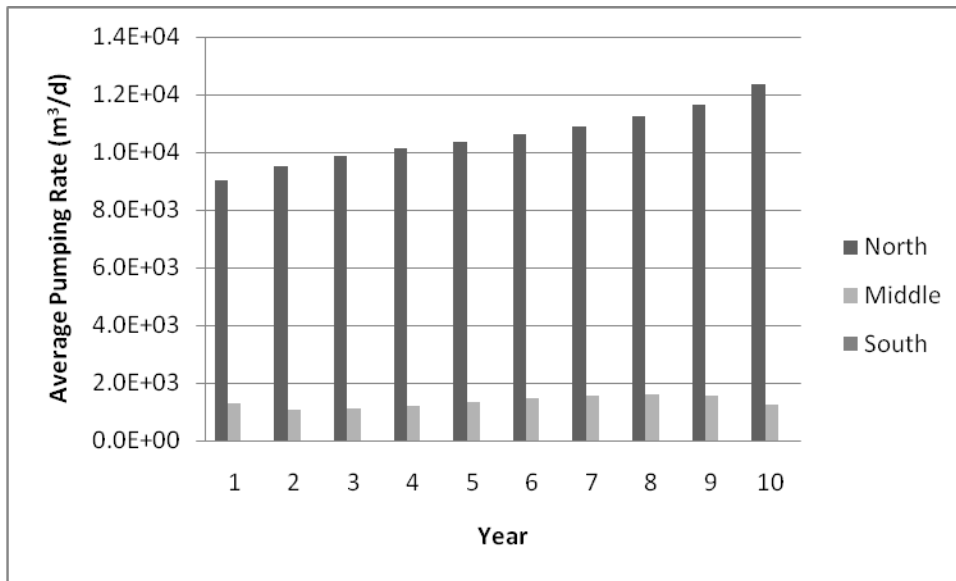


Figure 4-13. Distribution of pumping for the MINENG-GS-GS2 scenario

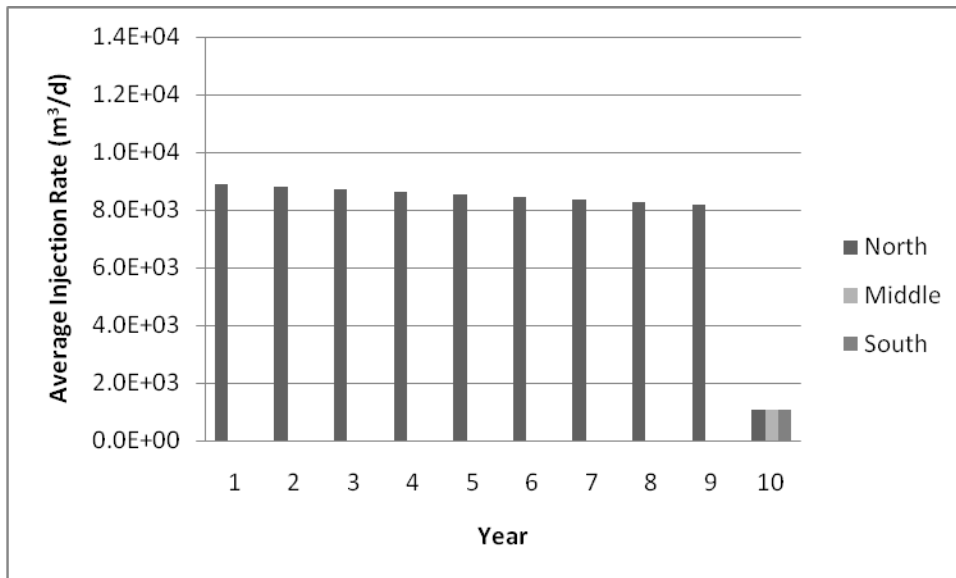


Figure 4-14. Distribution of injection for the MINENG-GS-GS2 scenario



By comparing the lift at the end of the last withdrawal period of the LANOPT-GS formulation to the initial lift, it can be seen that the lift generally decreased in the northern region and increased in the southern region due to the pumping and injection distribution and groundwater flow (Table 4-6). A negative change in lift indicates a rise in the head at that well as compared to the initial head, leading to a decrease in lift.

Table 4-6. Lifts at the end of the last withdrawal period of the LANOPT-GS scenario

Well	Ground Surface Elevation	Head	Lift	$\Delta$ Lift
	m	m	m	m
9A	707	669	39	-2.7
9B	706	668	37	-2.7
9E	707	665	42	-1.8
15R	727	656	71	-1.8
22B	724	654	70	0.0
27F	744	641	103	7.9
27H	745	645	100	5.2
27P	751	640	110	8.5
30B	728	658	70	0.3
34N	768	641	127	8.8

By comparing the lift at the end of the last withdrawal period of the MINENG-GS-GS1 scenario to the initial lift, it can be seen that the lift increased in the northern region, decreased in the middle and southern regions, and stayed approximately the same at well 30B, which is located farther west than any of the other wells (Table 4-7). Although no water was injected in the southern region, the lift decreased due to the flow of groundwater, including water injected in the northern region, from north to south since there was no pumping in the southern region either. The MINENG-GS-GS2 scenario gave similar results: the lift increased in the northern region, decreased in the middle and southern regions, and stayed approximately the same at well 30B (Table 4-8).

Table 4-7. Lifts at the end of the last withdrawal period of the MINENG-GS-GS1 scenario

Well	Ground Surface Elevation	Head	Lift	$\Delta$ Lift
	m	m	m	m
9A	707	659	48	6.6
9B	706	659	47	6.8
9E	707	656	51	7.1
15R	727	659	68	-4.4
22B	724	658	66	-3.4
27F	744	654	90	-5.5
27H	745	655	91	-4.3
27P	751	654	97	-5.2
30B	728	658	69	0.0
34N	768	653	115	-2.9

Table 4-8. Lifts at the end of the last withdrawal period of the MINENG-GS-GS2 scenario

Well	Ground Surface Elevation	Head	Lift	$\Delta$ Lift
	m	m	m	m
9A	707	656	51	9.9
9B	706	655	51	10.4
9E	707	653	54	10.3
15R	727	657	70	-2.5
22B	724	656	68	-1.4
27F	744	654	91	-5.0
27H	745	654	91	-3.9
27P	751	653	97	-4.8
30B	728	657	71	1.3
34N	768	653	115	-2.8

The MINIMAX formulation was not used for comparison with the minimize energy formulations for the case where the individual ground surface elevations at each well were used. The large variation in initial lifts makes this problem unsuitable for the MINIMAX formulation. Since the minimize energy formulation did not pump water from all wells, the MINIMAX formulation would be unlikely to pump from all wells either.

#### 4.5.2 Uniform reference elevation

The previous minimize energy formulations only consider the energy required to lift the water to the ground surface. They do not take into account movement of the water after it has been pumped to the ground surface. Due to the increased urban demand, it is assumed that more water will have to be used in the middle and southern regions of the Lancaster subbasin, where Lancaster and Palmdale are located. As such, the movement of water after extracting it from the aquifer should be considered in the formulation as well, particularly since the ground surface slopes upward from north to south. Since well 34N has the greatest ground surface elevation, its elevation of 768 m is used as the reference elevation for all of the wells.

##### 4.5.2.1 Minimize energy formulation using a uniform reference elevation

The MINENG-UE scenario requires  $19.2 \times 10^6$  kWh of energy over the ten-year simulation period. As before, the required energy increased each year, changing from  $1.73 \times 10^6$  kWh in the first year to  $2.19 \times 10^6$  kWh in the tenth year (Figure 4-15).

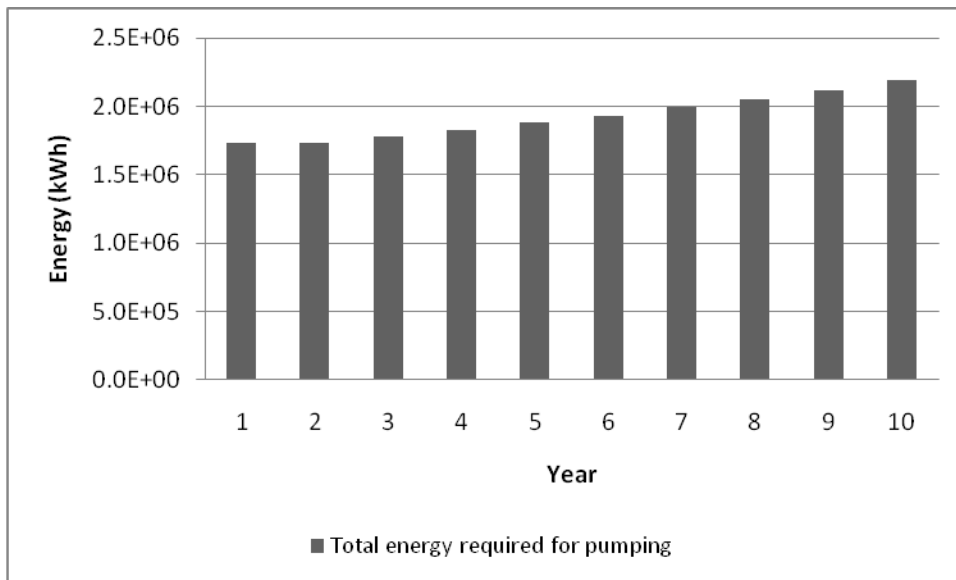


Figure 4-15. Energy required for pumping for the MINENG-UE scenario

For this scenario, the pumping is concentrated in the northern region (Figure 4-16), as expected, since the initial lift is the smallest in the north. The least amount of

water is pumped from the southern region. However, pumping occurs at every well in every withdrawal period (Figure 4-17, Figure 4-18, and Figure 4-19).

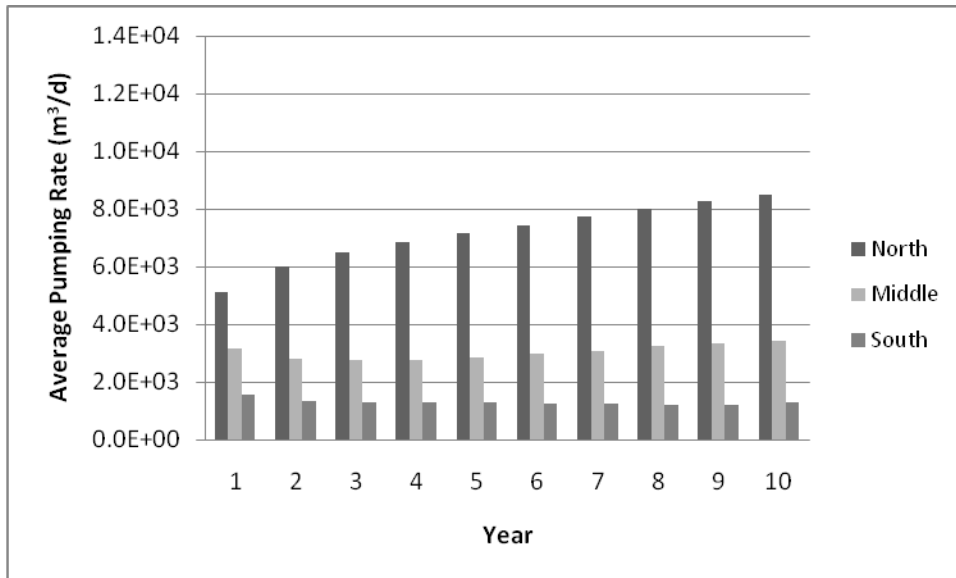


Figure 4-16. Regional pumping distribution for the MINENG-UE scenario

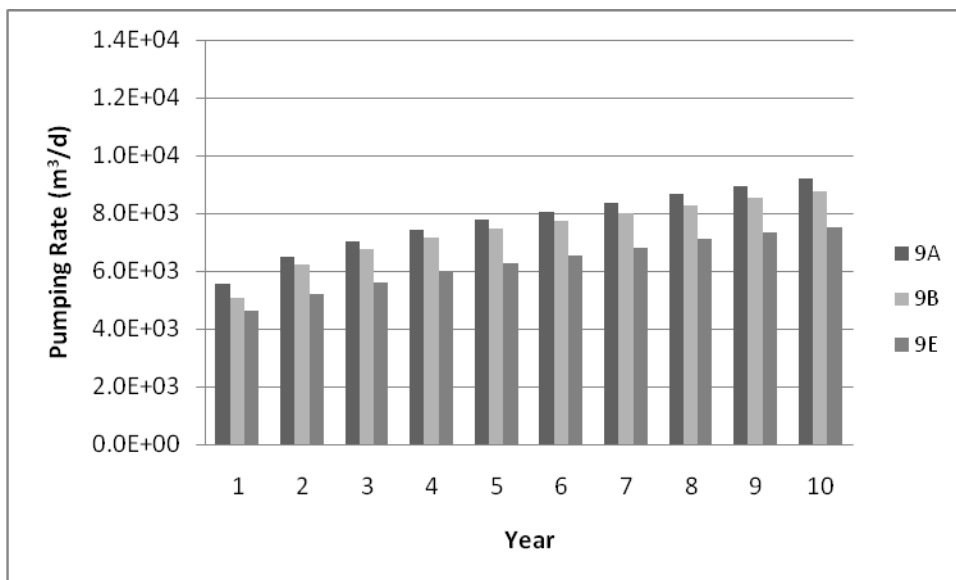


Figure 4-17. Pumping distribution within the northern region for the MINENG-UE scenario

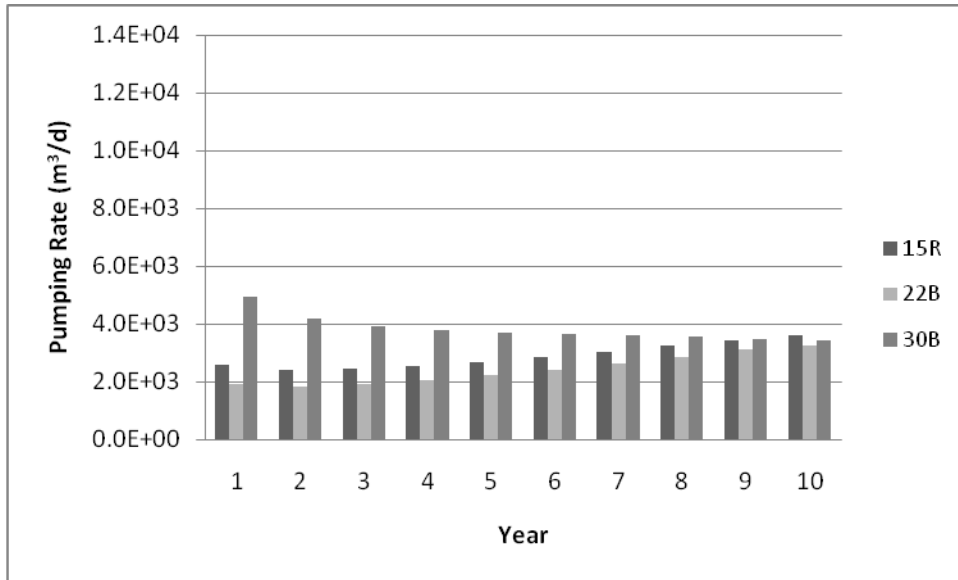


Figure 4-18. Pumping distribution within the middle region for the MINENG-UE scenario

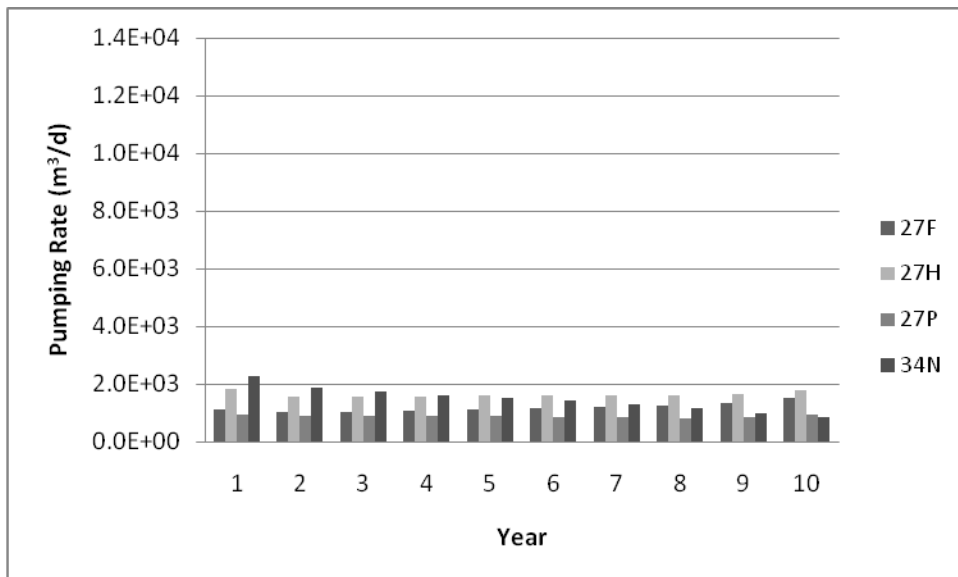


Figure 4-19. Pumping distribution within the southern region for the MINENG-UE scenario

The injection is again concentrated in the northern region, though injection occurs in the middle region during all time periods as well (Figure 4-20). Although water is injected into all wells in the northern region during all injection periods (Figure 4-21), only well 22B in the middle region has water injected into it during all ten injection periods (Figure 4-22). Well 34N in the southern region has the least amount of water injected into it, only having injection during the ninth and tenth years (Figure 4-23).

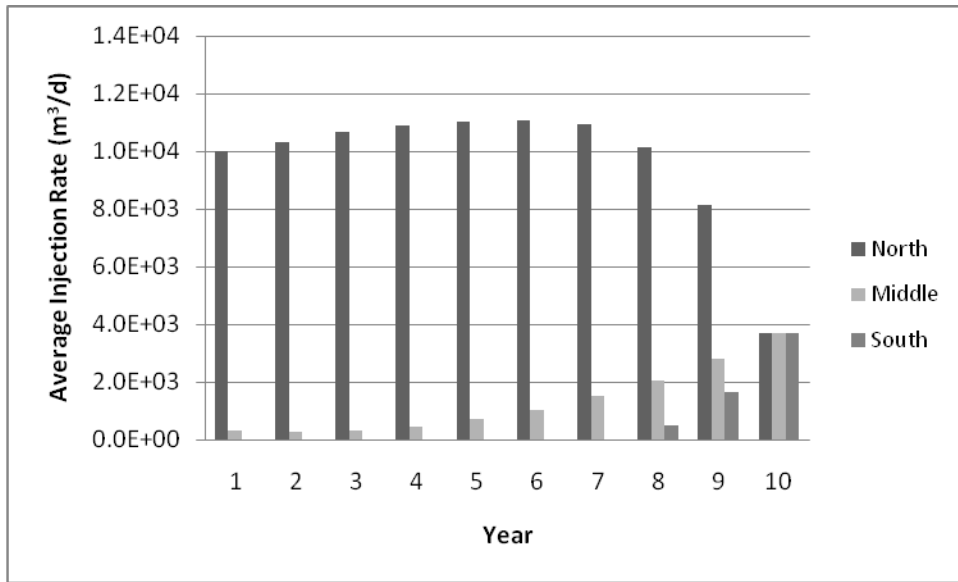


Figure 4-20. Regional injection distribution for the MINENG-UE scenario

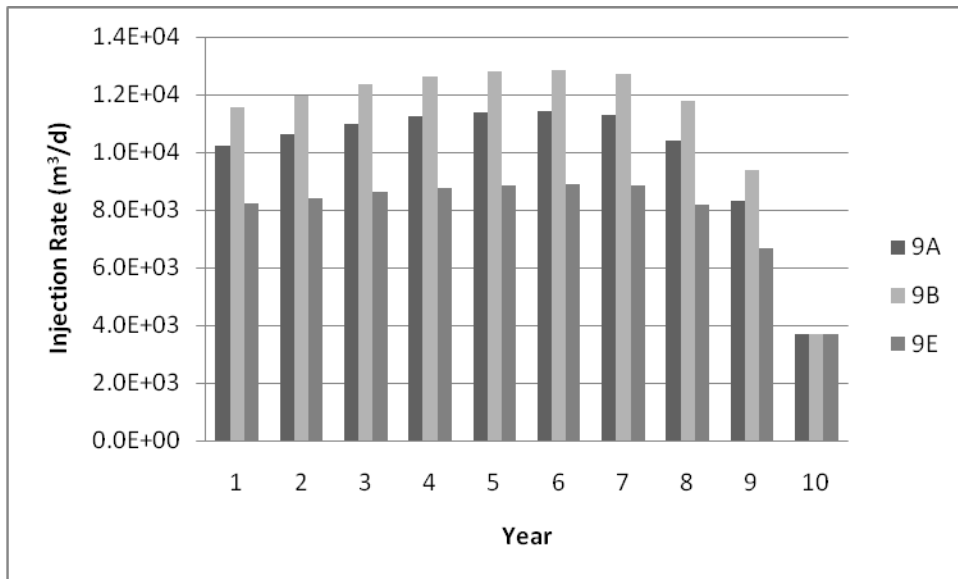


Figure 4-21. Injection distribution within the northern region for the MINENG-UE scenario

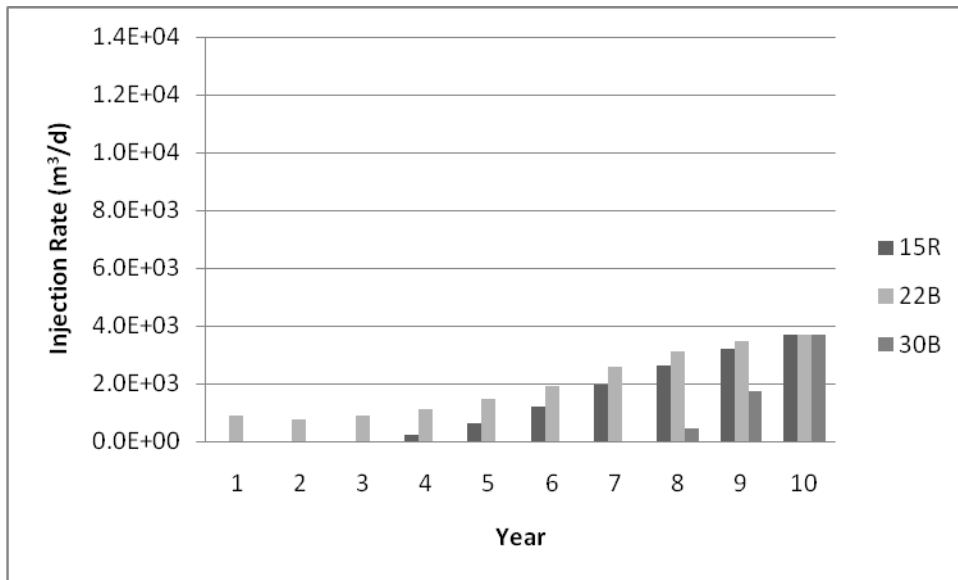


Figure 4-22. Injection distribution within the middle region for the MINENG-UE scenario

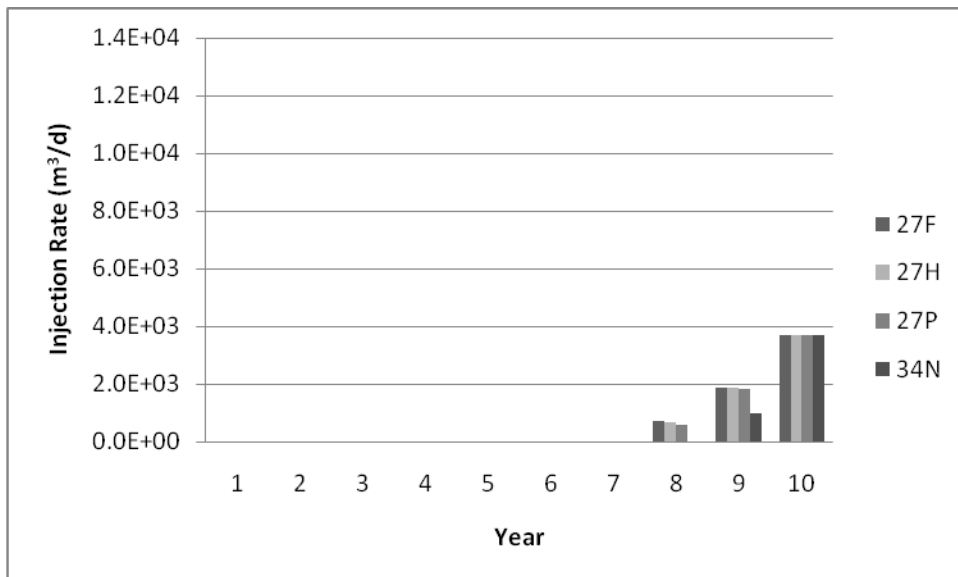


Figure 4-23. Injection distribution within the southern region for the MINENG-UE scenario

Overall, the heads in the aquifer increase over time due to the injection of water into the aquifer. All of the hydraulic heads at the wells have a yearly cycle in which they decrease during the withdrawal period and increase during the injection period. The heads in the northern region increase until the end of the seventh year, after which the injection shifts to more southern wells, causing decreases in the heads in the northern region (Figure 4-24). In the middle region, the head at well 30B remains relatively steady

from year to year, excluding the periodic variation due to the withdrawal and injection cycle, while the other two wells show increasing heads (Figure 4-25). All of the wells in the southern region show an increasing trend in head (Figure 4-26).

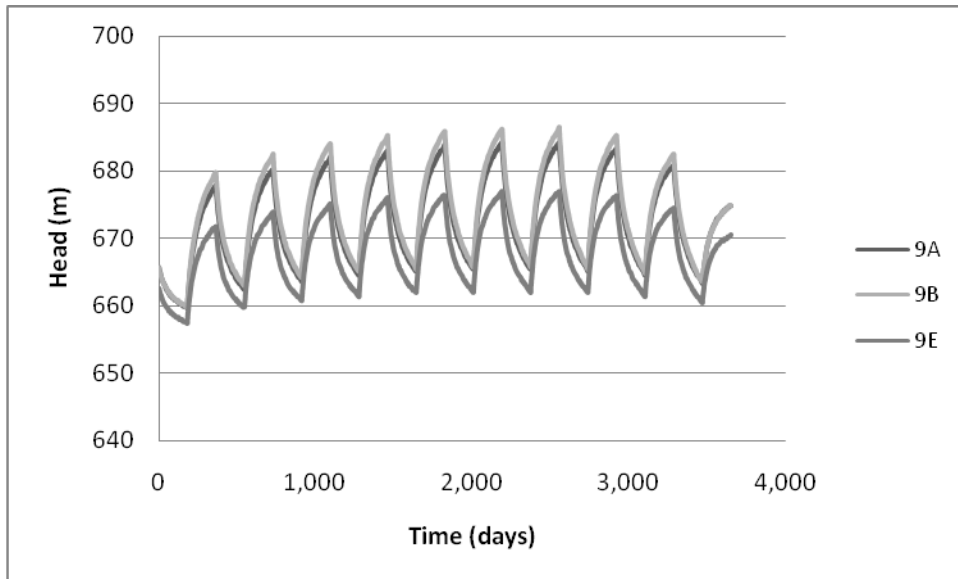


Figure 4-24. Heads at wells within the northern region for the MINENG-UE scenario

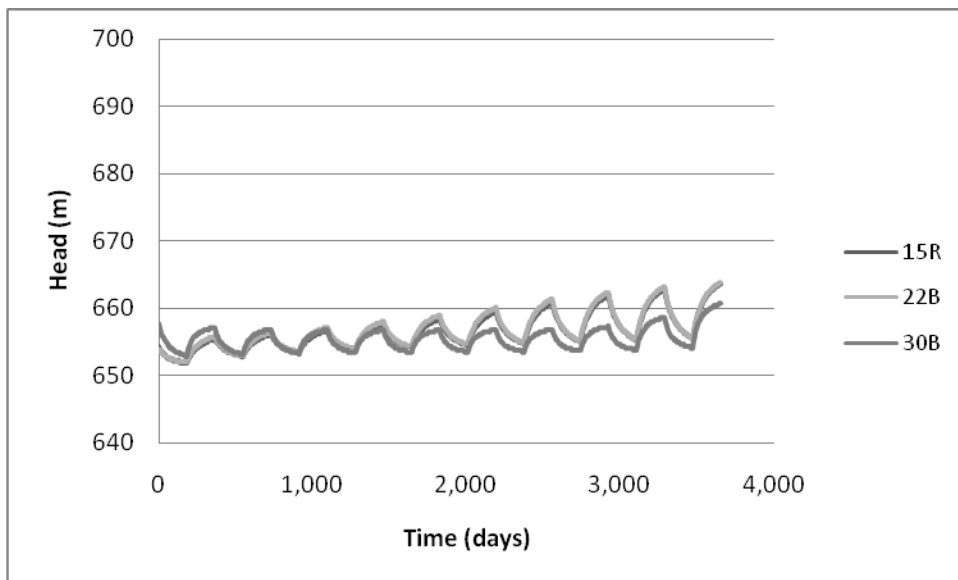


Figure 4-25. Heads at wells within the middle region for the MINENG-UE scenario



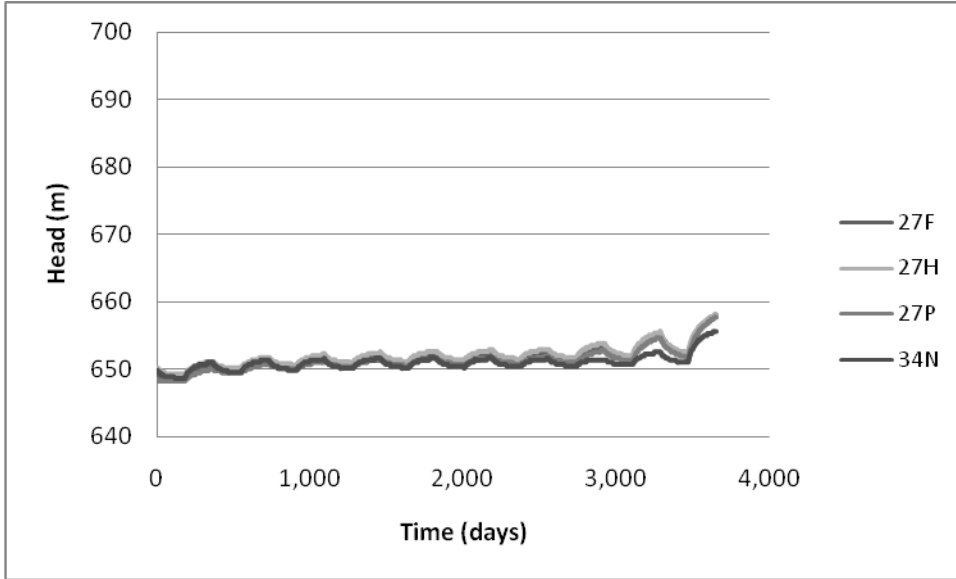


Figure 4-26. Heads at wells within the southern region for the MINENG-UE scenario

#### 4.5.2.2 MINIMAX formulation using a uniform reference elevation

The MINIMAX formulation for the MINIMAX-UE scenario takes the form

$$\text{Minimize} \quad Z = R \quad (\text{Eq. 4.4})$$

$$\text{such that} \quad \sum_{i,t} Q_{i,t} \geq D_t \text{ for each year}$$

$$\sum_i Q_{i,t} \geq \sum_i I_{i,t} \text{ for each year}$$

$$H - h_{i,t} \leq R, \quad i = 1, 2, \dots, n$$

$$\text{and} \quad h_{i,t} \leq 2300 \text{ ft}$$

where  $H = 768$  m and is the maximum elevation to which the water will be lifted. It is justifiable to attempt to use the MINIMAX formulation for the case using a uniform reference elevation, since using the uniform elevation rather than the individual ground surface elevations decreases the variability in initial lift among the wells. Since the MINENG-UE scenario resulted in pumping at all wells, it was hypothesized that the MINIMAX-UE formulation could provide an acceptable substitute for the minimize energy formulation.

The MINIMAX-UE scenario requires  $20.9 \times 10^6$  kWh of energy over the ten-year simulation period. As before, the required energy increased each year, changing from  $1.79 \times 10^6$  kWh in the first year to  $2.39 \times 10^6$  kWh in the tenth year (Figure 4-27).

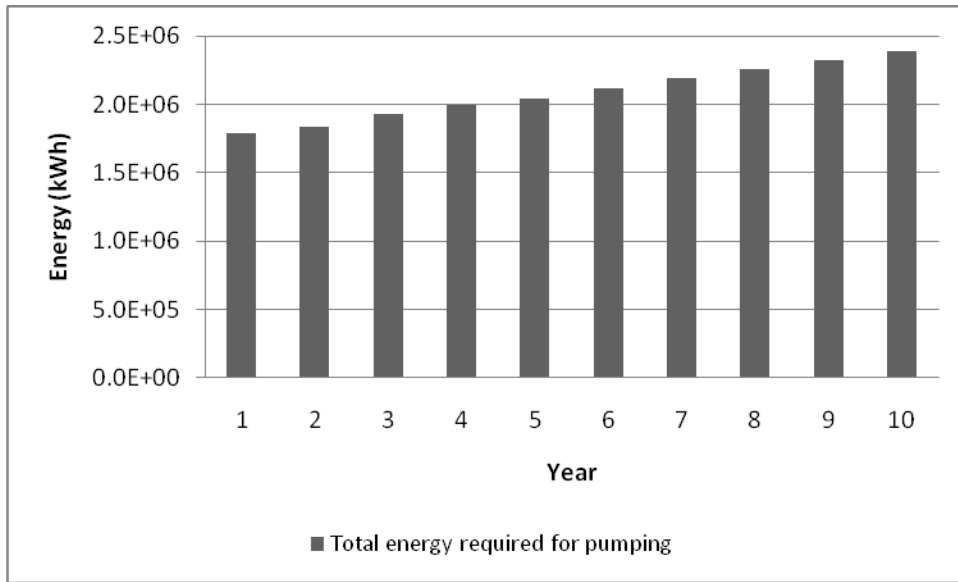


Figure 4-27. Energy required for pumping for the MINIMAX-UE scenario

Although the energy requirements for the MINIMAX-UE scenario are similar to those of the MINENG-UE scenario, the pumping and injection distributions are extremely different. Pumping occurs only in the northern region for the first year, and then is distributed among all three regions for the remaining years (Figure 4-28) in the MINIMAX-UE scenario. In the northern region, water is pumped from all three wells during the first year, then only from well 9A during the remaining years (Figure 4-29). In the middle region, pumping in the last nine years is distributed between wells 22B and 30B; well 15R does not have any pumping (Figure 4-30). Only well 34N pumps in the southern region (Figure 4-31).

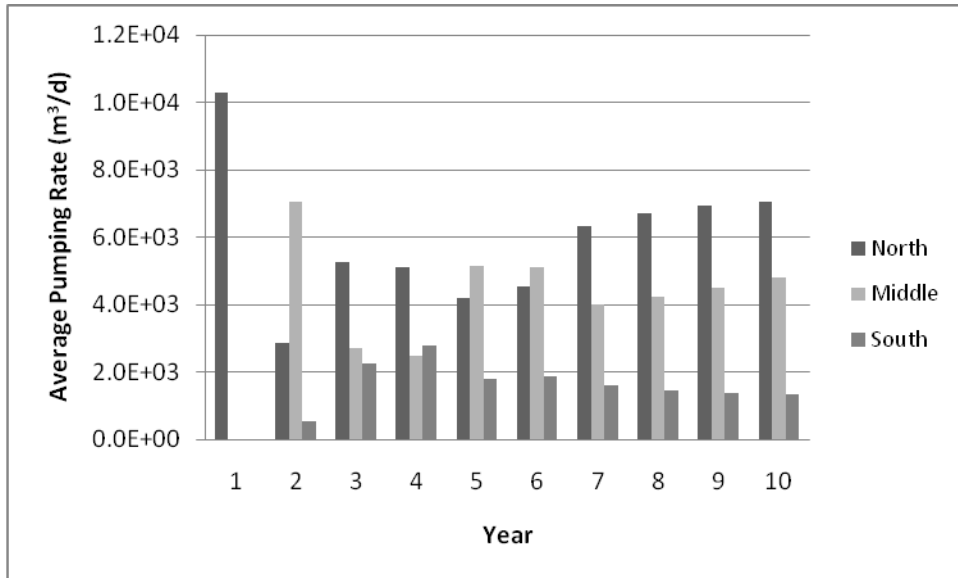


Figure 4-28. Regional pumping distribution for the MINIMAX-UE scenario

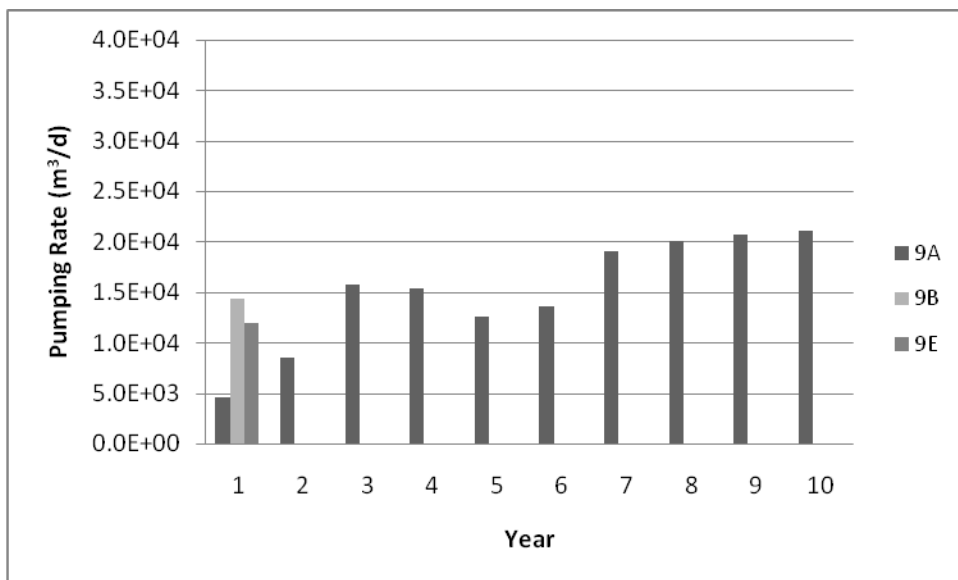


Figure 4-29. Pumping distribution within the northern region for the MINIMAX-UE scenario

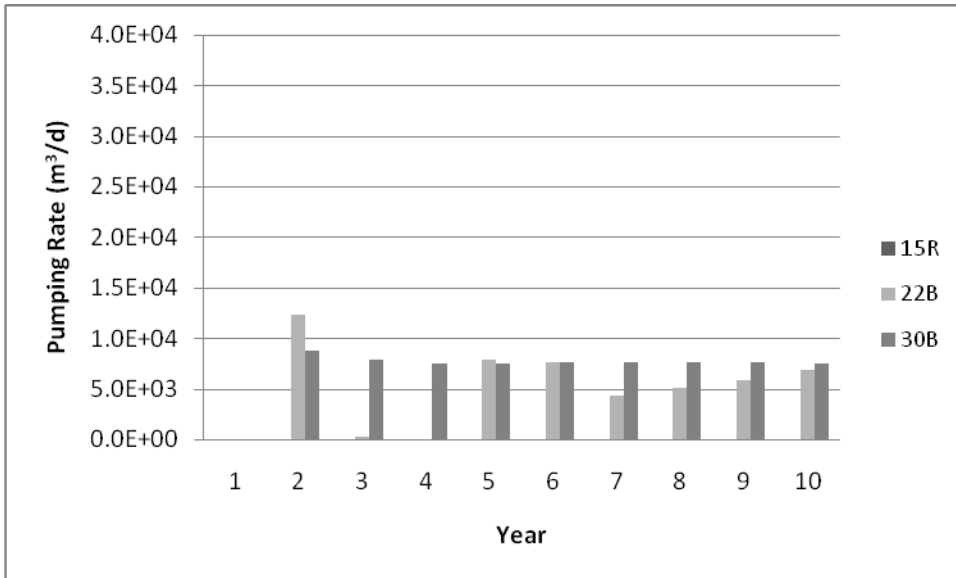


Figure 4-30. Pumping distribution within the middle region for the MINIMAX-UE scenario

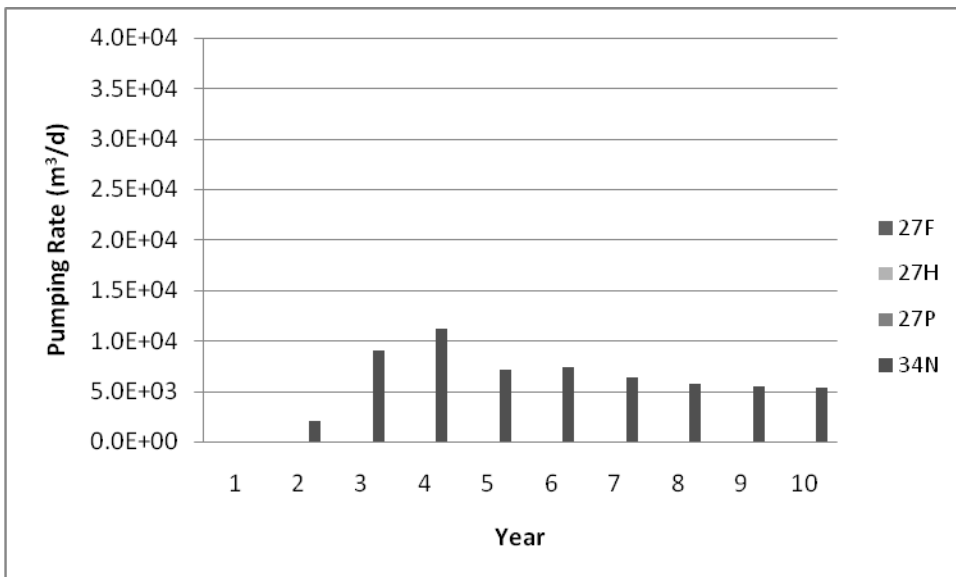


Figure 4-31. Pumping distribution within the southern region for the MINIMAX-UE scenario

Injection is even more clustered than the pumping. The middle region has injection during the first and last years, the southern region has injection during the last nine years, and the northern region has injection only during years six through nine (Figure 4-32). Within the regions, only well 9B injects water in the north (Figure 4-33), only well 22B injects water in the middle region (Figure 4-34), and well 34N injects

water during years 2, 3, and 10, while well 27P injects water during years four through nine (Figure 4-35).

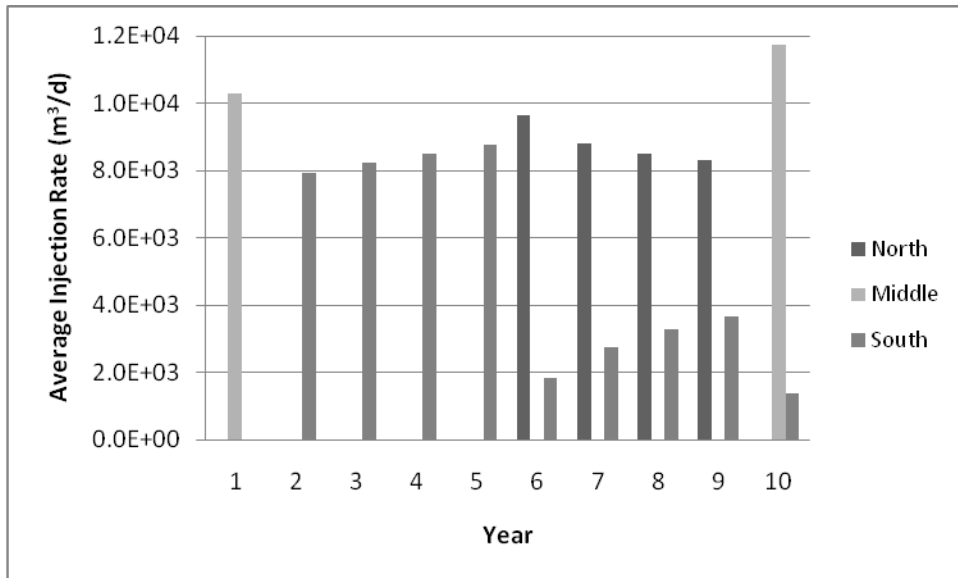


Figure 4-32. Regional injection distribution for the MINIMAX-UE scenario

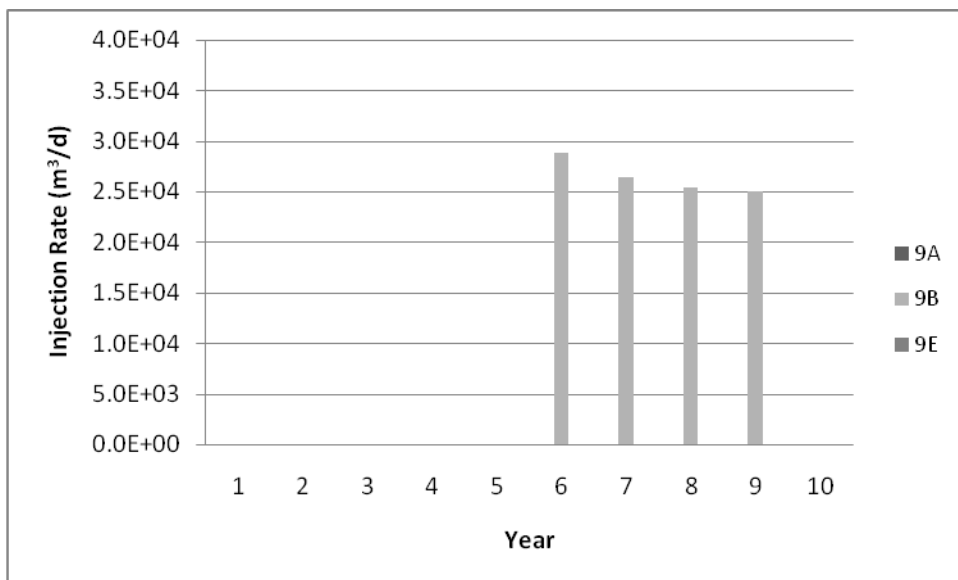


Figure 4-33. Injection distribution within the northern region for the MINIMAX-UE scenario

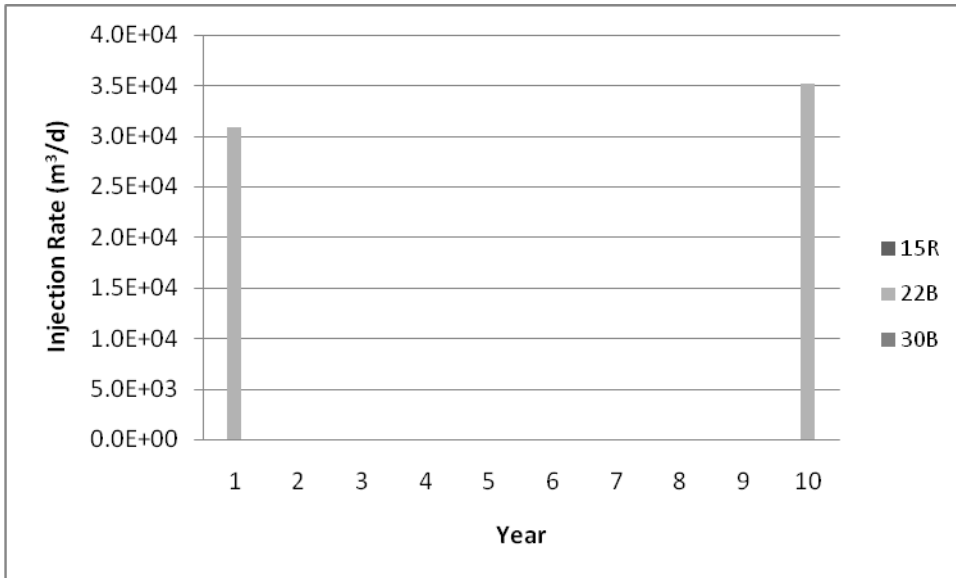


Figure 4-34. Injection distribution within the middle region for the MINIMAX-UE scenario

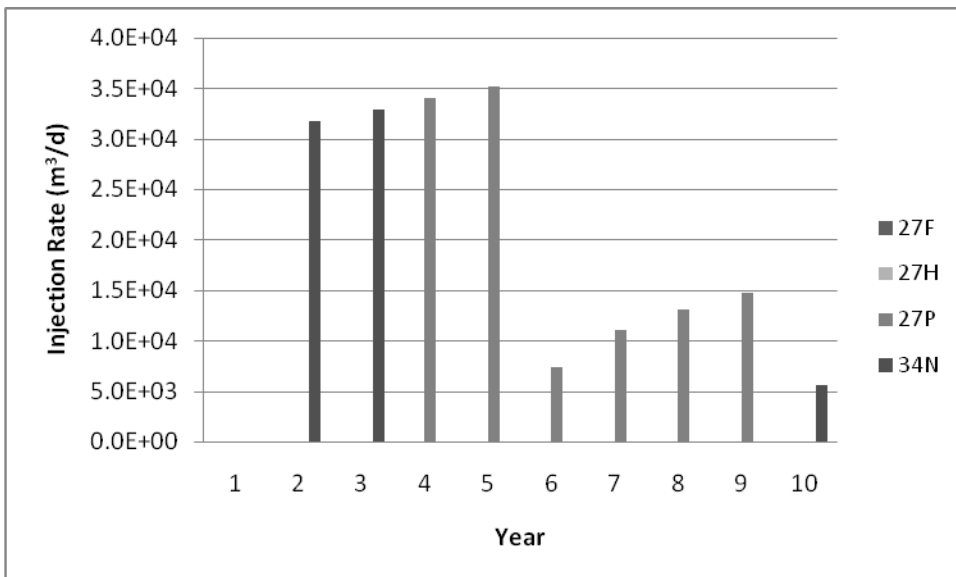


Figure 4-35. Injection distribution within the southern region for the MINIMAX-UE scenario

The objective of the MINIMAX formulation is to minimize the maximum lift in the aquifer at the end of the withdrawal periods. The concentrated pumping and injection at individual wells causes large changes in head with respect to time at those wells, while the response of the heads at other wells is much smaller (Figure 4-36, Figure 4-37, and Figure 4-38). However, the lift at each well at the end of each withdrawal period does not fluctuate much from the previous withdrawal period (Figure 4-39, Figure 4-40, and

Figure 4-41). The maximum lift is 118.0 m. The demand is not high enough to equalize the lifts at all of the wells; so many lifts are less than 118 m. The maximum lift is achieved 29 times out of a possible 100 times. The maximum lift resulting from the minimize energy formulation is 119.5 m.

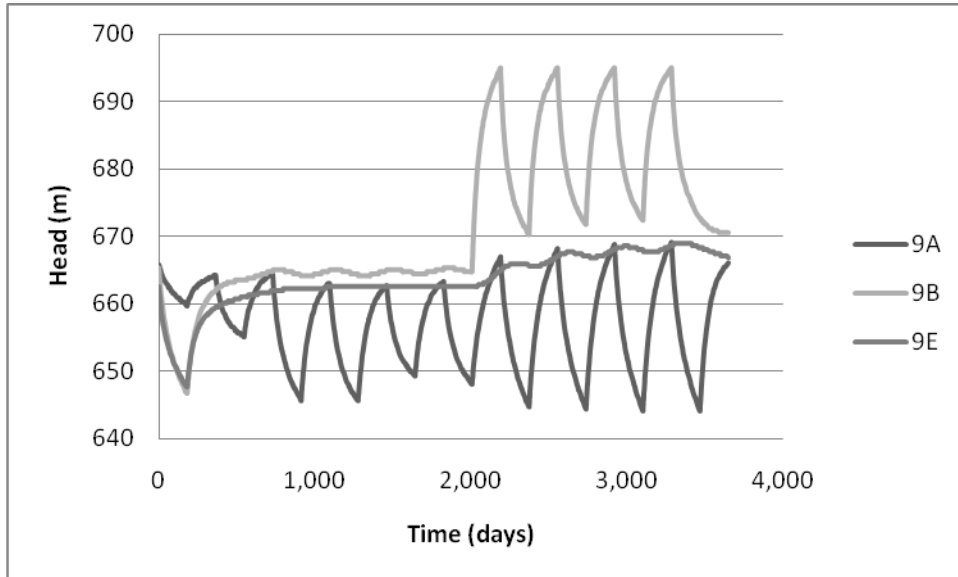


Figure 4-36. Heads at wells within the northern region for the MINIMAX-UE scenario

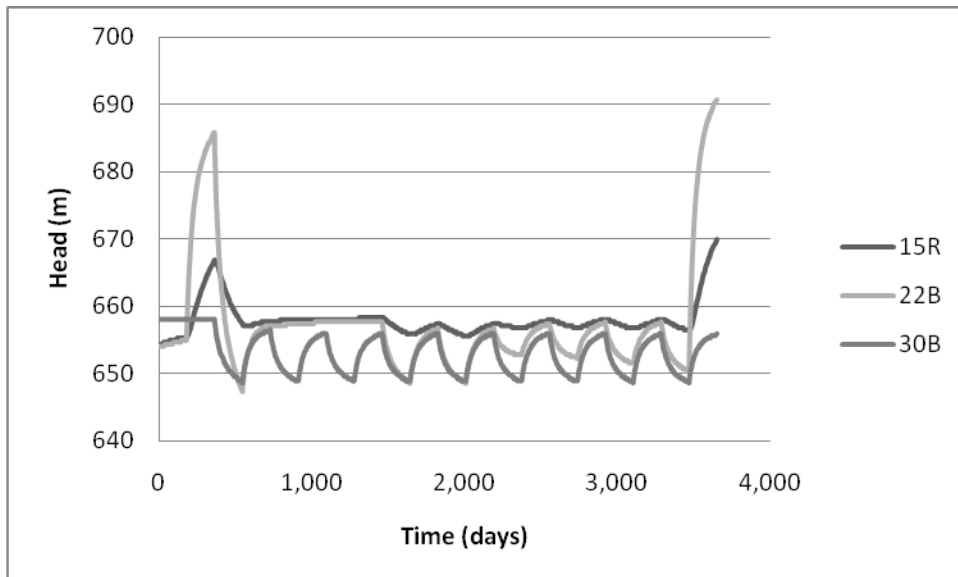


Figure 4-37. Heads at wells within the middle region for the MINIMAX-UE scenario

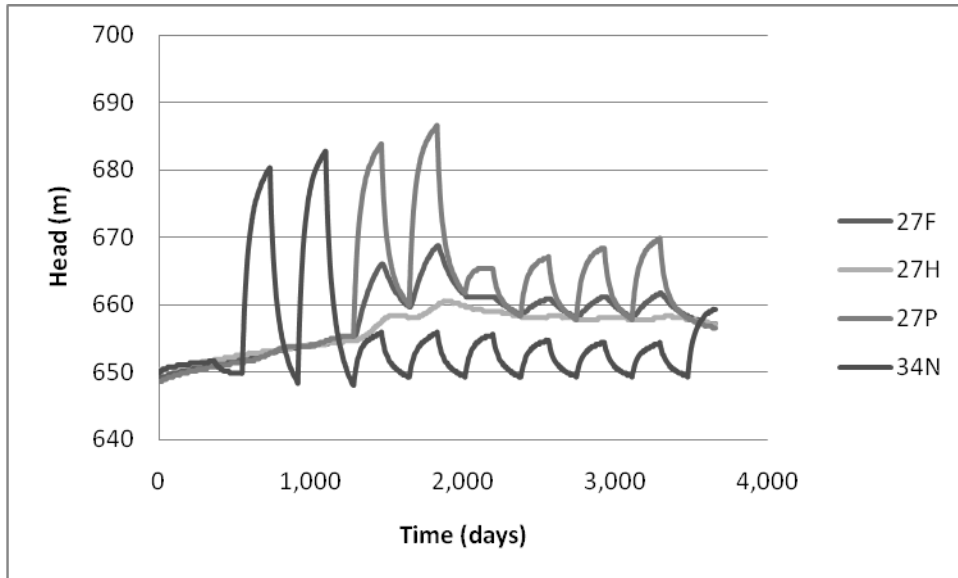


Figure 4-38. Heads at wells within the southern region for the MINIMAX-UE scenario

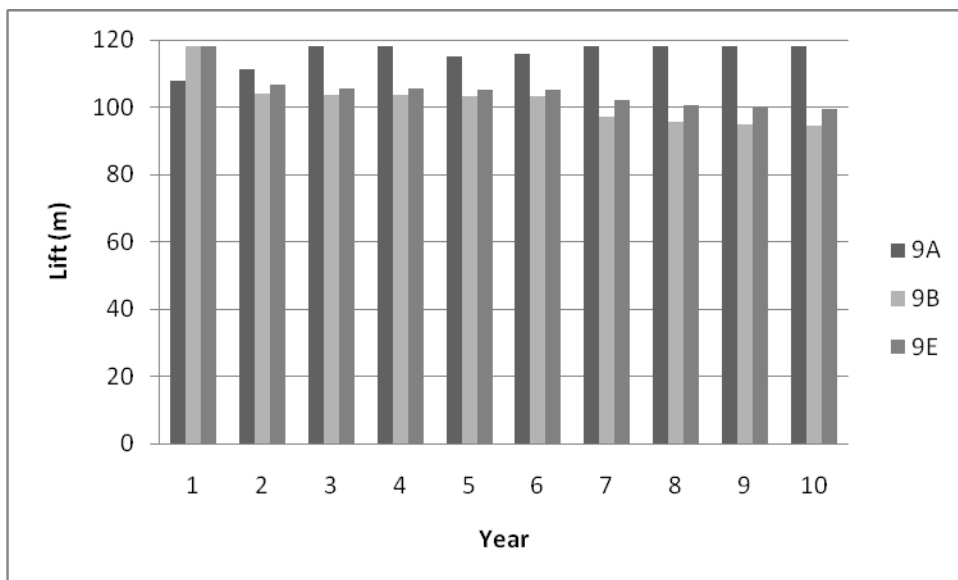


Figure 4-39. Lifts at wells within the northern region for the MINIMAX-UE scenario



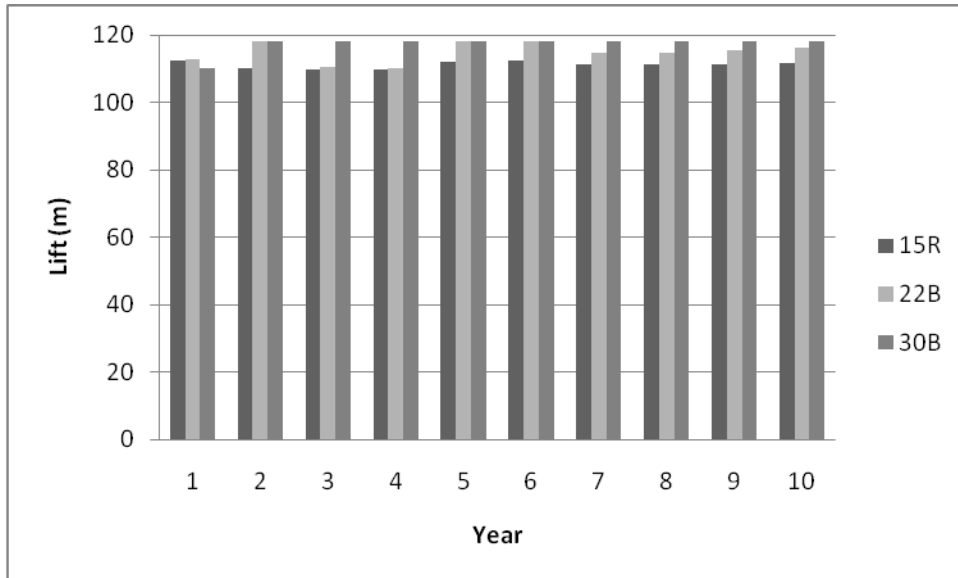


Figure 4-40. Lifts at wells within the middle region for the MINIMAX-UE scenario

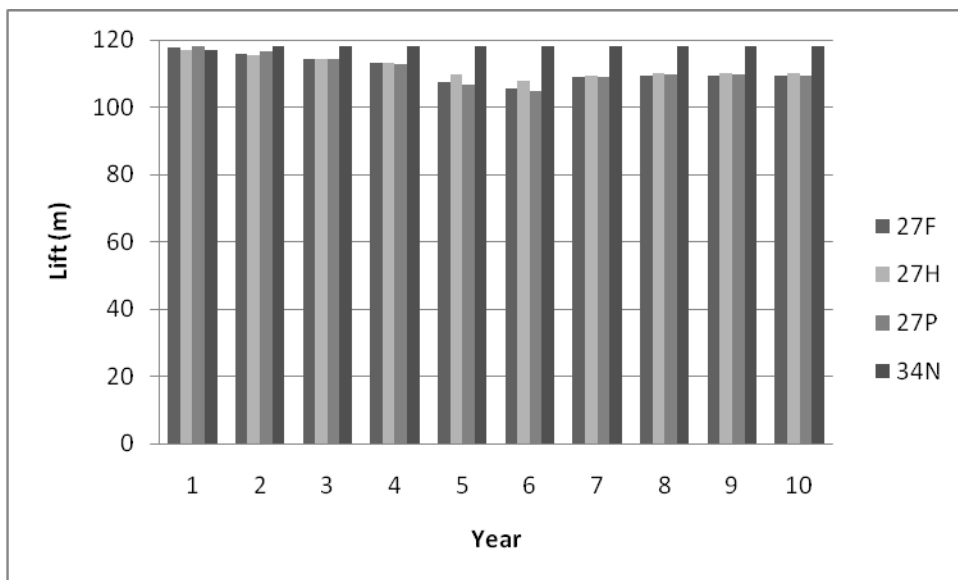


Figure 4-41. Lifts at wells within the southern region for the MINIMAX-UE scenario

### 4.5.3 Comparison of minimize energy and MINIMAX formulations

This section compares the results of the LANOPT, minimize energy formulations, and the MINIMAX formulation for the Lancaster subbasin. In order to compare the MINENG-GS-GS1 scenario to the MINENG-UE scenario, the energy use was recalculated to lift the water to the uniform reference elevation instead of the ground surface elevations, creating the MNINENG-GS-UE scenario. The same calculations were performed for the LANOPT-GS scenario, creating the LANOPT-UE scenario.

The LANOPT-GS scenario requires a total energy of  $33.4 \times 10^6$  kWh. The LANOPT-UE scenario, which uses the same pumping and injection distribution, but lifts the water to the uniform reference elevation of 768 m, increases the required energy to  $43.0 \times 10^6$  kWh. The MINENG-GS-GS1 scenario requires a total energy of  $8.9 \times 10^6$  kWh, which is 27% of the energy required in the LANOPT-GS scenario. The MINENG-GS-UE scenario, which uses the same pumping and injection distribution, but lifts the water to the uniform reference elevation of 768 m, increases the required energy to  $19.5 \times 10^6$  kWh. The MINENG-UE scenario requires  $19.2 \times 10^6$  kWh, which is 45% of the energy required for the LANOPT-UE scenario. The MINIMAX-UE scenario requires the most energy of the optimization scenarios, requiring  $20.9 \times 10^6$  kWh (Table 4-9). There is a 74% difference between the MINENG-GS-GS1 and the MINENG-UE scenarios. Lifting the water to the uniform reference elevation from the ground surface, results in a 1.4% error when comparing the MINENG-GS-UE scenario to the MINENG-UE scenario. The MINIMAX-UE scenario has an 8.5% error when comparing it to the MINENG-UE scenario.

Table 4-9. Comparison of energy requirements for each formulation

Scenario	Total energy (kWh)
LANOPT-GS	$33.4 \times 10^6$
LANOPT-UE	$43.0 \times 10^6$
MINENG-GS-GS1	$8.9 \times 10^6$
MINENG-GS-UE	$19.5 \times 10^6$
MINENG-UE	$19.2 \times 10^6$
MINIMAX-UE	$20.9 \times 10^6$

Figure 4-42, Figure 4-43, and Figure 4-44 show the regional pumping distributions for each scenario. The MINENG-GS-UE scenario withdraws the most water from the northern region. The MINIMAX-UE scenario withdraws the most water from the middle and southern regions. Figure 4-45, Figure 4-46, and Figure 4-47 show the regional injection distributions for each formulation. The MINENG-GS-UE scenario injects the most water into the northern region and the MINIMAX-UE scenario injects the most water into the middle and southern regions. Since the pumping distributions from the MINENG-GS-UE, MINENG-UE, and MINIMAX-UE scenarios do not cause an

overall decline in heads at the wells and actually increase heads at most wells, it is presumed that the pumping distribution will not cause additional subsidence, which meets the objective of the LANOPT scenario to which these results are compared.

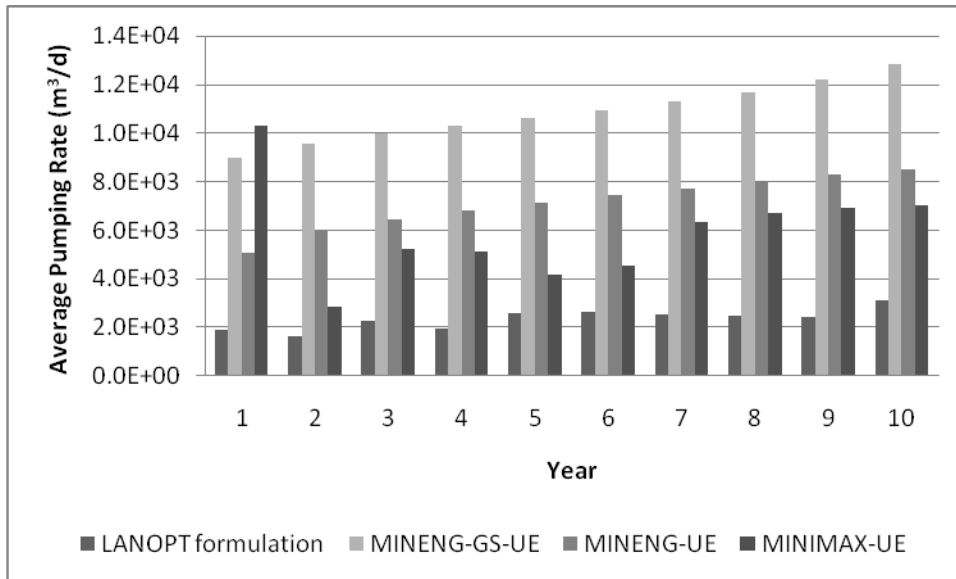


Figure 4-42. Comparison of pumping rates for the LANOPT-UE, MINENG-GS-UE, MINENG-UE, and MINIMAX-UE scenarios for the northern region

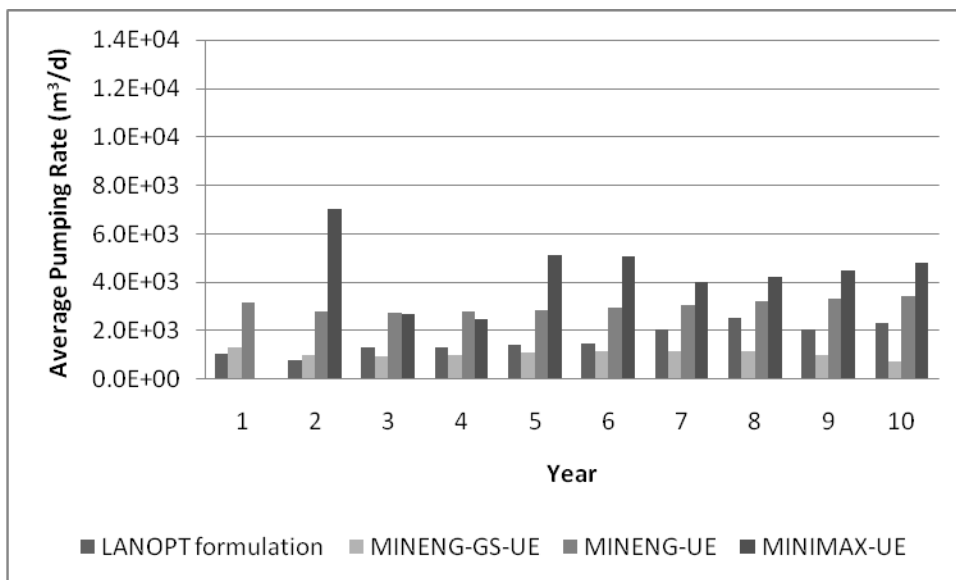


Figure 4-43. Comparison of pumping rates for the LANOPT-UE, MINENG-GS-UE, MINENG-UE, and MINIMAX-UE scenarios for the middle region

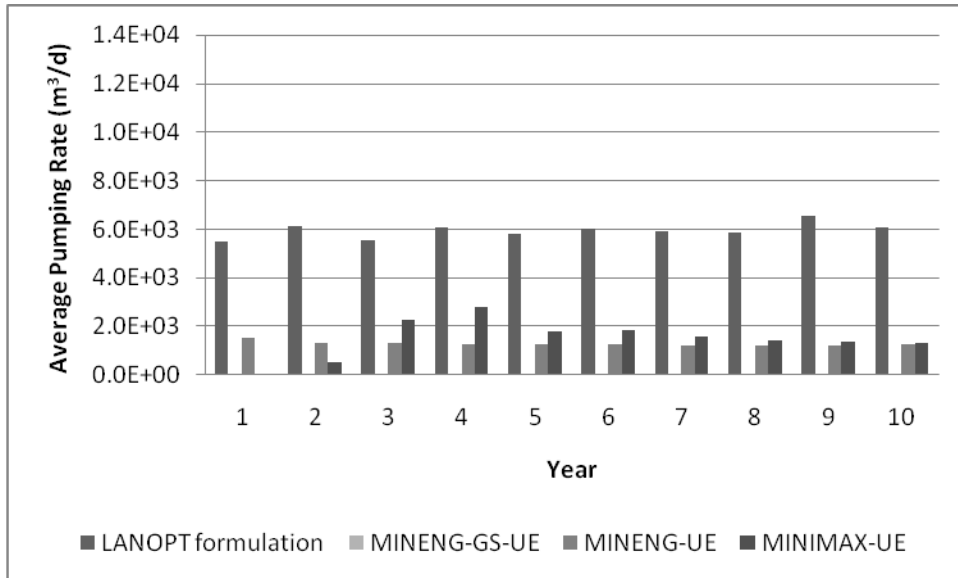


Figure 4-44. Comparison of pumping rates for the LANOPT-UE, MINENG-GS-UE, MINENG-UE, and MINIMAX-UE scenarios for the southern region

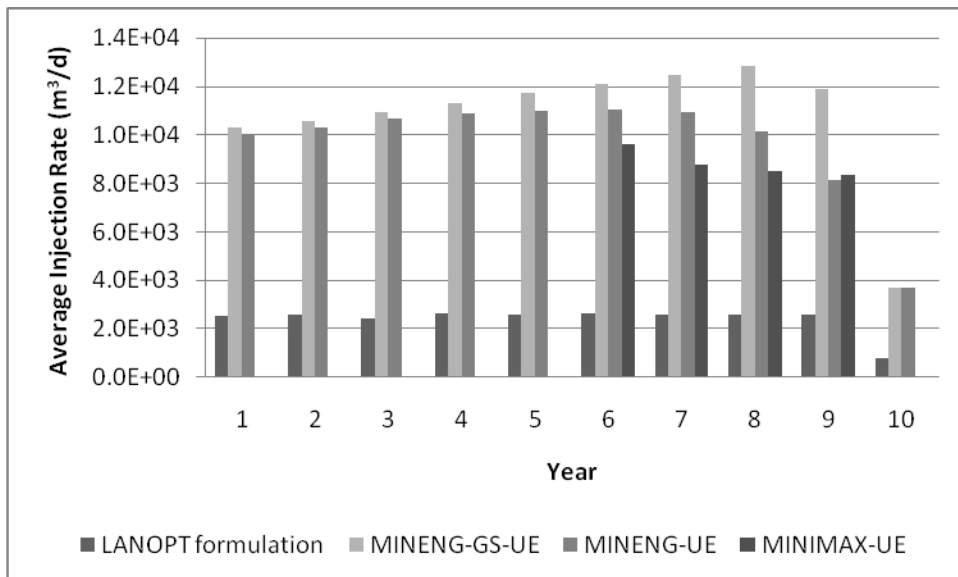


Figure 4-45. Comparison of injection rates for the LANOPT-UE, MINENG-GS-UE, MINENG-UE, and MINIMAX-UE scenarios for the northern region

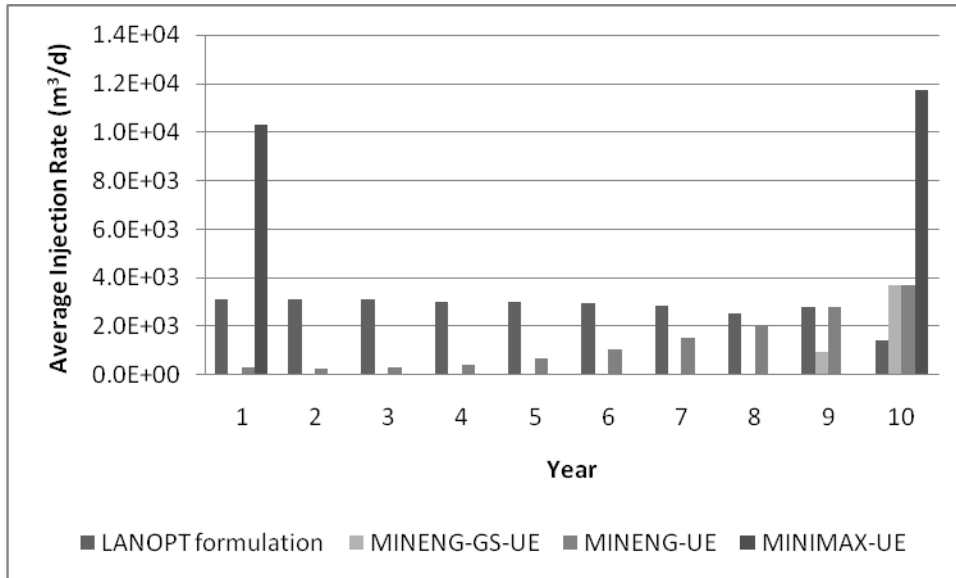


Figure 4-46. Comparison of injection rates for the LANOPT-UE, MINENG-GS-UE, MINENG-UE, and MINIMAX-UE scenarios for the middle region

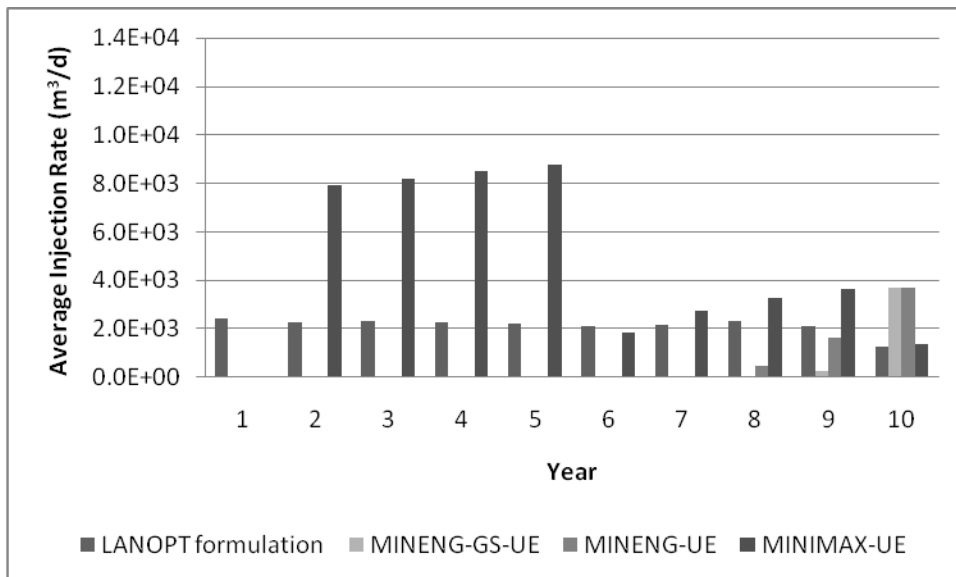


Figure 4-47. Comparison of injection rates for the LANOPT-UE, MINENG-GS-UE, MINENG-UE, and MINIMAX-UE scenarios for the southern region

#### 4.6 Conclusions from the Antelope Valley case study

The Antelope Valley case study shows that the minimize energy formulation can be effectively applied to a large groundwater supply system and can result in significant energy savings. Using two different scenarios for the elevation to which the water must be lifted provides upper and lower bounds on the required energy as determined by the minimize energy formulations. The MINIMAX formulation can be used when the

differences among initial lifts are not too large. However, although the difference in total energy between the MINIMAX-UE and MINENG-UE was less than 10%, the pumping and injection distributions varied greatly. The MINIMAX-UE scenario used a small number of wells for the pumping and injection as compared to the MINENG-UE scenario.

## 5 Conclusions

The minimize energy and MINIMAX formulations were applied to simple test models and to a large-scale case study. The results showed that the minimize energy formulation can be applied to large water supply systems and its use can result in significant energy savings. Using two different scenarios for the elevation to which the water must be lifted provides upper and lower bounds on the required energy as determined by the minimize energy formulations.

From the test models, it was determined that the MINIMAX formulation can be an acceptable alternative for the minimize energy formulation, substituting a linear formulation for a quadratic formulation. The MINIMAX formulation can be substituted for the minimize energy formulation when there are small variations among the initial lifts and when the demand is high enough that all wells are pumping, such that the MINIMAX formulation is able to equalize the lifts at all wells. However, the Antelope Valley case study shows that the MINIMAX formulation concentrates pumping among a small number of wells when there is large variation in initial lifts. Using a small number of available wells may not be a feasible solution for a water supply system due to physical limitations such as well capacity and pipe sizing. If so, additional constraints may need to be added to the formulation to limit the amount of water withdrawn at a single well.

## 6 References

- Ahlfeld, D. P., and A. E. Mulligan. 2000. *Optimal Management of Flow in Groundwater Systems*. San Diego: Academic Press.
- Ahlfeld, David P., Paul M. Barlow, and Ann E. Mulligan. 2005. *GWM - A Ground-Water Management Process for the U.S. Geological Survey Modular Ground-Water Model (MODFLOW-2000)*. Open-File Report 2005-1072. U.S. Geological Survey.
- Ahlfeld, David P., and Gemma Baro-Montes. 2008. Solving Unconfined Groundwater Flow Management Problems with Successive Linear Programming. *Journal of Water Resources Planning and Management* 134, no. 5: 404-412.
- Baker, Kris. 2008. Extension of MF2005-GWM (Ground-Water Management Process) to Solve Management Formulations which Optimize Hydraulic Head and Solve Quadratic Programming Problems. M.S. Environmental Engineering Project, University of Massachusetts.
- Baro-Montes, Gemma. 2007. Ground Water Management, GWM, Formulations to Control Subsidence in a Large Scale Transient Problem. M.S. Environmental Engineering Project, University of Massachusetts.
- Bartolino, J. R., and W. L. Cunningham. 2003. *Ground-water depletion across the nation*. U.S. Geological Survey.
- Bloyd, R. M. 1967. *Water Resources of the Antelope Valley-East Kern Water Agency Area, California*. Open-File Report 67-21. U.S. Geological Survey.
- California Energy Commission. 2004. Water Energy Use in California. <http://www.energy.ca.gov/research/iaw/industry/water.html>.
- Carlson, Carl S., David A. Leighton, Steven P. Phillips, and Loren F. Metzger. 1998. *Regional Water Table (1996) and Water-Table Changes in the Antelope Valley Ground-Water Basin, California*. Water\_Resources Investigations Report 98-4022. U.S. Geological Survey.
- Carlson, Carl S., and Steven P. Phillips. 1998. *Water-Level Changes (1975-98) in the Antelope Valley, California*. Water-Resources Investigations Report 98-561. U.S. Geological Survey.
- Das, A., and B. Datta. 2001. Application of optimisation techniques in groundwater quantity and quality management. *Sādhanā* 26, no. 4: 293-316.
- Durbin, Timothy J. 1978. *Calibration of a Mathematical Model of the Antelope Valley Ground-Water Basin, California*. Water-Supply Paper 2046. U.S. Geological Survey.



- Galloway, Devin L., Kenneth W. Hudnut, S. E. Ingebritsen, Steven P. Phillips, G. Peltzer, F. Rogez, and P. A. Rosen. 1998. Detection of Aquifer System Compaction and Land Subsidence Using Interferometric Synthetic Aperture Radar, Antelope Valley, Mojave Desert, California. *Water Resources Research* 34, no. 10: 2573-2585.
- Gorelick, S. M. 1983. A review of distributed parameter groundwater management modeling methods. *Water Resources Research* 19, no. 2: 305-319.
- Greenwald, R. M. 1993. *Documentation and User's Guide: MODMAN and Optimization Module for MODFLOW, Version 3.0*. Sterling, VA: GeoTrans.
- Harbaugh, Arlen W. 2005. *MODFLOW-2005, the U.S. Geological Survey modular ground-water model - the Ground-Water Flow Process*. U.S. Geological Survey Techniques and Methods 6-A16.
- Harbaugh, Arlen W., Edward R. Banta, Mary C. Hill, and Michael G. McDonald. 2000. *MODFLOW-2000, The U.S. Geological Survey Modular Ground-Water Model - User Guide to Modularization Concepts and the Ground-Water Flow Process*. Open-File Report 00-92. U.S. Geological Survey.
- Harbaugh, Arlen W., and Michael G. McDonald. 1996. *User's Documentation for MODFLOW-96, an Update to the U.S. Geological Survey Modular Finite-Difference Ground-Water Flow Model*. Open-File Report 96-485. U.S. Geological Survey.
- Hill, Mary C. 1990. *Preconditioned Conjugate-Gradient 2 (PCG2), a Computer Program for Solving Ground-Water Flow Equations*. Water-Resources Investigations Report 90-4048. U.S. Geological Survey.
- Hsieh, P. A., and J. R. Freckleton. 1993. *Documentation of a Computer Program to Simulate Horizontal-Flow Barriers Using the U.S. Geological Survey's Modular Three-Dimensional Finite-Difference Ground-Water Flow Model*. Open-File Report 92-477. U.S. Geological Survey.
- Ikehara, Marti E., and Steven P. Phillips. 1994. *Determination of Land Subsidence Related to Ground-Water-Level Declines Using Global Positioning System and Leveling Surveys in Antelope Valley, Los Angeles and Kern Counties, California, 1992*. Water-Resources Investigations Report 94-4184. U.S. Geological Survey.
- Johnson, Harry R. 1911. *Water Resources of Antelope Valley, California*. Water-Supply Paper 278. U.S. Geological Survey.
- Katsifarakis, K. L. 2008. Groundwater Pumping Cost Minimization – an Analytical Approach. *Water Resources Management* 22: 1089-1099.

- Leake, S. A., and D. E. Prudic. 1991. Documentation of a Computer Program to Simulate Aquifer-System Compaction Using the Modular Finite-Difference Ground-Water Flow Model. In *Techniques of Water-Resources Investigations of the U.S. Geological Survey, Book 6, Chapter A2*, 68.
- Leighton, David A., and Steven P. Phillips. 2003. *Simulation of Ground-Water Flow and Land Subsidence, Antelope Valley Ground-Water Basin, California*. Water-Resources Investigations Report 03-4016. U.S. Geological Survey.
- McDonald, Michael G., and Arlen W. Harbaugh. 1988. A Modular Three-Dimensional Finite-Difference Ground-Water Flow Model. In *U.S. Geological Survey Techniques of Water Resources Investigations, Book 6, Chapter A1*, 586.
- Metzger, Loren F., Marti E. Ikehara, and James F. Howle. 2002. *Vertical-Deformation, Water-Level, Microgravity, Geodetic, Water-Chemistry, and Flow-Rate Data Collected During Injection, Storage, and Recovery Tests at Lancaster, Antelope Valley, California, September 1995 through September 1998*. Open-File Report 01-414. U.S. Geological Survey.
- Nishikawa, Tracy, D. L. Rewis, and Peter Martin. 2001. *Numerical Simulation of Ground-Water Flow and Land Subsidence at Edwards Air Force Base, Antelope Valley, California*. Water-Resources Investigations Report 01-4038. U.S. Geological Survey.
- Phillips, Steven P., Carl S. Carlson, Loren F. Metzger, James F. Howle, Devin L. Galloway, Michelle Sneed, Marti E. Ikehara, Kenneth W. Hudnut, and Nancy E. King. 2003. *Analysis of Tests of Subsurface Injection, Storage, and Recovery of Freshwater in Lancaster, Antelope Valley, California*. Water-Resources Investigations Report 03-4061. U.S. Geological Survey.
- Schrage, Linus. 1991. *LINDO User's Manual Release 5.3*. New York: Boyd and Fraser.
- Thayer, W. N. 1946. *Geologic Features of Antelope Valley, California*. Los Angeles County Flood Control District Report.
- Theodossiou, N. P. 2004. Application of Non-Linear Simulation and Optimisation Models in Groundwater Aquifer Management. *Water Resources Management* 18: 125-141.
- Thompson, David G. 1929. *The Mojave Desert Region of California, a Geographic, Geologic, and Hydrologic Reconnaissance*. Water-Supply Paper 578. U.S. Geological Survey.

Tsai, F. T.-C., V. Katiyar, D. Toy, and R. A. Goff. 2009. Conjunctive Management of Large-Scale Pressurized Water Distribution and Groundwater Systems in Semi-Arid Area with Parallel Genetic Algorithm. *Water Resources Management* 23: 1497-1517.

Western Regional Climate Center. Southern California Climate Summaries.  
<http://www.wrcc.dri.edu/summary/Climsmsca.html>.